University of New Hampshire
University of New Hampshire Scholars' Repository

Doctoral Dissertations | Student Scholarship

Spring 2005

Chemical sensors based on swelling polymer microspheres and uncrosslinked fluorescently-labelled molecularly imprinted polymers

George K. Mwangi
University of New Hampshire, Durham

Follow this and additional works at: https://scholars.unh.edu/dissertation

Recommended Citation
Mwangi, George K., "Chemical sensors based on swelling polymer microspheres and uncrosslinked fluorescently-labelled molecularly imprinted polymers" (2005). *Doctoral Dissertations*. 270.
https://scholars.unh.edu/dissertation/270

This Dissertation is brought to you for free and open access by the Student Scholarship at University of New Hampshire Scholars' Repository. It has been accepted for inclusion in Doctoral Dissertations by an authorized administrator of University of New Hampshire Scholars' Repository. For more information, please contact nicole.hentz@unh.edu.

NOTE TO USERS

Page(s) not included in the original manuscript and are unavailable from the author or university. The manuscript was scanned as received.

53

This reproduction is the best copy available.

UMI®

Reproduced with permission of the copyright owner. Further reproduction prohibited without permission.

Reproduced with permission of the copyright owner. Further reproduction prohibited without permission.

CHEMICAL SENSORS BASED ON SWELLING POLYMER MICROSPHERES AND UNCROSSLINKED FLUORESCENTLY-LABELLED MOLECULARLY IMPRINTED POLYMERS

By

George K. Mwangi
B.S., University of Pune, India, 1985
M.S., University of Nairobi, Kenya, 1990

DISSERTATION

Submitted to the University of New Hampshire
in Partial Fulfillment of
the Requirement for the Degree of

Doctor of Philosophy

In

Chemistry

May 2005

Reproduced with permission of the copyright owner. Further reproduction prohibited without permission.

UMI Number: 3169087

INFORMATION TO USERS

The quality of this reproduction is dependent upon the quality of the copy submitted. Broken or indistinct print, colored or poor quality illustrations and photographs, print bleed-through, substandard margins, and improper alignment can adversely affect reproduction.

In the unlikely event that the author did not send a complete manuscript and there are missing pages, these will be noted. Also, if unauthorized copyright material had to be removed, a note will indicate the deletion.

UMI®

UMI Microform 3169087

Copyright 2005 by ProQuest Information and Learning Company.

All rights reserved. This microform edition is protected against unauthorized copying under Title 17, United States Code.

ProQuest Information and Learning Company
300 North Zeeb Road
P.O. Box 1346
Ann Arbor, MI 48106-1346

Reproduced with permission of the copyright owner. Further reproduction prohibited without permission.

This dissertation has been examined and approved.

Dissertation Director, Dr. W. Rudolf Seitz
Professor of Chemistry

Dr. Sterling A. Tomellini
Professor of Chemistry

Dr. Howard R. Mayne
Professor of Chemistry

Dr. Richard P. Johnson
Professor of Chemistry

Dr. Barkley C. Sive
Research Assistant Professor
Climate Change Research Center

5/12/05

Date

Reproduced with permission of the copyright owner. Further reproduction prohibited without permission.

DEDICATION

This dissertation is dedicated to my wife, soul mate and my best friend Lucy Wanjiru, to my lovely daughters, Ann Wagathuitu and Ruth Wanjuhi, to my parents Arthur Mwangi and Jennifer Muthoni for their love, support and constant encouragement. Last but not least to my mother-in-law, Ruth Wanjuhi Mbugua, for her love and prayers.

Reproduced with permission of the copyright owner. Further reproduction prohibited without permission.

ACKNOWLEDGEMENTS

First I would like to sincerely thank my research advisor, Professor W. Rudolf Seitz for his constant guidance, mentoring and encouragement all throughout my studies at UNH. He taught me to think independently and brought out the very best in me. I also extend my appreciation to my other committee members: Dr. Sterling A. Tomellini, Dr. Howard R. Mayne, Dr. Richard P. Johnson and Dr. Barkley C. Sive for their time and assistance.

I would like to sincerely thank the following that have in their own ways helped to make this study a success:

Dr. Dennis N. Chasteen for his assistance in running the EPR spectra and for his help in interpreting the data.

Dr. Barry Lavine of the Oklahoma State University for his encouragement and support during and after his sabbatical at the UNH.

I am very thankful to my fellow group members for their friendly and collaborative atmosphere, which made working with them fun. I am especially grateful to Dr. Necati Kaval who taught me to make my first microspheres.

Nancy Cherim, UNH instrumentation center, for her help with the Scanning Electron Microscopy and CHN analysis.

To Cindi Rohwer, Peggy Torch, Susan Higgins, Amy Linsday, Kathy Gallagher, Kristin McFarlane and Bob Constantine I say thank you for your help and support.

Last but not least my gratitude goes the Department of Chemistry and the University of New Hampshire for their financial support without which all this would not have been possible.

Reproduced with permission of the copyright owner. Further reproduction prohibited without permission.

Table of Contents

DEDICATION iv

ACKNOWLEDGEMENTS v

LIST OF TABLES ix

LIST OF FIGURES x

ABSTRACT xv

CHAPTER PAGE

I. INTRODUCTION
- 1.1. Chemical Sensors 1
- 1.2. Sensor Classification 5
- 1.3. Chemical Sensors Based on Molecularly Imprinted Polymers 12
- 1.4. Chemical Sensors Based on Swellable Polymers 14
- 1.5. Objectives 19

II. THEORY
- 2.1. Polymer Background 21
- 2.2. Free Radical Polymerization 24
- 2.3. Dispersion Polymerization 30
- 2.4. Particle Growth In Dispersion Polymerization 32
- 2.5. Theory of Polymer Swelling 35
- 2.6 Free radical polymerization techniques 41
- 2.7. Shirazu Porous Glass Emulsification Method 42
- 2.8. Phase Transition Temperatures of Acrylamide Polymers 47
- 2.9. Background of Molecular Imprinted Polymers 48
- 2.10 Optical Measurement of Particle Suspended in a Hydrogel 52

III. EXPERIMENTAL
- 3.1. Reagents 54
- 3.2. Apparatus 58
- 3.3. Procedures 59
- 3.4. Preparation of the Fluorescent monomer (NBD-AE2) 67
- 3.5. Preparation of theophylline imprinted, PolyNNPAM-co-AAc-co-NBD-AE2 71
- 3.6. Dialysis for template extraction 74
- 3.7. Preparation of hydrogel membranes 77
- 3.8. Evaluation of microparticles 80

Reproduced with permission of the copyright owner. Further reproduction prohibited without permission.

IV. SUSPENSION POLYMERIZATION SYNTHESIS AND EVALUATION OF AMINATED POLY (VBC) MICROSPHERES FOR pH OPTICAL SENSING

4.1 Introduction 85
4.2. Preparation of Poly (VBC) Microparticles 88
4.3. Derivatization of Poly (VBC) Microparticles 91
4.4. Results and Discussion 92
4.5. Conclusion 102

V. DISPERSION POLYMERIZATION SYNTHESIS AND EVALUATION OF AMINATED POLYMER MICROSPHERES FOR pH AND Cu^{2+} SENSING

5.1. Introduction 104
5.2 Light microscope images of the swelling and shrinking of aminated polyHEMA microspheres 107
5.3. Evaluation of aminated polyHEMA microspheres for pH sensing 109
5.4. Titration of aminated polyHEMA microspheres with Cu^{2+} 114
5.5 Copper turbidity spectra for ethylenediamine derivatised microspheres 117
5.6. Determination of Cu^{2+} :N complexation ratio 119
5.7. Electron Paramagnetic Resonance Spectra 123
5.8. Conclusion 129

VI MOLECULARLY IMPRINTED POLYMER MICROSPHERES FOR ROOM TEMPERATURE THGEOPHYLLINE SENSING

6.1. Introduction 131
6.2. Results and discussion 134
6.3. Conclusion 138

Reproduced with permission of the copyright owner. Further reproduction prohibited without permission.

VII. MOLECULAR IMPRINTED POLYMERS BASED ON UNCROSSLINKED AND FLUORESCENTLY LABELLED POLYMERS

7.1. Introduction 139
7.2 Temperature response of uncrosslinked templated polyNNPAM 144
7.3. Selectivity of PolyNNPAM-co-AAc-co-NBD-AE2 in buffer solutions at constant temperature 146
7.5. Response of uncrosslinked, imprinted polymer to theophylline 149
7.6 Response time 152
7.7 Conclusions 153

VII. CONCLUSIONS 154

Reproduced with permission of the copyright owner. Further reproduction prohibited without permission.

LIST OF TABLES

		PAGE
Table 1.1	Ideal Characteristics of a sensor.	3
Table 3.1	Formulation for the suspension polymerization of VBC.	60
Table 3.2	Typical recipe for the dispersion polymerization of HEMA.	64
Table 3.3	Typical formulation for the synthesis of NBD-AE2 Fluorophore.	69
Table 3.4	Typical formulation for the dispersion polymerization of theophylline templated polyNNPAM-co-AAc-co-NBD-AE2 co-polymer.	76
Table 4.1	Results from CHN analysis for the amination of poly (VBC) microspheres at different temperatures.	97

Reproduced with permission of the copyright owner. Further reproduction prohibited without permission.

LIST OF FIGURES

		PAGE
Figure 1.1	Classification of FOCS. (a) direct spectroscopic sensors (b) reagent-mediated sensors.	8
Figure 1.2	Schematic representation of a remote distributive optic chemical sensor.	18
Figure 2.1	Initiation stage of the free radical polymerization of HEMA with AIBN as the initiator.	27
Figure 2.2	Propagation stage of the free radical polymerization of HEMA with AIBN as the initiator.	28
Figure 2.3	Termination stage of the Free Radical Polymerization of Poly (HEMA) with AIBN as the initiator, a) Combination b) Disproportionation.	29
Figure 2.4	Schematic of particle growth by dispersion polymerization.	34
Figure 2.5	Schematic illustration of ionic polymer swelling. (1) Shows the unswollen polymer, (2) the swollen polymer. The circles represent mobile charge in solution; squares represent fixed charges on the polymer skeleton.	40
Figure 2.6	Schematic diagram of the Shirazu porous glass (SPG) membrane emulsification apparatus .	44
Figure 2.7	Scheme of an emulsification module.	45
Figure 2.8	Schematic showing droplet formation as pressure is applied.	47
Figure 2.9	Schematic of the molecular imprinting principle, in which the template is the structural analogue of the target analyte.	50
Figure 3.1	Three-neck reactor flask with overhead mechanical stirrer.	61
Figure 3.2	Synthesis of N-n-Propylacrylamide from Acryloyl Chloride and N-n-Propylamine.	66
Figure 3.3	Synthesis of 4-(6-Hydroxyamino)-7-nitro-2, 1, 3-benzoxadiazole.	68

Reproduced with permission of the copyright owner. Further reproduction prohibited without permission.

Figure 3.4 Synthesis of 4-(6-Acryloyloxyhexylamino)-7-nitro-2, 1,3-benzoxadiazole (NBD-AE2) fluorophore. 70

Figure 3.5 Synthesis of uncrosslinked poly (NNPAM-co-AAc-co-NBD-AE2). 72

Figure 3.6 Preparation of theophylline selective molecularly imprinted polymers. 73

Figure 3.7 Dialysis apparatus used for extracting the template from the polymer. 75

Figure 3.8 Membrane holders for turbidity determinations. 83

Figure 4.1 Non-uniform and large Poly (VBC) particles prepared initially. 89

Figure 4.2 Uniform and monodisperse polyVBC microspheres prepared after some practice with the SPG apparatus. 90

Figure 4.3 Derivatization of poly (VBC) microspheres. 91

Figure 4.4 pH titration of NNN'-trimethylenediamine derivatized poly (VBC) with 0.1 M NaOH solution. 92

Figure 4.5 Turbidity vs. wavelength spectra of NNN-trimethylenediamine derivatized poly (VBC) microspheres suspended in PVA membrane. 94

Figure 4.6 Turbidity vs. wavelength spectra of NNN-trimethylenediamine derivatized poly (VBC) microspheres. Monitored at 500 nm. 95

Figure 4.7 Turbidity spectra for aminated Poly (HEMA) microspheres in pH 4 and pH 10 buffers. The amount of N derivatized on the microspheres was 3.38%. 98

Figure 4.8 Turbidity spectra for aminated Poly (HEMA) microspheres in pH 4 and pH 10 buffers. The amount of N derivatized on the microspheres was 5.78%. 99

Figure 4.9 Turbidity spectra for aminated Poly (HEMA) microspheres in pH 4 and pH 10 buffers. The amount of N derivatized on the microspheres was 11.27%. 100

Reproduced with permission of the copyright owner. Further reproduction prohibited without permission.

Figure 4.10 Response time of NNN'-trimethylenediamine derivatized poly (HEMA) in pH 4 and pH 10 buffer solutions. 101

Figure 5.1 Activation of poly (HEMA) to introduce the imidazolyl Carbamate group. 105

Figure 5.2 Coupling the activated poly (HEMA) matrix with functionality diethylenetriamine to introduce the pH and metal sensing. 106

Figure 5.3 Light micrograph images of aminated poly (HEMA) in the swelling process when immersed in buffers from pH 11 to pH 2. 108

Figure 5.4 Turbidity vs. pH of 1 % diethylenetriamine derivatized Poly (HEMA) particles suspended in 76 micrometer thick polyurethane membrane. 110

Figure 5.5 Turbidity vs. pH of 1 % diethylenetriamine derivatized Poly (HEMA) particles monitored at 500 nm. 110

Figure 5.6 pH response curve of CDI-activated Poly (HEMA) microspheres derivatized with diethylenetriamine. 111

Figure 5.7 0.2 % Diethylenetriamine derivatized poly (HEMA) Microspheres suspended in Poly (Vinyl alcohol) membrane. 112

Figure 5.8 0.2 % Diethylenetriamine derivatized poly (HEMA) microspheres suspended in Poly (Vinyl alcohol) membrane monitored at 500 nm. 113

Figure 5.9 Potentimetric titration of Poly HEMA-CDI-Diethylenetriamine with 0.02 M Cu^{2+} buffered at pH 3.8. 115

Figure 5.10 Response time of polyHEMA-CDI-Diethylenetriamine to Cu^{2+} 116

Figure 5.11 Turbidity response of polyHEMA-CDI-Diethylenetriamine. 117

Figure 5.12 PolyHEMA-CDI-Diethylenetriamine 3% in polyurethane Membrane. 118

Reproduced with permission of the copyright owner. Further reproduction prohibited without permission.

Figure 5.13 Copper complexation of PolyHEMA-CDI-Diethylenetriamine derivatized microspheres 3% suspended in Polyurethane membrane. 120

Figure 5.14 Copper complexation of Poly HEMA-CDI-Diethylenetriamine derivatized microspheres 1% suspended in Polyurethane membrane. 122

Figure 5.15 A and B Electron paramagnetic spectra of the complexes of Cu^{2+} Ethylenediamine as the model ligand. 124

Figure 5.15 C and D Electron paramagnetic spectra of the complexes of Cu^{2+} with the model ligand Ethylenediamine. 125

Figure 5.16 EPR spectrum of diethylenetriamine derivatized polyHEMA buffered at pH 5.5. 126

Figure 5.17 EPR spectrum of diethylenetriamine derivatized polyHEMA buffered at pH 7.0. 127

Figure 6.1 Response of templated polyNIPA-co-MAA to theophylline Concentration at room temperature. 135

Figure 6.2 Response of templated polyNIPA-co-MAA to theophylline Concentration at 500 nm. 136

Figure 6.3 Response of templated polyNIPA-co-MAA to theophylline At pH 7 with 10 % MAA used in formulation. 137

Figure 7.1 The structures of Theophylline and Caffeine. 143

Figure 7.2 Temperature response of uncrosslinked and templated Poly NNPAM-co-AAc-co-AE2. 144

Figure 7.3 Temperature response of uncrosslinked PolyNIPA-co-AAc-co-NTBA-co-AE2. 145

Figure 7.4 Fluorescence intensity of uncrosslinked and templated PolyNNPAM- co-AAc-co-AE2 as a function of wavelength and theophylline concentration at pH 4. 147

Figure 7.5 Fluorescence intensity of uncrosslinked and templated PolyNNPAM- co-AAc-co-AE2 as a function of wavelength and caffeine concentration at pH4. 148

Reproduced with permission of the copyright owner. Further reproduction prohibited without permission.

Figure 7.6 Fluorescence intensity of uncrosslinked and templated PolyNNPAM- co-MAA-co-AE2 as a function of wavelength and theophylline concentration at pH 2. 150

Figure 7.7 Fluorescence intensity of uncrosslinked and untemplated PolyNNPAM- co-MAA-co-AE2 as a function of wavelength and THO concentration. 151

Figure 7.8 Response time of uncrosslinked polyNNPAM-co-AAc-co-AE2. 152

Reproduced with permission of the copyright owner. Further reproduction prohibited without permission.

ABSTRACT

CHEMICAL SENSORS BASED ON SWELLING POLYMER MICROSPHERES AND UNCROSSLINKED FLUORESCENTLY-LABELLED MOLECULAR IMPRINTED POLYMERS

By

George K. Mwangi

University of New Hampshire, May 2005

Polymer swelling can be achieved by derivatizing a functional group onto the polymer that selectively binds a particular analyte. For example, at low pH, the particles in a hydrogel membrane swell in response to the increased hydrogen ion concentration and the membrane reflects less light. When the refractive index of the membrane is less than that of the particles, swelling decreases the refractive index of the particles. This brings it closer to the refractive index of the membrane, and decreases the scattering of light making the membrane more transparent.

On the other hand if the refractive index of the membrane is higher than that of the microspheres, swelling of the microspheres increases the difference between the refractive indices of the two media. This makes the membrane less transparent. By coupling selective polymer swelling with a transduction method that responds to the changes in polymer size, it is possible to make a chemical sensor.

Reproduced with permission of the copyright owner. Further reproduction prohibited without permission.

Polymer microspheres that change size as a function of pH and metal ion concentration have been prepared by suspension and dispersion polymerization respectively. For the pH sensor, poly (vinylbenzylchloride) was prepared by suspension polymerization using the Shirazu porous glass (SPG) method. The particles were lightly crosslinked with divinylbenzene followed by amination with NNN'- trimethylethylenediamine.

Poly (hydroxyethylmethacrylate)(polyHEMA) microspheres were prepared by dispersion polymerization and then derivatized with diethylenetriamine. These aminated polymer microspheres suspended in PVA and polyurethane hydrogels respond to Cu^{2+} ions in solution. The complexation ratio of Cu^{2+}: N was determined to be 1:2. The response time is ~ 7 minutes, which is much longer than was observed with pH response. This was attributed to the bigger size of Cu^{2+}, which restricts their movement into the polymer microspheres.

A new design of a molecularly imprinted polymer was developed. It was based on theophylline templated, uncrosslinked poly N-n-propylacrylamide (polyNNPAM) (principal monomer), co-polymerized with 4-(2-acroyloyloxyethylamino)-7-nitro-2, 1,3-benzoxadiazole (NBD-AE2) (fluorophore) and methacrylic acid (MAA) (functional monomer). This polymer was prepared by dispersion polymerization in acetonitrile solvent. Since the co-polymer remains in solution rather than as a separate phase (because of the absence of crosslinks), dialysis was the method chosen to extract the template, with many changes of the external solution. The sensor responds by increase in fluorescence with increased

Reproduced with permission of the copyright owner. Further reproduction prohibited without permission.

concentrations of theophylline. It was shown to have a high sensitivity ($1x10^{-7}$M) and was highly selective because there was no change in fluorescence for increasing caffeine concentration up to 1 $x10^{-3}$M.

Reproduced with permission of the copyright owner. Further reproduction prohibited without permission.

CHAPTER 1

INTRODUCTION

1.1 Chemical Sensors

A chemical sensor is a measurement system designed to exhibit an experimental response that can be related to the quantity of a sample chemical species or a class of chemical species.[1] A chemical sensor can be distinguished from a physical transducer in that it provides the user with information about the chemical nature of its environment. While it may contain a physical transducer (e.g., a thermister or piezoelectric crystal) or reference electrode (eg, a Ag/AgCl wire) at its core, its overall character is usually determined by some type of chemically selective membrane, film or layer at the sensing tip.[2] Chemical sensing is part of an information acquisition process in which some insight is obtained about the chemical composition of the system in real time. Generally it consists of two distinct steps: recognition and amplification. The recognition (also known as selectivity) is provided by some chemical interaction, while the amplification can be provided by some physical means. The coupling of the chemically selective layer to the physical part of the sensor is very important because it can have a profound effect on chemical selectivity.[3]

Reproduced with permission of the copyright owner. Further reproduction prohibited without permission.

There is no such thing as an 'ideal' sensor. A sensor that performs well for monitoring a particular analyte in a given situation may be totally unsuitable for monitoring the same analyte in a different matrix. Factors that contribute to the suitability of a device for a particular assay may include physical parameters such as temperature, pressure, or chemical interferences arising from the sample matrix. Table 1.1 lists some desirable characteristics of sensors.

There seems to be a natural division between chemical and physical sensors. However there are those that do not classify easily, like humidity sensors, a chemical sensor traditionally lumped with physical sensors. Biosensors are defined as sensors that use biomolecules and/or structures to measure an analyte with a biological significance or bioactivity. The biosensor can be considered a subset of chemical sensors because the transduction methods, sometimes referred to as the sensor platforms, are the same as those for chemical sensors. Chemical sensor arrays with instrumentation, having popular names like the electronic nose or electronic tongue, have been constructed to address chemically complex parameters like taste, odor, toxicity or freshness.

Reproduced with permission of the copyright owner. Further reproduction prohibited without permission.

Table 1.1 Ideal Characteristics of a Sensor[2]

Characteristic	**Comments**
Signal output should be proportional, or bear a simple mathematical relationship, to the amount of species in the sample	This is becoming less important with the advent of on-device electronics and integration of complex signal processing options to produce so-called smart sensors
No hysteresis	The signal should return to baseline after responding to the analyte
Fast response times	Slow response times arising from multiple sensing membranes or sluggish exchange kinetics can seriously limit the range of possible application and prevent use in real-time monitoring situations
Good signal-to-noise (S/N) characteristics	The S/N ratio determines the limit of detection; can be improved by using the sensor in a flow analysis situation rather than for steady state measurements-S/N ratio can be improved by filter or impedance conversion circuitry built into the device ('smart' sensor)
Selective	Without adequate selectivity, the user cannot relate the signal obtained to the target species concentration with any confidence
Sensitive	Sensitivity is defined as the change in signal per change in concentration (i.e. the slope of the calibration curve); this determines the ability of the device to discriminate accurately and precisely between small differences in analyte concentration

Reproduced with permission of the copyright owner. Further reproduction prohibited without permission.

There is a growing need for sensitive sensors in several industrial areas such as process technology, health care, environmental control, biotechnology, etc.[4] For practical applications these sensors should be very sensitive, small, fast, cheap and have the possibility of remote sensing. The most effective method to construct a long-term sensor for underwater use is to promote measurement principles that are not susceptible to interference or drift. Although electrochemical techniques are traditional and easy to adopt, very few are suitable for long-term use because they do not posses long term stability, resistance to high salt concentrations, mechanical ruggedness, or compatibility with various anti-fouling regimes.[5] Calibration of chemical sensors is essential to the absolute accuracy and long-term deployment of the sensor. It can be difficult to maintain a calibration and there is often a trade off between sensitivity and response rate.[5]

Spectroscopic detectors are easy to adapt for many applications and numerous research groups have developed new optical sensors. There are a number of easily measured optical properties such as absorption, polarization, luminescence and decay times. The vitality of the chemical sensing field can be seen from the growing number of published papers. In his review of 2070 papers published during the period from 1994-97, Janata found that electrochemical sensors represented the largest group of sensors, followed by optical and mass sensors.[6] Thus chemical sensors have become an integral tool of diverse scientific studies.

Reproduced with permission of the copyright owner. Further reproduction prohibited without permission.

1.2 Sensor Classification

There are four broad categories of sensors, which are classified according to their transduction principle. These are: thermal, mass, electrochemical and optical.

1.2.1 Thermal Sensors

Classical thermal sensors involve thermometers, thermocouples and thermisters. These devices measure temperature change by its effect on the volume of a liquid; induced emf changes from a bimetallic contact, or changing resistance values respectively[1]. Thermal sensors are the least published group of sensors. In the period between 1990-97, less than 100 papers were published on this topic.[6]

However, several new ideas have emerged, in the thermosensing of gases. These include the solid-state catharometer, which exhibit selectivity for gases[7] and organic vapors by a photopyroelectric effect.[8]

1.2.2. Mass Sensors

Sensors that use acoustic waves are a very versatile. Because they are highly sensitive to surface mass changes, they have many applications as chemical sensors. It is customary to add a layer to the device surface that can recognize and bind the analyte of interest.[9]

Binding transfers the analyte from the medium being analyzed to the device surface, where it alters one or more of the physical properties to which the acoustic wave responds. For example, absorption of a vapor from the gas phase into a polymer thin film increases the mass and decreases the modulus of the thin film. Both of these changes reduce acoustic wave velocities in the substrate.[9]

Reproduced with permission of the copyright owner. Further reproduction prohibited without permission.

1.2.3. Electrochemical Sensors

As a class of sensors, electrochemical sensors constitute one of the broadest and oldest types. Most of these devices fall into two major categories, amperometric and potentiometric. Amperometric sensors are based on the detection of electroactive species involved in the chemical or biological recognition process. The signal transduction process is accomplished by controlling the potential of the working electrode at a fixed value (relative to a reference electrode) while monitoring the current as function of time.[10] In potentiometric sensors, the analytical information is obtained by converting the recognition process into a potential signal, which is related to the activity.[10]

1.2.4. Fiber Optic Chemical Sensors (FOCS)

Chemists were quick to recognize that chemicals sensors could be developed using the high quality inexpensive fiber optics that became available in the late 1970s.[6] Like electrochemical sensors that use an electrical conductor to transmit information between the meter and the sensing mechanism, an optical chemical sensor could be made with fiber optics acting as a light conduit to and from an optically–based sensor.[6] Considerable interest in chemical applications for industrial, medical and environmental monitoring stimulated a large amount of research into these sensors, now called Fiber Optic Chemical Sensors (FOCS) or sometimes 'optodes.'

Reproduced with permission of the copyright owner. Further reproduction prohibited without permission.

Optical fibers, also known as light guides or optical wave-guides, permit the low loss transmission of light though the fiber core by the phenomenon of total internal reflection. Fibers can also be used in a bi-directional mode, in which light propagates through a fiber and returns via the same or a second fiber, thereby allowing spectroscopy to be performed at a distance. The optical fiber functions as a conduit for light and can be used to monitor changes in absorption, reflectance, chemiluminescence and fluorescence in the sample.[21]

1.2.4.1 Types of Optic Fibers

Fiber-optic chemical sensors are classified conveniently in two categories (Figure 1.1):

- Direct Spectroscopic Sensors. In this case, the fiber functions solely as a simple light guide that separates the sensing location from the monitoring instrumentation (source, detector, spectral filtering, etc.). The fiber facilitates direct spectral analysis (e.g., fluorescence, absorption, Raman scattering) of a sample at a distance. Naturally fluorescent groundwater contaminants have been monitored in this manner at sub-ppm levels over distances of hundreds of meters.[11]

Reproduced with permission of the copyright owner. Further reproduction prohibited without permission.

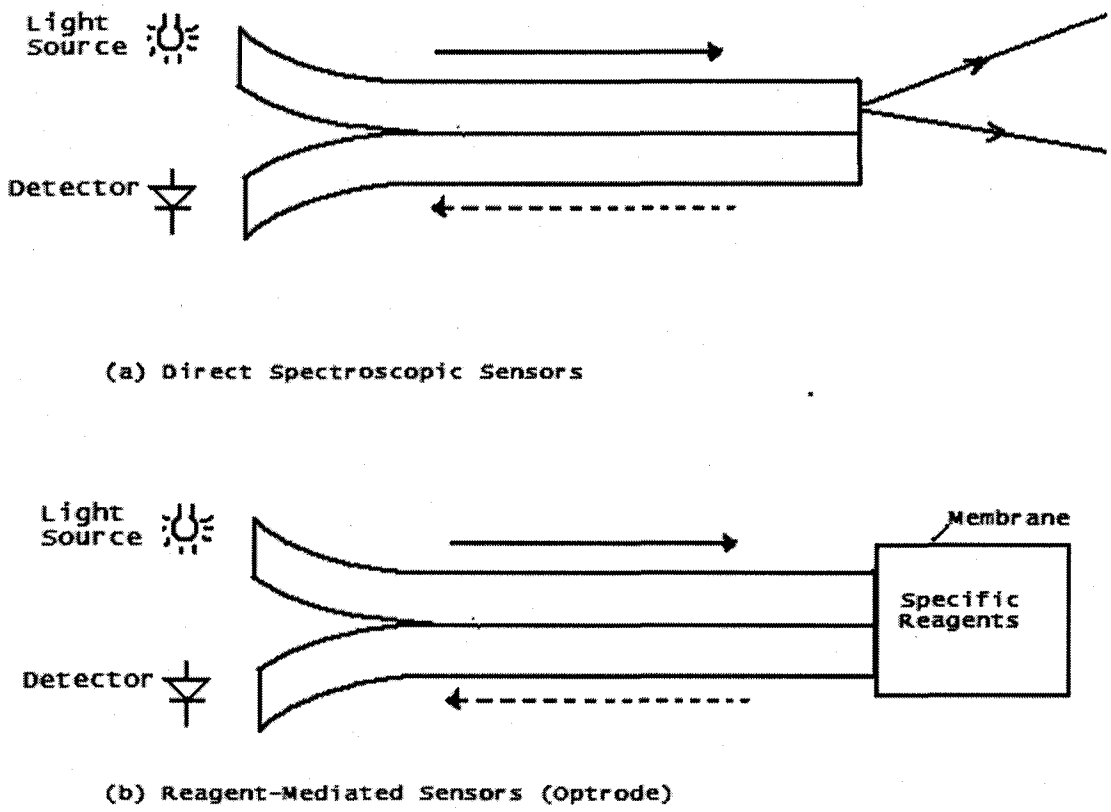

Figure 1.1. Classification of FOCS: (a) direct Spectroscopic Sensors; (b) reagent-mediated sensors (Optrodes).

- Reagent–Mediated Sensors (Optrodes). An indicator phase can interact with analyte to produce an optically detectable signal. A reagent is chosen that reacts sensitively and specifically with the analyte so that the resultant changes in optical properties (e.g. fluorescence or absorption) is a direct measure of the analyte concentration. A number of configurations may be used. For example, at the far end of the fiber specific reagents can be contained in a miniature reservoir attached to the fiber tip and separated from the sample by means of an appropriate membrane.[11]

Reproduced with permission of the copyright owner. Further reproduction prohibited without permission.

Direct immobilization of suitable reagent in a support matrix on the fiber tip or along the core of a decladded optical fiber are also widely used.

In addition, the terms intrinsic and extrinsic are sometimes applied to FOCS.

- With intrinsic sensors, the optical fiber acts as an optical component, its properties are modulated directly by a change in a physical parameter, thus altering the transmitted light. It is possible to detect very subtle influences by coiling a long length of fiber in the modulating area. Intrinsic sensors exist for the measurement of temperature, magnetic field, acoustics, strain and electrical current, as well as other physical parameters.
- An extrinsic sensor is used for specific chemical detection and requires an association of an optical transducer with the fiber. The transducer must induce an optical signal change (absorption, fluorescence or reflectance) in response to the selective detection of an analyte in a complex mixture. Fluorescence is preferred due to its inherent sensitivity, the easy separation between exciting and emitted light and the technical expediency of coupling laser excitation to optical fibers. In this research we will further explore and discuss this type of sensor.

Peterson *et al*[12] designed the first fiber optic probe for pH monitoring that was based on the use of a dye indicator in 1980. This non-electrical pH probe has some advantages for physiological applications over conventional micro-pH electrodes. An important safety feature for human use is that no possible electrical contact to the body is involved.[12] The use of a plastic optical fiber allows a high degree of mechanical flexibility combined with small size and low cost, disposable construction. In this sensor, microspheres of polyacrylamide microspheres for light

Reproduced with permission of the copyright owner. Further reproduction prohibited without permission.

scattering were packed in an envelope of cellulose dialysis tubing at the end of a pair of plastic optical fibers.

The probe can be inserted into tissue or a blood vessel through a 22-gauge (0.41-mm i.d) hypodermic needle. It is used for monitoring pH in studies of respiration and tissue oxygenation.[12] The probe designed by Peterson *et al*[12] was suitable for measuring blood pH over the physiological range of pH 7.0-7.4 with an accuracy of 0.01 pH unit.

Saari and Seitz[13]demonstrated the viability of sensors based on immobilized fluorigenic agents two years later. Fluorescence measurements were made by attaching and immobilizing fluorescein to the end of the optical fiber and immersing the fiber in a solution of 0.1 M acetic acid. The measurements were made as the pH was varied by adding 4.0 M KOH.[13]

Later in 1986, Munkholm and co-workers prepared a pH fiber optic sensor based on fluorescence intensity. This sensor used fluoresceinamine, which was incorporated into an acrylamide-methylenebis (acrylamide) copolymer, which in turn was attached to a surface modified glass fiber via photopolymerization. This sensor gave instantaneous responses and reversible measurements over the pH range of 4.0-8.0 with S/N ratios typically 275/1.[13]

St. John and co-workers[15] fabricated an optical detector that is specific for bacterial cells. In their study, an antichoriogonadotrophin antibody was immobilized to a silicon wafer surface[3] and was used to capture the antigen from sample solutions.

Detection of the bound choriogonadotrophin was achieved by illuminating the surface with a laser that diffracts due to binding of the biological material.

Progress in the field of optical hardware has inspired the development of many

Reproduced with permission of the copyright owner. Further reproduction prohibited without permission.

chemical optical sensors (optodes or optrodes), which comprise an expanding area of analytical chemistry. Optical fiber wave-guides have often been used to transmit light to and from the sensing layer, allowing the fabrication of cheap and operationally simple sensor systems.[16]

The development of optical ion sensors has been initiated by the availability of suitable optical hardware, which promises a wide field of novel applications.[17] There have been many efforts to develop ion-selective optodes based on the immobilization of sensing components on the surface of an optical waveguide. It has been recognized that the non-thermodynamic assumptions for the determination of single ion activities, are in this case more difficult when compared to ion selective electrodes.[17]

Array-based sensors provide architecture for multi-analyte sensing. Michael *et al*[18] reported a new approach for sensor fabrication in which they made sensors by immobilizing different reactive chemistries on the surfaces of microspheres. They made randomly ordered, addressable, high-density optical sensor arrays by combining optical imaging fibers, selective etching, chemical assays, and optical encoding schemes.

An optical imaging fiber was chemically etched to produce a high-density array of micrometer-sized wells. A one step procedure was then developed for dispersing tens of thousands of chemically modified microspheres in an etched fiber to create a high-density sensor array.[18]

The first optical enzyme biosensor was developed by Lubbers and Opitz[11] for the measurement of glucose. The feasibility of using an enzyme in an optrode was also demonstrated by Arnold.[19] Kulp *et al* [20] prepared two enzyme based optrodes that

Reproduced with permission of the copyright owner. Further reproduction prohibited without permission.

detected penicillin. The enzyme penicillinase catalyzes the cleavage of the beta-lactam ring of penicillin to form penicilloic acid, which dissociates to penicilloate and a proton, thus producing a pH change in the medium, which is monitored by a pH dependent fluorescent dye.[20]

An exciting development in the field of chemical sensors is the recent development of sub-micrometer fiber optic chemical sensors. To fabricate a sub-micrometer fiber optic sensor, an optical fiber is pulled in a modified micropipette puller to produce a tip with a typical diameter of 100 nanometers. The sides of the pulled fiber are then coated with aluminum leaving the end face of the fiber as a transmittive aperture.[22]

1.3 Chemical Sensors Based on Molecularly Imprinted Polymers (MIPs).

The term 'molecular recognition' has been recognized all over the world since the Nobel prize was awarded to Cram, Lehn and Pederson in 1987. Since the early work by Dickey,[29] about 50 years ago, molecular imprinting has now reached a stage where commercial uses of imprinted material are being evaluated, notably for separations requiring strong and selective binding in small molecules.

The methodology is based on the prearrangement of print molecules and functional monomers prior to initiation of the polymerization. A rigid crosslinked macroporous polymer is formed which contains sites complementary to the print molecule both in shape and in the arrangement of functional groups. Removal of the print molecule by extraction leaves sites specific for print molecules and free for binding.

Reproduced with permission of the copyright owner. Further reproduction prohibited without permission.

Many imprinted polymers specific for different compounds have been prepared in several laboratories over the last few years, including theophylline specific polymers, which have been used as antibody mimics.[30] Most imprinted polymers though have been prepared as particles or polymer monoliths for HPLC.[31-34]

The use of MIP stationary phases for chromatographic or electrophoretic methodology provides predetermined selectivity for pharmaceutical substances. The ability of MIPs to stereoselectively separate racemic mixtures in combination with their physical properties render them attractive separation materials.[35-39] Early work utilizing MIP-based Chiral stationary phases (CSPs) was almost exclusively carried out with liquid chromatography.[36-39]

This technique has been shown to demonstrate remarkable enantioselectivity for a broad range of compound classes including drugs,[40] amino acid derivatives,[39] peptides,[41] antibiotics,[42] synthetic enzymes[43] and sensors.[44,45] The MIP based CSP is produced using covalent or non-covalent imprinting techniques with pure enantiomeric template molecules, resulting in highly selective polymeric CSP. The polymer is then crushed, extracted and sieved to a suitable particle size for subsequent packing into a chromatographic column.[37]

Affinity assays such as immunoassays are widely applied for routine chemical analysis. Therefore the incorporation of MIPs into these assays may have a high impact in the analytical field. In immunoassays analyte recognition occurs by an antibody, which offers a high affinity, specific binding site.[46]

In spite of the recent upsurge in publications concerning imprinted polymers there is relative dearth of reports regarding fluorescent imprinted polymers.[47-50] However there is work on imprinted polymers for detection of fluorescent analytes[40,41] or for

Reproduced with permission of the copyright owner. Further reproduction prohibited without permission.

non-fluorescent analytes by competitive displacement by the analyte of a fluorescent compound.[51] In the cases where the polymers rather than the analytes, contain the covalently bound fluorophores, these are fabricated by means of fluorescent functional monomers. Once the crosslinked-imprinted polymer has been obtained, the fluorophore is covalently located in the polymer cavities. The imprinting template associates non-covalently with the fluorophore, usually by hydrogen binding, and the presence or absence of the analyte may be detected via changes in the fluorescence properties of the polymer.[47, 52]

Recently, a fluorescent polymer that recognizes the related cyclic nucleotide second messenger, adenosine 3', 5'-cyclic monophosphate (camp) has been reported.[41] A molecularly imprinted polymer based on immobilized gold nanoparticles (Au-MIP) had been reported by Matsui *et al.*[53] The sensing mechanism was based upon the variable proximity of the Au nanoparticles particles immobilized in the imprinting polymer. Using adrenaline as the model analyte, it was shown that molecular imprinting effectively enhanced the selectivity and sensitivity, and accordingly, Au-MIP selectivity detected the analyte at 5μM.[53]

1.4 Chemical Sensors Based on Swellable Polymers.

Polymers can be designed to selectively swell and shrink as a function of analyte concentration by introducing a functional group that selectively binds to the analyte. For example, protonation of lightly crosslinked aminated polystyrene in acidic media leads to swelling by introducing a positive charge onto the polystyrene backbone and increasing the affinity of the polymer for aqueous media.

Reproduced with permission of the copyright owner. Further reproduction prohibited without permission.

Our research group has concerned itself with the development of polymers for chemical sensing for many years.[13, 23-28] McCurley[26] developed the first fiber optic chemical sensor that was based on polymer swelling coupled to optical displacement in 1990. The sensing element was a crosslinked polymer that swelled or shrank as a function of analyte concentration. It used ion exchange materials, sulfonated polystyrene (Dowex 50 W) and sulfonated dextran (SP Sephadex) for detecting the ionic strengths of aqueous solutions. The swelling of a polymer bead was transduced by the optical displacement of a reflecting surface within the optrode.

Conway[24] and others did a factorial experiment to investigate how properties relevant to sensing depend on polymer formulation. The polymer was formed by suspension polymerization of vinyl benzyl chloride, crosslinker (divinyl benzene), toughening agent (Kraton G1652 which is a styrene-ethylene, butylene-styrene triblock co-polymer), porogenic solvent and free radical initiator at 85° C. It was then aminated to introduce a pH sensitive functional group. They measured the rate and magnitude of the change in diameter of the beads, with changing pH and the penetration modulus, which is a measure of the force necessary to deform the bead. They found that the percentage of Kraton, divinylbenzene and total diluents, all affect the penetration modulus at the 99% confidence level.

In 1994, Shakhsher and Seitz[25] prepared fiber optic sensors consisting of a small drop of aminated polystyrene on the tip of a single optical fiber with a core diameter of 100 μm. The sensor was prepared by dip-coating a partially polymerized solution and then completing the polymerization on the fiber. This was followed by amination with diethanolamine. Protonation of the amine groups caused the polymer to swell. This was accompanied by an increase in clarity of the polymer and a

Reproduced with permission of the copyright owner. Further reproduction prohibited without permission.

decrease in the intensity of light reflected back into the optical fiber. The intensity was found to decrease by a factor of 2 as the pH decreased from 8.0 to 6.5. The changes in clarity involved refractive index changes and led to the idea of suspended swellable microspheres in a hydrogel. In most cases, swelling causes the microsphere refractive index to be closer to the hydrogel refractive index resulting in a decrease in the membrane turbidity.[97] When microspheres are suspended in a membrane, they are free to swell freely in all directions, increasing the volume change due to swelling and circumventing the problem of delamination.[97]

Polyvinylbenzylchloride, lightly crosslinked with divinylbenzene was derivatized as the dicarboxylate.[27] the derivatized microspheres were dispersed in a hydrogel membrane of polyvinyl alcohol crosslinked with gluteraldehyde. When the deprotonated dicarboxylic acid groups bound calcium, or copper cations their negative charges were neutralized. Protons also had the same effect.[27] The polymer microspheres shrank causing a change in the optical properties of the sensing element. This was related to the change in the difference in the refractive indices, between the dispersed microspheres and that of the hydrogels.

The most significant advantage to this approach to sensing is that it can be implemented at any wavelength including near-infrared wavelengths used for fiber optic telecommunications. It enables coupling of state-of-the-art optic technology with chemical sensing. Also, because photoexcitation of an indicator is not required, slow photodegradation is not a problem and response can be stable for long periods of time.[97]

Instrumentation for fiber-optic chemical sensors constructed by Civiello[28] is shown in Figure 1.2. The system consists of a NIR laser diode, which is pulsed at a

Reproduced with permission of the copyright owner. Further reproduction prohibited without permission.

frequency of 33 kHz along a fiber optic cable. This cable is split by a 2x2 coupler into two fibers of unequal lengths, 300 and 500 meters. The significance of this is that it allows the resolution and analysis of the two signals independently, based on differences in transit time through the fiber. After attachment of the polymer at the distal end of the fiber, the light is reflected off the polymer surface and back through the same fiber, to the photodiode detector. The data is acquired and displayed using the LABVIEW acquisition program. The magnitude of scattering is indicative of the concentration of the analyte. Despite a low S/N ratio, this apparatus proved to be feasible and research on the system has continued.

Reproduced with permission of the copyright owner. Further reproduction prohibited without permission.

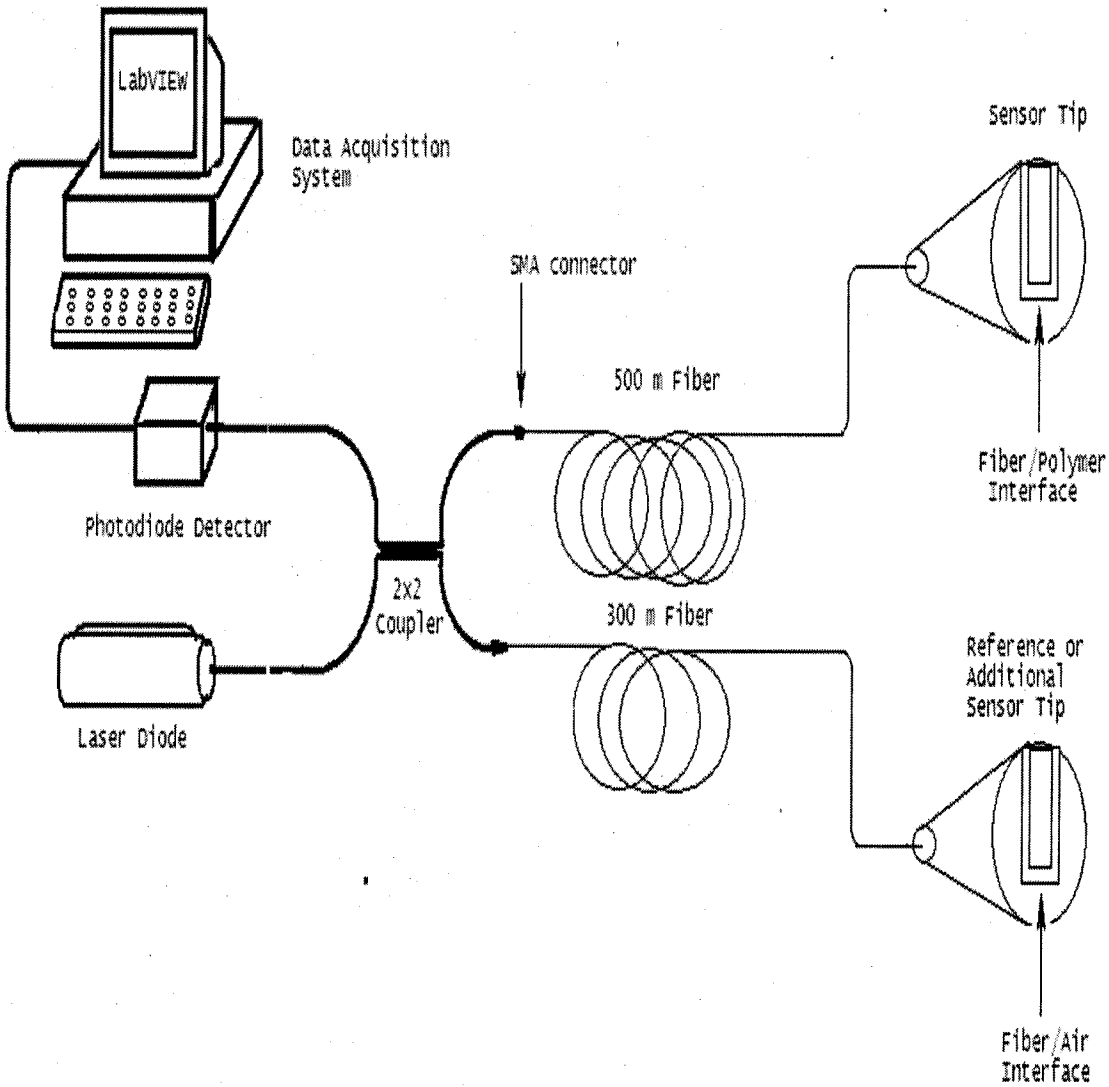

Figure 1.2 Schematic representation of a remote distributive optic chemical sensor

Reproduced with permission of the copyright owner. Further reproduction prohibited without permission.

1.5 Objectives

The first goal of my research was to develop improved swellable polymer microspheres for optical pH and metal ion sensing. To achieve this, polymer microspheres that produce large changes in turbidity as a function of analyte concentration were synthesized. The first part of this research focused on preparing monodispersed polyvinyl (benzyl chloride) microspheres. These microspheres were synthesized by suspension polymerization using the new Shirazu porous glass (SPG) method.[61] In conventional suspension polymerization vigorous stirring is required to break up the emulsion into droplets. In the SPG method, the emulsification is done by forcing the monomer phase through a porous membrane into the water phase. This results in a more uniform distribution of microspheres that are then suspended in various hydrogel membranes.

The second goal was to investigate different functional monomers and their effect on the effective swelling and shrinking properties of the polymer microspheres in which they were derivatized. The functional monomers ethylenediamine, diethylenetriamine and NNN-trimethyl ethylenediamine are pH and metal ion sensitive. These ions introduce positive charge on the functionalized polymer microspheres that causes them to swell due to the electrostatic repulsive forces.

The third goal of my research was to develop chemical sensors based on molecularly imprinted polymers for drugs such as theophylline. The initial part of this project involved the synthesis of swellable molecularly imprinted polymers that undergo swelling and shrinking as a function of template-analyte concentration.

Reproduced with permission of the copyright owner. Further reproduction prohibited without permission.

PolyNIPA and polyNNPAM are co-polymerized with methacrylic acid in the presence to theophylline template by dispersion polymerization. Studies were done on various formulations of stabilizer, crosslinker, functional monomer and template concentration.

The second part of the project was to develop a new molecularly imprinted polymer that changes fluorescence on binding the analyte. A method of dispersion polymerization using acetonitrile has been developed to prepare theophylline templated uncrosslinked polyNNPAM that is co-polymerized with a fluorophore. A number of formulation variables like percent functional monomer, template concentration and reaction conditions, such as pH and temperature, have been studied to obtain polymers that are have high sensitivities, are selective and give optimum fluorescence as function of analyte concentration.

Reproduced with permission of the copyright owner. Further reproduction prohibited without permission.

CHAPTER 2

THEORY

2.1 Polymer Background

The word polymer is derived from the Greek words *poly* (many) and *meros (part).* The original concept of polymerism was applied to situations where molecules had identical empirical formulae but different chemical and physical properties. It was not until the 1920s that the basic nature of those materials now called polymers was well understood.[54] Herman Standiger suggested the term 'macromolecules' which means 'large molecule' to describe these types of molecules. This term is presently used almost interchangeably with the word polymer.[54]

Polymers are produced from simple molecules known as monomers (single part), by a process known as polymerization. A structural unit of the polymer is enclosed by parenthesis[55]. This is known as the repeating or monomeric unit. Monomeric units are groups having two or more available bonding sites and are linked together through covalent bonds in the polymer molecule.[55]

The units can be arranged and connected in a variety of ways. In the most straightforward type of polymer, the linear polymer, the units are connected one to another in a chain arrangement such as X-M-M-M-M----Y or $X\text{-}(M)_n\text{-}Y$, where M is a structural unit or a monomer and n is the *degree of polymerization*. The degree

Reproduced with permission of the copyright owner. Further reproduction prohibited without permission.

of polymerization (d.p) represents the molecular size.[56] The molecular weight of the polymer is the product of the molecular weight of the repeat unit and the degree of polymerization. Using poly (vinyl chloride) as an example, a polymer of degree of polymerization 1000 has a molecular weight of 63 x 1000 = 63,000. Most high polymers useful for plastics, rubbers, or fibers have molecular weights between 10,000 and 1,000,000.[57]

Classically, polymers have been divided into two main groups on the basis of a comparison of the structure of the repeating unit of the polymer with the structure of the monomer from which the polymer was derived. These two general divisions are *addition polymers* and *condensation polymers*.

In addition polymers, the molecular formula of the repeating unit is identical to that of the monomer, and the molecular weight of the polymer is a simple summation of the molecular weights of all combined monomer units in the chain. For example polystyrene having the molecular formula $(C_8H_8)_n$, is the addition polymer of styrene, which has the molecular formula C_8H_8.[57]

Condensation polymers are polymers in which the repeating unit contains fewer atoms than that of the monomer or monomers, so that the molecular weight of the polymer is less than the sum of molecular weights of all the original monomer units. For example, poly (hexamethylene adipamide), which has the molecular formula $(C_{12}H_{22}N_2O_2)_n$, is the condensation polymer of hexamethylenediamine, $C_6H_{16}N_2$ and adipic acid $C_6H_{10}N_4$. The secondary product of the condensation is water.[57]

Reproduced with permission of the copyright owner. Further reproduction prohibited without permission.

While these definitions were perfectly adequate at the time, it soon became obvious that notable exceptions existed and that a fundamentally sounder classification should be based on description of the chain growth mechanism. It is preferable to replace the term condensation with *step-growth* polymerization, which includes polymers such as polyurethanes, which grow by a step reaction mechanism without elimination of a small molecule. In step-growth polymerization, a linear chain of monomer residues is obtained by a stepwise intermolecular condensation or addition of the reactive groups in bifunctional monomers. These reactions are analogous to simple reactions involving monofunctional units as typified by a polyesterification reaction involving a diol and a dibasic acid.

$$HO-R-OH + HOOC-R'-COOH \longrightarrow HO-R-OCO-R'-COOH + H_2O$$

If the water is removed as it is formed, no equilibrium is established and the first stage in the reaction is the formation of a dimer, which is also bifunctional. As the reaction proceeds, longer chains, trimers, tetramers, and so on, will form through other esterification reactions, all essentially identical in rate and mechanism, until ultimately the reaction contains a mixture of polymer chains of large molar masses M.

Two major groups, both distinguished by the type of monomer involved, can be identified in step-growth polymerization. In the first group two polyfunctional monomers take part in the reaction, and each posses only one distinct type of functional group as in the esterification reaction, or more generally:

Reproduced with permission of the copyright owner. Further reproduction prohibited without permission.

$$A-A + B-B \longrightarrow \left(A-AB-B\right)$$

The second group is encountered when the monomer contains more than one type of functional group such as a hydroxylacid (HO-R-COOH), represented generally as A-B where the reaction is

$$nA-B \longrightarrow \left(AB\right)_n$$

or

$$n(HO-R-COOH) \longrightarrow H\left(ORCO\right)_n OH$$

One basic simplifying assumption proposed by Flory[60], when analyzing the kinetics of step growth systems, was that all functional groups could be considered as being equally reactive.

2.2 Free Radical Polymerization

Free radical polymerization is the most widely practiced method of chain polymerization and is used almost exclusively for the preparation of polymers from olefinic monomers of the general type $CH_2=CR^1R^2$, where R^1 and R^2 are two substituent groups which may be identical, but more often are different. In common with other types of polymerization, free radical polymerization can be divided into three distinct stages: initiation, propagation and termination.

Reproduced with permission of the copyright owner. Further reproduction prohibited without permission.

2.2.1 Initiation

This stage of the reaction involves creation of the free radical active center and usually takes place in two steps (Figure 2.1). The first is the formation of the free radicals from an initiator, and the second is the addition of one of these free radicals to a molecule of monomer.

Free radicals may be formed in two different ways: 1) homolytic scission (homolysis) of a single bond and 2) single electron transfer to or from an ion or molecule (e.g. redox reactions). Many compounds are known to undergo thermolysis (heat mediated homolysis), in the convenient temperature range of between 50-100°C. The most important initiators are those that have the peroxide (-O-O-) or azo (-N=N-) groups.

Radiation (especially ultraviolet radiation) can also cause homolysis, in which case it is known as photolysis. Examples of this reaction include the dissociation of 2,2'-azobis(2-cyanopropane) and the formation of free radicals from benzophenone (PhCOPh) and benzoin (PhCOCH (OH) Ph). An advantage of photolysis is that the formation of free radicals begins the instant of exposure and ceases as the light source is removed.

2.2.2 Propagation

The propagation stage involves growth of the polymer chain by sequential addition of molecules of monomer to the active center (Figure 2.2). The time

Reproduced with permission of the copyright owner. Further reproduction prohibited without permission.

required for each monomer addition typically is of the order of a millisecond and so several thousand additions take place within a few seconds. There are two possible modes of propagation; head to head and head to tail additions.

The polymer chains principally consists of head to tail linkages, although an occasional head to head linkage can be expected. The proportion of head to head linkages depends upon the substituent group attached to the vinyl group. If this group is small and offers little or no mesomeric stabilization, then a high proportion of head to head linkages results. The propagation proceeds until the termination steps of combination or disproportionation occur to stop the polymerization process.

2.2.3 Termination

In the termination stage of the reaction, growth of the polymer chain is terminated (Figure 2.3). Combination and disproportionation are the two most common termination reactions; both involve reaction between two growing polymer chains. Combination involves the coupling together of two growing chains to form a single polymer molecule and results in a head to head linkage at the point of coupling. In dispropotionation, a hydrogen atom is abstracted from one growing chain by another, resulting in the formation of two polymer molecules, one with a saturated end-group and the other with an unsaturated end-group. It is important to note that the chains have initiator fragments at only one end, in contrast to combination, which yields polymer molecules with initiator fragments at both ends. Generally, both these termination reactions contribute, but to different extents depending upon the monomer and the polymerization conditions.

Reproduced with permission of the copyright owner. Further reproduction prohibited without permission.

1) Initiation

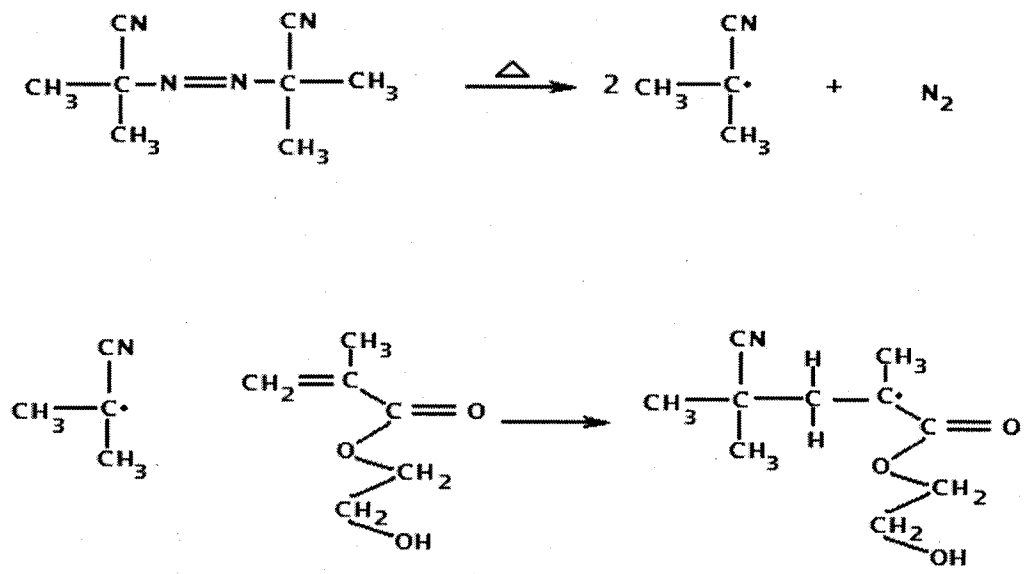

Figure 2.1 Initiation stage of the Free Radical Polymerization of HEMA with AIBN as the initiator

Reproduced with permission of the copyright owner. Further reproduction prohibited without permission.

2) Propagation

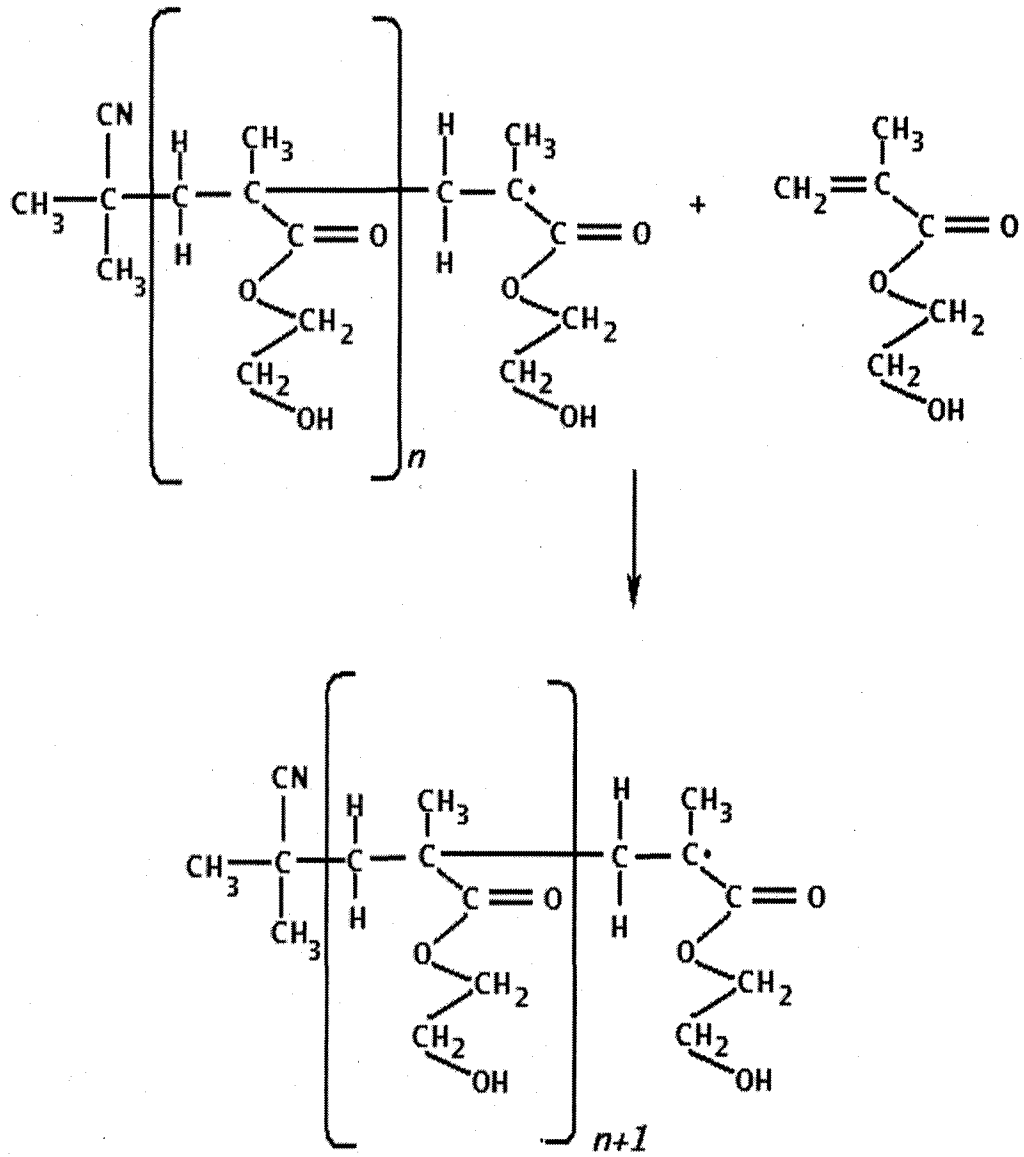

Figure 2.2 Propagation stage of the Free Radical Polymerization of HEMA with AIBN as the initiator

Reproduced with permission of the copyright owner. Further reproduction prohibited without permission.

3) Termination

a) Combination

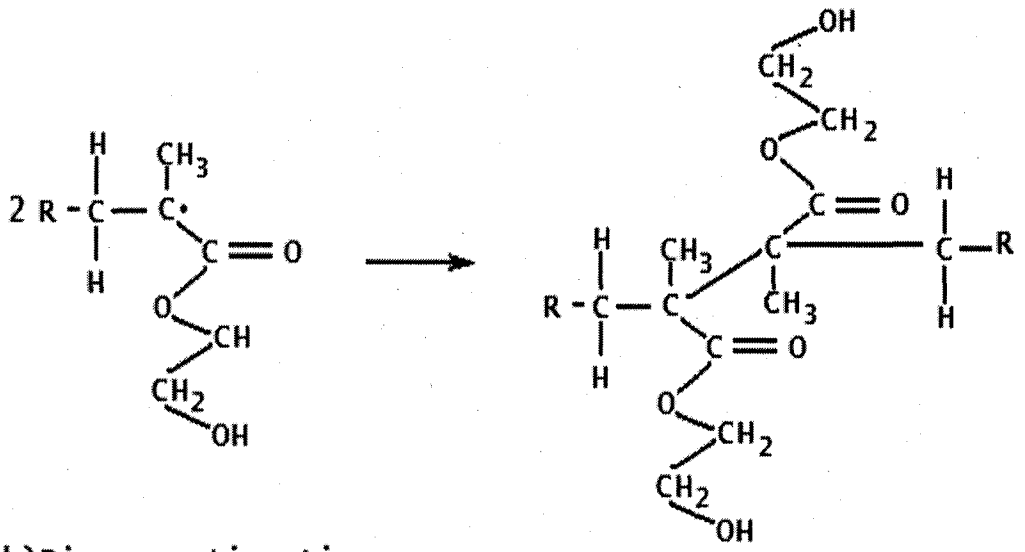

b)Disproportionation

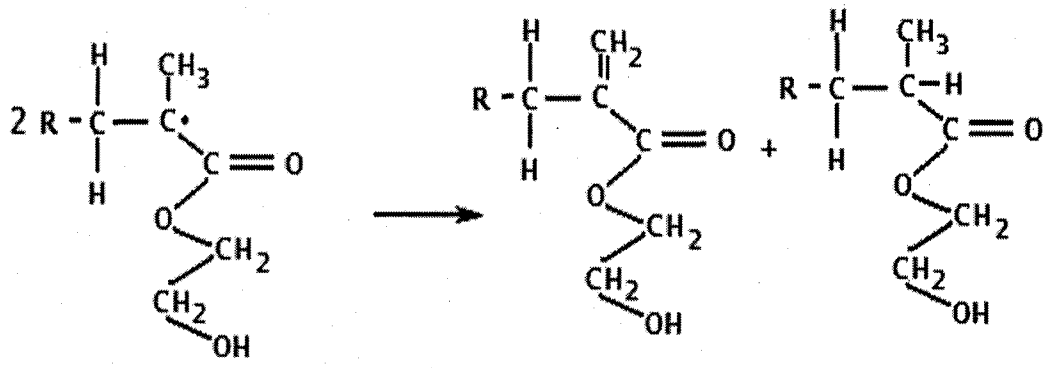

Figure 2.3 Termination stage of the Free Radical Polymerization of Poly (HEMA) with AIBN as the initiator, a) Combination b) Disproportionation

Reproduced with permission of the copyright owner. Further reproduction prohibited without permission.

2.3 Dispersion Polymerization

Dispersion polymerization is a modified precipitation polymerization that is used to produce latex particles with diameters from 0.1 to 15μm. In this method all the components of the reaction are added simultaneously to the polymerization reaction flask. The flask is then heated to start the reaction. The heating is continued for a period of between 8-20 hours to achieve a high yield. Initially the mixture appears as a faint grayish-white color that indicates the particles nucleation stage in the process. On further heating the solution turns completely white as the polymer particles fall out of solution.

2.3.1 Typical Components for Dispersion Polymerization.

The essential components that are required to perform dispersion polymerization are monomer, initiator, steric stabilizer, and solvent/non-solvent. Some researchers have applied co-stabilizers, which consist of low molecular mass cationic or anionic surfactants.[58,102] These surfactants have been said to be necessary for the formation of monodisperse microspheres in some systems.[102]

2.3.2 Monomers

Many different monomers have been used in dispersion polymerization. The monomer must have high solubility in the reaction mixture while the polymer it forms must be insoluble. There are many solvent and monomer systems that meet the above requirements. There are a few monomers like methyl methacrylate and

Reproduced with permission of the copyright owner. Further reproduction prohibited without permission.

styrene, which have been subjected to exhaustive research. In this research, we investigate the dispersion polymerization of poly (hydroxyethylmethacrylate) (polyHEMA) and propylacrylamides co-polymerized with acrylic acid or methacrylic acid.

2.3.3.Stabilizers

Stabilizers play an important role in the polymerization process because they prevent the polymer from coagulating or sticking together. The use of stabilizers becomes vital in dispersion polymerization because the solvents used are of low dielectric stabilization, therefore they do not have the benefit of electrostatic stabilization. Stabilizers are generally amphipathic; one section has an affinity for the final polymer particle surface, and the other is soluble in the solvent. There are three types of amphipathic stabilizers 1) block and graft copolymers 2) macromonomers 3) homopolymers

The first type is especially effective as stabilizers because they already have the two chemically distinct segments, while the second type is able to co-polymerize with the principal monomer to yield graft co-polymers. Homopolymers are potentially good stabilizers because in the course of reaction, a graft is formed though chain transfer from the growing oligomer to the originally present homopolymer stabilizer. This results in a graft copolymer.

2.3.4. Initiators

A vital requirement of initiators is that they should be soluble in the dispersion medium. The type of initiator used can have a significant influence on

Reproduced with permission of the copyright owner. Further reproduction prohibited without permission.

the nature of the final polymer obtained. In this study two types of initiators were used; benzyl peroxide and 2,2 -azobisisobutyronitrile, which are also the most commonly used initiators for dispersion polymerization.

2.3.5 Dispersion Medium

It is essential for the solvent to fulfill the requirement of dissolving the monomer but not the forming polymer. It must also dissolve all the other reactants used in the formulation (initiator, stabilizer and the monomer). Polar and non-polar solvents may be applied in dispersion polymerization. In the past, petroleum distillates and aliphatic hydrocarbons were used as solvents, but recently polar solvents such as ethanol and methanol[58] have been used increasingly. In the present study, toluene was used in the synthesis of polyHEMA while acetonitrile was used to prepare polyNNPAM.

2.4 Particle Growth in Dispersion Polymerization

Figure 2.4 illustrates the main stages of particle growth during dispersion polymerization. At the beginning all the components are in homogeneous solution (Figure 2.4 A). The commencement of polymerization is marked by the appearance of oligomers, which grow until they reach a critical chain length, at which point there is a phase separation. This phase separation results in the formation of particle nuclei, which have colloidal instability. The nucleation process takes place over a short period of time (Figure 2.4 B). Homocoagulation of the monomers or self-nucleation, results in the formation of even larger unstable species.

Reproduced with permission of the copyright owner. Further reproduction prohibited without permission.

At the same time nuclei may also coalesce with oligomers and adsorb onto the steric stabilizer. The growth of nuclei continues to propagate giving rise to mature particles when optimum stabilizer has been adsorbed onto the stabilizer (Figure 2.4 C &D). Paine[59] suggests that for small particles, growth proceeds via capture of oligomers with termination in the particle; for large particles, initiation and growth both occur in the solvent phase leading to particle growth by the accretion of dead polymer. Figure 2.4 E shows the particles that have grown to their final sizes. They remain suspended in the stabilizer to prevent coagulation.

Reproduced with permission of the copyright owner. Further reproduction prohibited without permission.

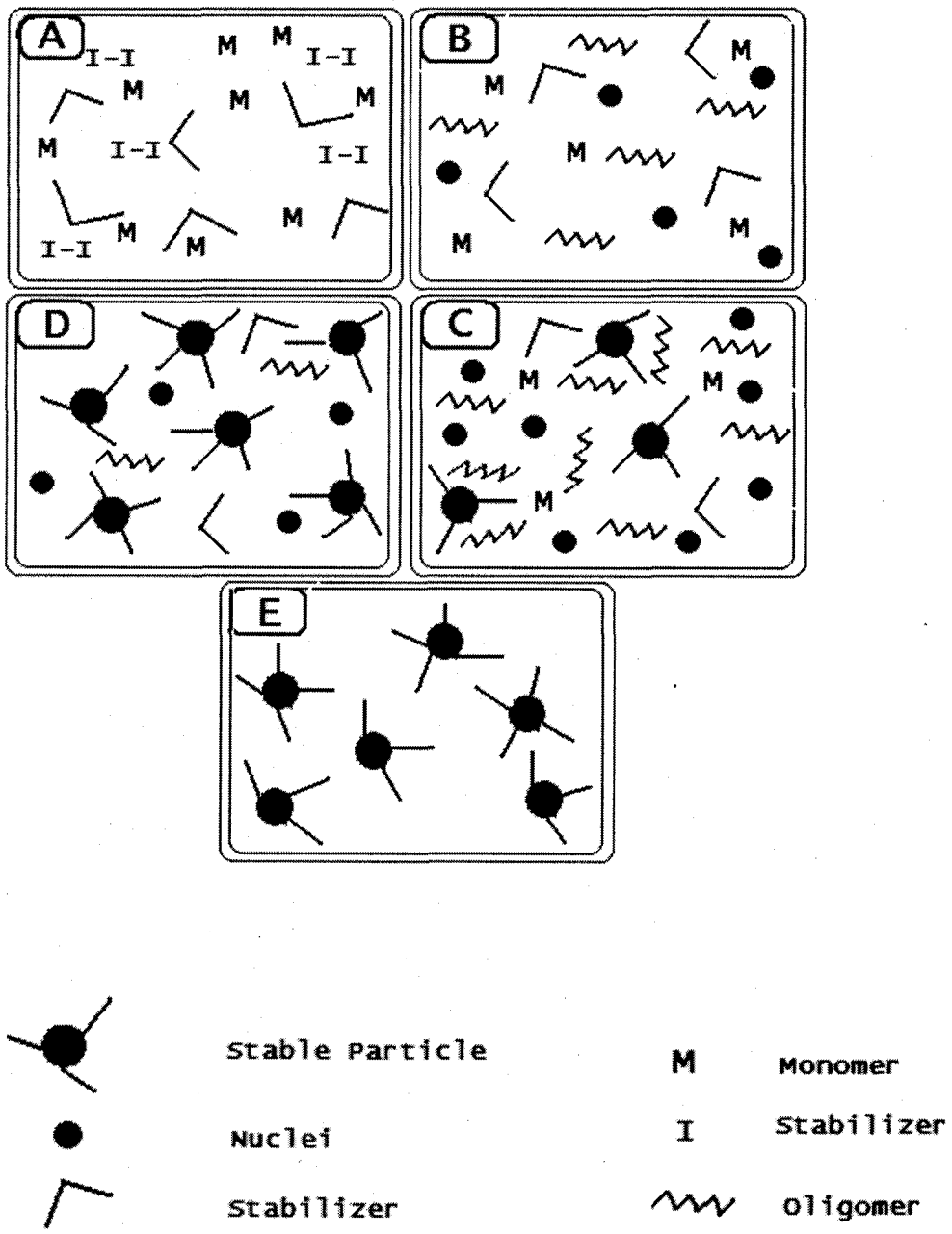

Figure 2.4 Schematic of particle growth by dispersion polymerization

Reproduced with permission of the copyright owner. Further reproduction prohibited without permission.

2.5 Theory of Polymer Swelling

A crosslinked polymer does not dissolve in a compatible solvent, but instead absorbs the solvent and swells until it attains equilibrium. At this point the swelling forces caused by the solvation are counterbalanced by the retractive forces due to the stretching of the bonds in the polymer. The extent to which a polymer swells is therefore determined by the solvent affinity for the polymer. For charged polymers, there is an extra swelling force, which is caused by electrostatic repulsion between neighboring charges on the polymer. The strength of this force is determined by the charge density in the polymer compared to the charge density in the external solution as well as other parameters like ionic strength and dielectric constant of absorbed solvent.

We are developing chemical sensors based on the principle of polymer swelling. The main focus of our research has been to utilize polymer swelling to cause a change in optical properties. The original design of our sensors was based on a swelling polymer bead that was coupled to a moving diaphragm that changed the amount of light on an optical fiber.

Rooney[98] extensively investigated swellable polymers for reflectance-based chemical sensing. In this study, he investigated two different approaches to chemical sensing. The first one involved the use of bulk membranes that were pH sensitive, while the second one made use of pH sensitive polymer microspheres that were suspended in non-swellable and pH insensitive hydrogels. There are many

Reproduced with permission of the copyright owner. Further reproduction prohibited without permission.

advantages to the second design. Because the amount of pH sensitive material per membrane is low, it significantly reduces the response time for the membrane. The hydrogel membrane can easily be attached to fiber optic material for more effective sensing.

2.5.1 Non-ionic Swelling

Non-ionic swelling takes place when a polymer is placed in a suitable solvent. Uncrosslinked polymers dissolve when immersed in a suitable solvent system. However, with light crosslinking the polymer will not dissolve, but will absorb a portion of the solvent and subsequently swell. The extent of swelling represents a competition between two forces. The free energy will cause the solvent to penetrate and try to dilute the polymer solution. This entropic increase will be enhanced by increasing the temperature. As the polymer chains in the crosslinked polymer network begin to elongate under the swelling action of the solvent, they generate an elastic retractive force in opposition to this deformation. These opposite forces will balance each other at equilibrium.

Reproduced with permission of the copyright owner. Further reproduction prohibited without permission.

The following equation which was derived by Flory[60], describes the non-ionic swelling process:

$$q_m^{5/3} \cong \frac{(\bar{v}M_c)\left(1-\frac{2M_c}{M}\right)\left(\frac{1}{2}-X_1\right)}{V_1} \qquad (1)$$

Where:

q_m = equilibrium swelling ratio

$\bar{v}$ = Specific volume of the polymer

M_c = molecular weight per crosslinked unit

M = molecular weight of polymer network

X_1 = polymer-solvent interaction parameter

V_1 = molar volume of the solvent

q_m, the equilibrium swelling ratio is the volume of the swollen polymer (V) divided by the unswollen volume (V_o).The second term in the equation, expresses the correction for polymer network imperfections due to the polymer chain ends. This term reduces to unity for a perfect network. X_1 depicts the compatibility or affinity

Reproduced with permission of the copyright owner. Further reproduction prohibited without permission.

of the polymer for the solvent. Benzene and toluene, for example, are solvents used in the preparation of polystyrene. The polymer-solvent interaction parameters for the polystyrene with these solvents are 0.37- 0.4 and 0.39-0.4 respectively at 25 °C. Typical values for other polymer-solvent pairs are available in the polymer handbook.[103]

From the equation we see that the swelling ratio depends on 1) the degree of crosslinking and 2) the affinity of the polymer to the solvent. In a good solvent, the swelling ratio decreases with increased degree of crosslinking and with an increase in the molecular weight of the polymer. Also increasing the polymer affinity of the solvent will increase the swelling ratio. In the equation, the second term is a correction for polymer network imperfection due the chain extremities.

2.5.2 Ionic Swelling

Ionic polymer swelling is caused by the accumulation of charge in the polymer. These charges cause electrostatic repulsion on the polymer backbone causing it to swell. Therefore expansion due to the swelling minimizes the repulsive effect of the charges, as they are located further away from one another. This forms the basis of the sensing work done in this dissertation.

For pH sensing, the electrostatic repulsive charges were concentrated in the polymer by incorporating, amines, trimethylethylenediamine (TMEN) and NNN'-diethylenetriamine, onto polyvinylbenzylchloride (PolyVBC) and polyhydroxyethylmethacrylate (PolyHEMA) polymers, respectively. In both cases when the polymer is immersed in acid the amino groups become protonated.

Reproduced with permission of the copyright owner. Further reproduction prohibited without permission.

Flory[60] described the ionic swelling process of polymers in equation 2:

$$q_m^{5/3} \cong \frac{\left(\frac{i}{2V_u\sqrt{S}}\right)^2 + \frac{\left(\frac{1}{2} - X_1\right)}{V_1}}{\frac{v_e}{V_o}} \qquad (2)$$

Where:

q_m = equilibrium swelling ratio

i = number of electronic charges per unit polymer unit

V_u= molecular volume of polymer repeating unit

S = molar ionic strength of free solvent

X_1 = polymer-solvent interaction parameter

V_1 = molar volume of the solvent

v_e = effective number of chains in the network

V_o = unswollen network volume

Reproduced with permission of the copyright owner. Further reproduction prohibited without permission.

From the first term of the equation, we can see that an increase in ionic charge on the linkages causes the equilibrium-swelling ratio to increase. The polymer-solvent interaction has the same effect as for the non-ionic polymer swelling. Low ionic strength causes an increase in the equilibrium-swelling ratio because of the absence of shielding of charges by the solvent ions, which are present in high ionic strength solvents. Figure 2.5 shows the ionic polymer swelling and shrinking process.

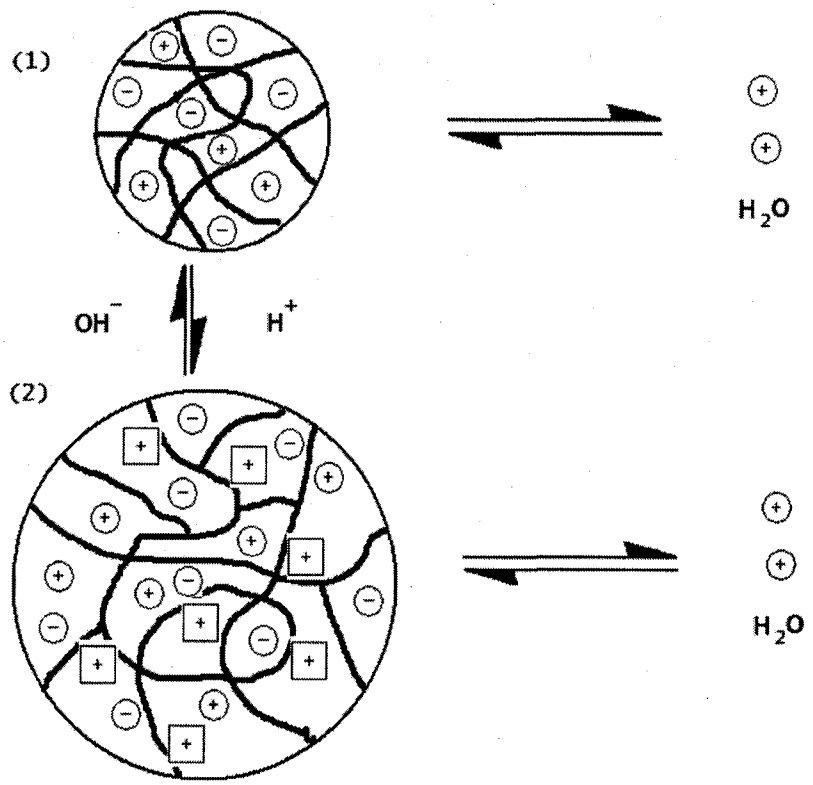

Figure 2.5 Schematic illustration of ionic polymer swelling.(1) Shows the unswollen polymer, (2) the swollen polymer. The circles represent mobile charge in solution; squares represent fixed charges on the polymer skeleton.

Reproduced with permission of the copyright owner. Further reproduction prohibited without permission.

2.6 Free Radical Polymerization Techniques

Free radical polymerization may be classified into homogeneous and heterogeneous systems. Suspension polymerization is an example of homogeneous polymerization. In this type of polymerization, the initiator is soluble in the monomer phase, which is dispersed by comminuting into the dispersion medium (usually water) to form droplets.

The solubility of the dispersed monomer (droplet) phase and also the resultant polymer in the dispersion medium are usually low. Polymerization proceeds in the droplet phase by a free radical mechanism. Suspension polymerization usually requires the addition of a small amount of stabilizer to hinder coalescence. In conventional suspension polymerization, which is widely adopted as a production process for commercially available polymeric microspheres, the problem of low yield and high cost is unavoidable. Suspension polymerization is usually carried out in a three-neck reactor flask that has a rough inner surface and is stirred vigorously with a magnetic stirrer[103]

In heterogeneous polymerization the initiator, monomer and polymer are not soluble in the same phase and the polymer forms a distinctly different phase. Heterogeneous polymerization includes dispersion, emulsion and suspension polymerization techniques.

Dispersion polymerization starts off as a homogeneous system where the monomer, initiator, stabilizer and crosslinker are all dissolved in an organic solvent forming a homogeneous solution, but as the process continues it becomes a heterogeneous system. This is because the polymer particles are insoluble in the

Reproduced with permission of the copyright owner. Further reproduction prohibited without permission.

organic medium and separate into a colloidal dispersion by precipitation. The particle size obtained in this method is between 1-5 μm.[97]

High speeds stirring and the high frictional force created against the rough surface serve to break down the dispersed monomer into small droplets. The speed of stirring causes a variation in molecular weight distribution[60] and it is difficult to narrow down the size distribution of the resulting microspheres when using conventional polymerization. To prepare emulsion droplets with a narrow range size distribution it is necessary to apply a large mechanical force into the reactor system.[61]

Emulsion polymerization is different from suspension polymerization in that the water immiscible monomer is emulsified in an aqueous continuous medium using an oil-in-water emulsifier. The initiator used in this process is water-soluble. The dimensions of the monomer droplets are between 0.05-5 μm. The polymer particles are smaller than 5μm.

2.7 Shirazu Porous Glass Method

In this research we applied a newly developed emulsification technique known as the Shirazu Porous Glass (SPG) Membrane Emulsification.[61] Figure 2.6 shows the main components of the SPG emulsification apparatus. These include a dispersion phase module, which is connected to a nitrogen gas tank, and a pressure tight steel membrane module, inside which is the porous membrane. The membrane module is connected to a pump, which circulates the emulsion from the emulsion tank

Reproduced with permission of the copyright owner. Further reproduction prohibited without permission.

A mixture of the monomer, solvent and initiator are mixed in the dispersion phase storage tank and on the application of pressure it permeates though the pores of the glass membrane and into the circulating flow of the aqueous phase components (aqueous solution of surfactants and stabilizers) as shown in Figure 2.7. The resulting suspension accumulates the droplets over time in the emulsion tank.

Reproduced with permission of the copyright owner. Further reproduction prohibited without permission.

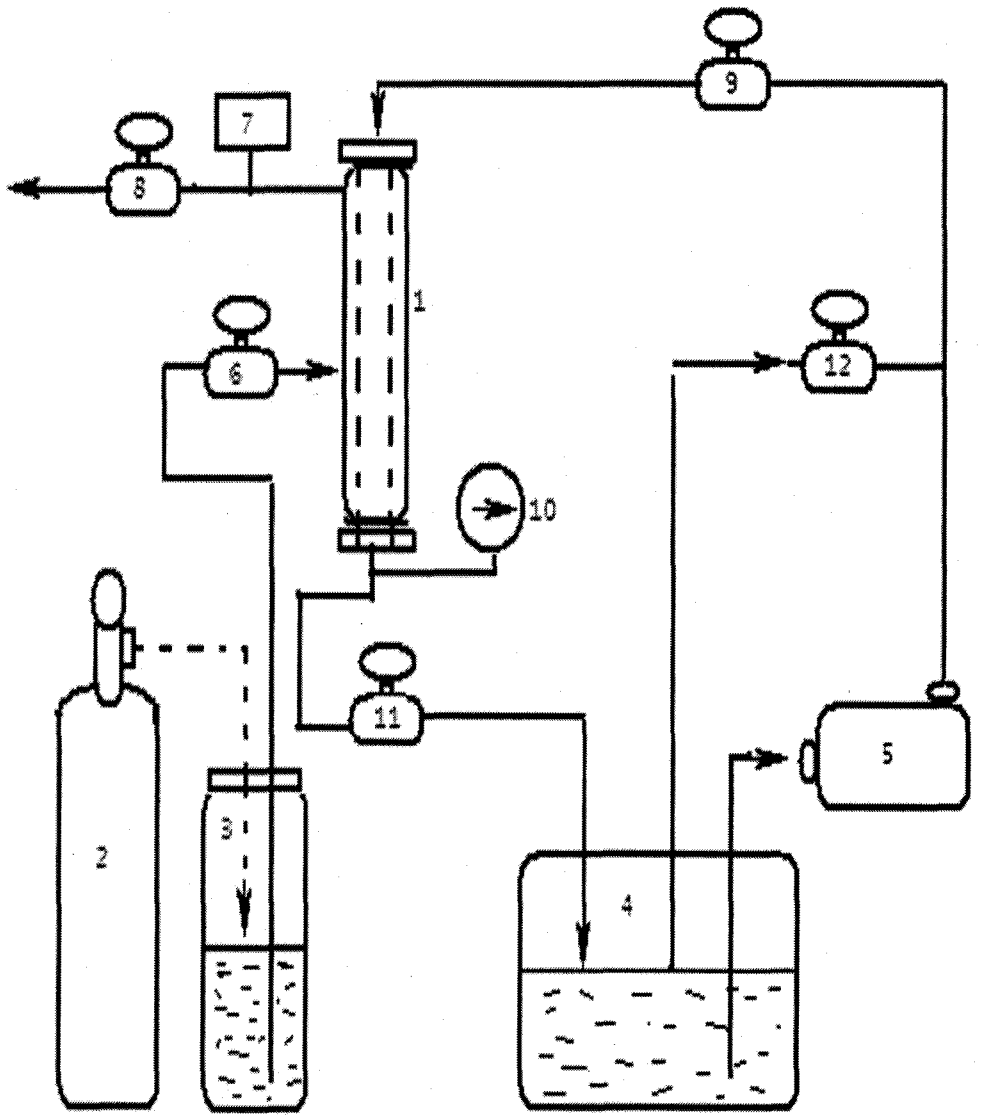

1 membrane module	5 circulation pump	9 needle valve
2 nitrogen gas tank	6 needle valve	10 pressure gauge
3 dispersion phase storage tank	7 pressure gauge	11 needle valve
4 emulsion tank	8 valve	12 needle valve

Figure 2.6 Schematic diagram of the Shirazu porous glass (SPG) membrane emulsification apparatus

Reproduced with permission of the copyright owner. Further reproduction prohibited without permission.

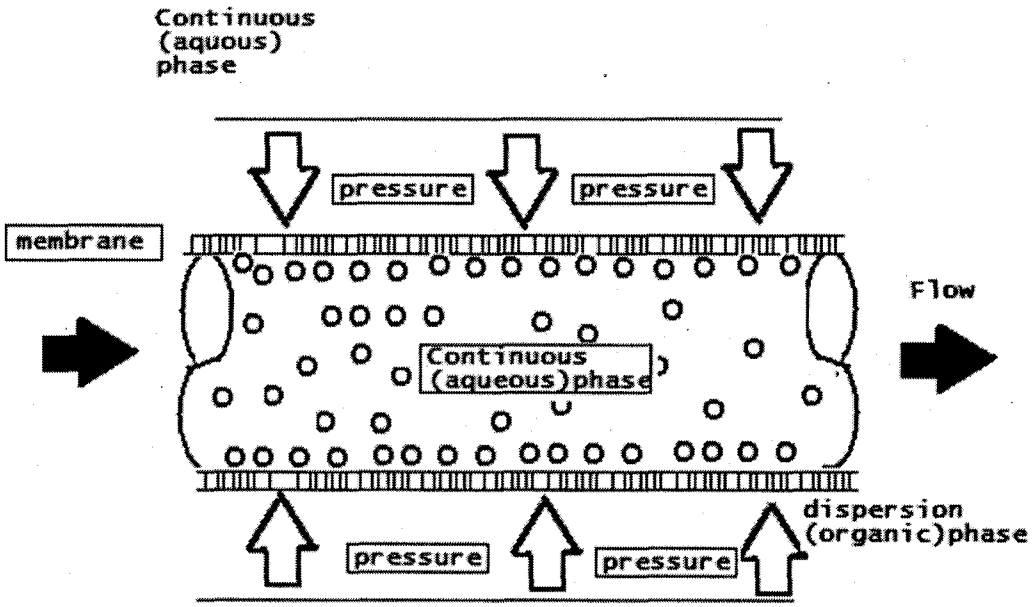

Figure 2.7 Scheme of an emulsification module.

The membrane emulsification method uses the surface chemistry of a microporous membrane for the dispersion of one of two immiscible liquids. This dispersion is achieved by the application of pressure, which forces the dispersion phase to permeate through the membrane. This method makes it possible not only to continuously produce oil in water (O in W) or (W in O) emulsion but is also capable of producing O in W in O or W in O in W type double emulsions.

For successful utilization of membrane emulsification, there are three vital factors must first be addressed:

- The microporous membrane must provide uniform pore size distribution as well as reasonable mechanical strength. This is because the membrane must

Reproduced with permission of the copyright owner. Further reproduction prohibited without permission.

withstand high pressures of up to 2000 kPa or even more. Also there should be a variety of available pore sizes and the pore size should be uniform as far as possible in the membrane being used.

- The membrane must be wetted with the continuous phase prior to contact with the dispersion phase. Membrane wetting with the dispersion phase must be avoided.

  The surface chemical properties of the membrane such as the dispersion phase wettability are critically important, therefore when an O in W emulsion is prepared, the membrane needs to be hydrophilic to prevent its wetting with the oil phase. On the other hand, to prepare a W in O, it necessarily should be hydrophobic to prevent the water phase from wetting it.

- To stabilize the emulsion, a surfactant must be added to both the dispersion phase and the continuous phase or to the latter. Although this is important, generally the amount of surfactant that needs to be added is remarkably small compared to when an emulsion is made using a conventional homogenizer.

The best microporous membrane that meets the first two requirements, is a microporous glass membrane, which is made from CaO-Al_2O_3-B_2O_3-SiO_3.This membrane is made by washing out CaO-B_2O_3 with acid, thus the remaining Al_2O_3-SiO_3 forms uniform pores. The membrane posses a unique porous structure with the cylindrical interconnected micropores with a high degree of uniformity when compared to other known microporous membranes. Figure 2.8 shows the droplet

Reproduced with permission of the copyright owner. Further reproduction prohibited without permission.

emulsification process and how the applied pressure determines the droplets formed.

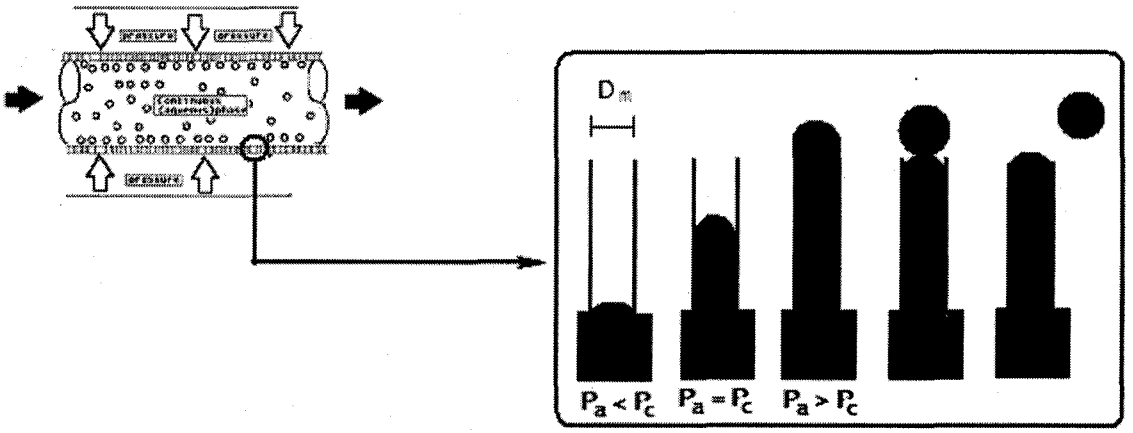

Figure 2.8 Schematic showing droplet formation as pressure is applied.

2.8 Phase Transition Temperatures of Acrylamide Polymers

Some N-alkylamide polymers undergo a phase transition in aqueous solution above a lower critical solution temperature (LCST). For such polymers, the microenvironmental polarities near the main chains change considerably with the phase transition[62]. Since its discovery, this phase transition has been well studied by various methods including calorimetry and with fluorescent additives. These studies support the viewpoint that the phase transition is due to the collapse of an open coil to a more globular stucture.[62] Furthermore, the microenvironmental polarities near the main chains of the polymer that undergo the temperature induced phase transition at around the human internal temperature has been of interest in the

Reproduced with permission of the copyright owner. Further reproduction prohibited without permission.

pharmaceutical industry, since the polymers are potential carriers of drugs.[63] Poly N-Isopropylacrylamide (PolyNIPA) shows a temperature –induced phase transition in aqueous solution, with a LCST value of ~32°C.[64] One way in which the transition temperature can be controlled, is by co-polymerizing the NIPA with co-monomers that have varying hydrophobicity. [65]

This method has been used extensively[67] in the past decade to control the thermally induced volume phase transition of many N-alkylacrylamide gels. Many researchers[66-71] have investigated and characterized many co-polymer gels such as N-acryloxysuccinimide-co-acrylamide, N,N-diethylacrylamide-co-NIPA , N,N-dimethylacrylamide-co-acrylate, NIPA-co-N-*tert*-butylacrylamide, NIPA-co-N-cyclopropylacrylamide and Poly (N-n-propylacrylamide)-co-NIPA. Properties that are intrinsic to polymers have already brought some special features to the field of molecular sensing. For example Whitten's team[72] constructed fluorescent sensors for biological targets.

2.9 Background of Molecular Imprinted Polymers

The idea of molecular specificity that could be tailored in sorbents has been around for a long time.[73] In 1931, Polyakov[74] demonstrated that molecular specificity could be imprinted on silica gel by pretreating silicic acid with organic adsorbates before polycondensation. Later Dickey[29] performed more extensive investigations. He precipitated silicic acid in the presence of alkyl orange dyes and found that after drying the hydrogel and removing as much of the imprinting agent as possible, the resulting xyrogel has a greatly increased adsorption capacity for the particular dye

Reproduced with permission of the copyright owner. Further reproduction prohibited without permission.

present during gelation. Modern molecular imprinting has its roots in Europe with the extensive investigations of Wulff and co-workers[75] and Ramstrom and colleagues.[76]

2.9.1 The Process of Molecular Imprinting

The principle of molecular imprinting is illustrated in Figure 2.9. It involves the following three steps.[77]

I. Complex formation of a specific target molecule (the template molecule) with polymerizable monomers bearing functional group(s) capable of interacting with the target molecule (functional monomers) by covalent and/or noncovalent bonding. In this stage pre-organization of the binding sites is achieved by assembling the functional monomers around the template.

II. Polymerization in order to maintain the alignment of the functional group(s), which are optimally set for binding the template molecule.

III. Removal of the template from the resulting polymer matrices, allowing 'tailor-made' binding sites for the template molecule to be generated.

Reproduced with permission of the copyright owner. Further reproduction prohibited without permission.

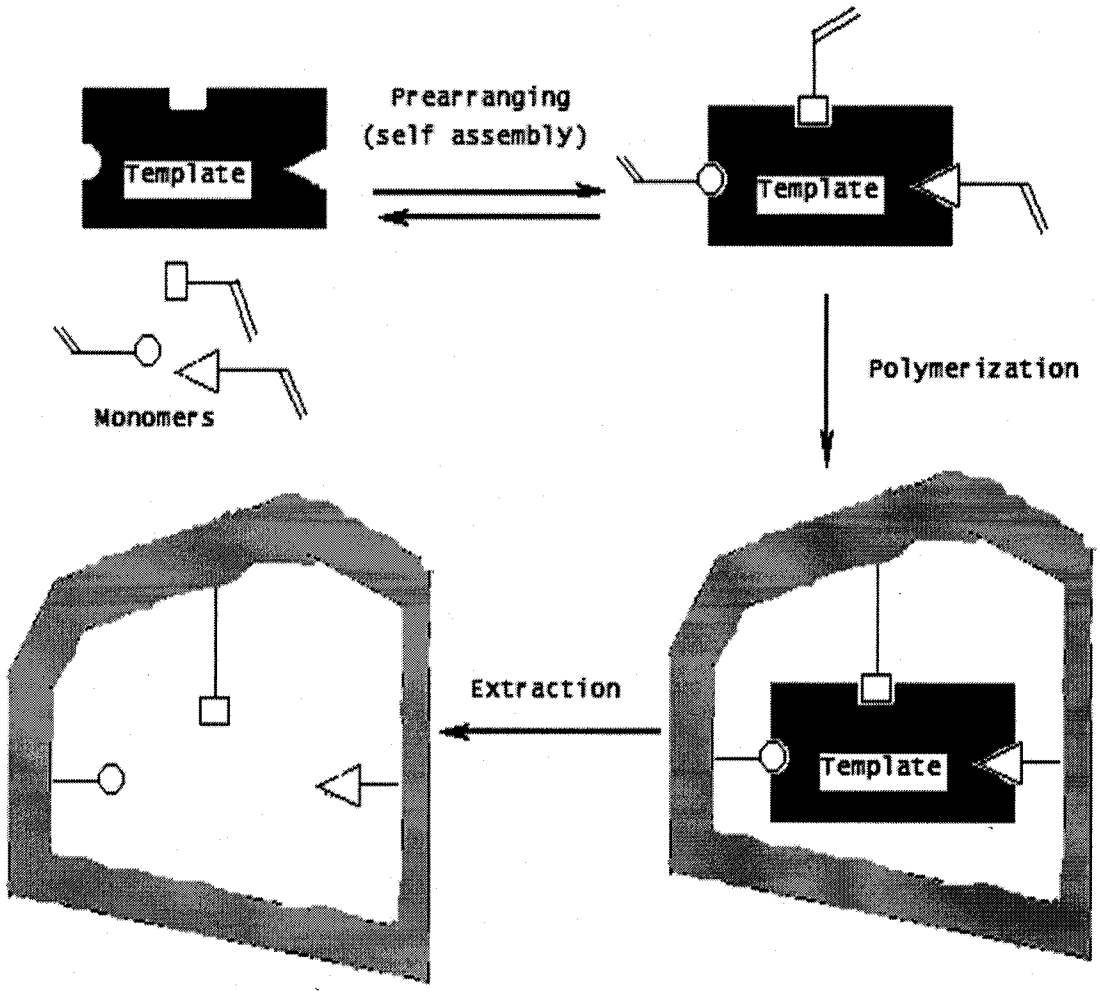

Figure 2.9 Schematic of the molecular imprinting principle, in which the template is the structural analogue of the target analyte.

Molecular imprinting may be classified in two ways depending on the type of bonds formed between the template and the target molecules. These are the covalent and noncovalent imprinting.

Reproduced with permission of the copyright owner. Further reproduction prohibited without permission.

2.9.2 Covalent Imprinting

This type of imprinting involves the formation of reversible covalent bonds between the template and the target molecule. The covalent bonds formed may involve ester linkages, acetal/ketal, metal coordination, etc. While this type of imprinting leads to strong bonds, which result in stable imprinted polymers, the technique has a number of drawbacks. These include the inability of covalent bonds to break and rebind easily and they have relatively slow binding kinetics, which may not be suitable for use in chromatographic systems.

2.9.3 Noncovalent Imprinting

Noncovalent imprinting relies on the self-assembly of functional monomers and a template in solution, freezing the resultant assemblies by crosslinking polymerization, and the subsequent removal of the template by extraction. Methacrylic acid is the most commonly used functional monomer to date. The self-assembly of the functional monomer and the template takes place by ion pairing, hydrogen bonding, or a combination of these interactions between the carboxylic acid groups of the methacrylic acid and the interaction sites on the template.[78]

The driving force for rebinding of the template to the sites is strongly medium dependent. The electrostatic contribution predominates in low polarity, weakly hydrogen-bonding solvents,[79] whereas a selective hydrophobic contribution to the binding can be seen with increasing aqueous content of the medium.

Easy preparation and quick binding kinetics have led to the use of non-covalent molecularly imprinted polymers in many applications and have caused the

Reproduced with permission of the copyright owner. Further reproduction prohibited without permission.

method to be extremely popular. It is applied in areas such as chiral separation of pharmaceutical compounds,[80] the preparation of samples using solid phase extraction,[73] drug determination by the use of competitive ligand binding assay[81,82] and as a recognition element in the construction of biomimetic sensors.[31] In this research we have focused on noncovalent methods of imprinting, therefore there will be no further reference to the covalent imprinting methods.

2.10 Optical Measurement of Particles Suspended in a Hydrogel Membrane

The Fresnel equation[33] shows for normal incidence, the relation between the amount of light reflected from materials with different refractive indices:

$$R(\lambda) = \left(\frac{(n_2 - n_1)}{(n_1 + n_2)} \right)^2$$

Where:

R = reflectance

n_1 = refractive index of medium 1

n_2= refractive index of medium 2

From this equation we see that as the difference in the refractive indices of the two media increases, so does the reflectance. This results in a change in reflectance when microspheres suspended in a hydrogel change refractive index.

Reproduced with permission of the copyright owner. Further reproduction prohibited without permission.

CHAPTER 3

EXPERIMENTAL

3.1 Reagents

Aldrich Chemical Company Inc., Milwaukee, WI 53233

Acetonitrile, anhydrous 99.8 %, F.W. 41.05, b.p. 81-82 °C

Acrylic acid (AAc), 99%, F.W. 70.06, b.p. 139 °C

Acryloyl chloride, F.W. 90.51, b.p. 72-76 °C 96%

6-Amino-1-hexanol, 97%, F.W.117.19, b.p. 135-140 °C

Ammonium hydroxide 28%

2,2 -Azobisisobutyronitrile (AIBN), 98%, F.W 164.21, m.p. 103-105 °C

Benzoyl peroxide (BPO) F.W 242.23

Caffeine, 99%, F.W. 194.19, m.p. 234-236 °C

1,1-Carbodiimidazole F.W 162.19 m.p 116 °C

7-Chloro-4-nitro-2, 1,3-benzoxadiazole (NBD-Cl),98% F.W. 199.55, m.p.97-99

Copper sulfate ACS reagent 98%

Dichloromethane, 99.8%, F.W. 84.93

Diethylenetraimine, 99.0%, F.W. 103.17, b.p. 199.209 °C

1,4-Dioxane, anhydrous, 99.8%, F.W. 88.11, b.p. 100-102 °C

Divinyl benzene (DVB), 97% mixture of isomers, F.W 130.19, b.p.195 °C

Reproduced with permission of the copyright owner. Further reproduction prohibited without permission.

Dodecane, 99%, F.W.170.34, b.p. 215-217 °C

Ethanol

Ethyl acetate 99.5% F.W. 88.11 b.p. 76.5-77.5 °C

Ethylene glycol dimethacrylate (EGDMA), 98%, F.W 198.22, b.p.98-100 °C/5 mm

Hexanes, 98.5% b.p.68-70 °C

2-Hydroxyethylmethacrylate (HEMA), 97%, F.W. 130.14, b.p. 67 °C/3.5 mm

Poly(vinyl alcohol), 87-89% hydrolyzed, Av. Mw: 85,000-146,000

Poly(vinyl alcohol), 98% hydrolyzed, Av. Mw: 11,000-31,000

Poly(vinyl alcohol), 100% hydrolyzed, Av. Mw: 14,000

Propylamine F.W. 59.11 b.p. 48 °C

Magnesium sulfate, F.W 120.37

Methacrylic acid (MAA), 99%, F.W. 86.09, b.p. 163 °C

Methanol

Methyl sulfoxide (DMSO), 99.9%, F.W. 78.13, b.p. 189 °C

N-Isopropylacrylamide (NIPA), 97%, F.W. 113.16, m.p. 60-63 °C, b.p.89-92 °C

Silica gel, grade 12 28-200 mesh

Sodium acetate, 99% F.W.82.03

Sodium hydroxide 97% F.W. 40.00

Sodium chloride, 99 % F.W. 58.44

Sodium phosphate: NaH_2PO_4, Na_2HPO_4

N-tert-butylacrylamide (NTBA), 97% F.W. 127.19, m.p. 128-129 °C

Theophylline (THO), anhydrous, 99% F.W. 180.2, m.p 274-275 °C

Xylenes, 98.51% F.W.106.17, b.p. 136-140 °C

Reproduced with permission of the copyright owner. Further reproduction prohibited without permission.

Bio-Rad Laboratories, 32nd & Griffin Ave., Richmond, CA 94894

N, N'-Methylene-bis-acrylamide (MBA)

Fisher Scientific Company., Fair Lawn, NJ 08540

Acetone, F.W 58.08, b.p 56.01 °C

Glutaraldehyde, 50% aqueous solution

Sodium bicarbonate, F.W. 84.01

HYMEDIX International., Inc. Dayton, NJ 08540

HYPAN HN 50, HN 68 and HN 80 Structural Hydrogels

Shell Chemical Co., P.O Box 325, Belpere, OH 45714

Kraton G 1650, LOT # 08RBL1526

Pharmco Products Inc., 58 Vale Road, Brookfield, CT, 06804

Methanol, 99.9 %

Diethylether, 99%

VWR Inc., West Chester, PA 19380

Acetic acid, 99.7%, F.W. 60.05

Reproduced with permission of the copyright owner. Further reproduction prohibited without permission.

Emd Chemicals Inc., Darmstadt, Germany

Hydrochloric acid, 36.5-37%, F.W. 36.46

All aqueous solutions were prepared with pure deionized, distilled water from a Corning Mega-Pure distillation equipment

Reproduced with permission of the copyright owner. Further reproduction prohibited without permission.

3.2 Apparatus

Preliminary observation of the microparticles was done with a Fisher Scientific microscope. They were then characterized for size and distribution with a Carl Zeiss KS200 microscope, which had a CCD camera for taking images. A Fisher laboratory centrifuge (3400 rpm) was used for separating and washing the microspheres. A Branson model 1210 sonicator was used for dispersing the microparticles and cleaning the porous glass membrane. A Bausch and Lomb refractometer was used to measure the refractive indices. An Orion 901 digital analyzer with a 91/55 pH electrode was used in the preparation of buffer solutions.

A VWR 1217 reciprocal shaker equipped with a temperature programmable water bath was used to derivatize and functionalize the microparticles. Scanning electron microscope (SEM) images were obtained and CHN analysis performed, using an Amray 3300 FE scanning electron microscope and a Perkin Elmer Model 2400 CHN Analyzer respectively. These instruments were operated by Nancy Cherim of the University of New Hampshire Instrumentation Center. A Spectr*AA*-220 Atomic absorption spectrometer was used to quantify copper ions removed from the microspheres.

The turbidities of the microspheres suspended in hydrogel membranes were monitored with a Cary 500 UV-Vis spectrophotometer. All fluorescence determinations were done with a Cary Eclipse spectrophotometer, which was integrated with a Thermomix 1414 heater and water bath for temperature regulation. The temperature was monitored with a Markson digital thermometer. A Nicolet Model Avatar 370 FT-IR spectrophotometer and a 400 MHz Varian NMR

Reproduced with permission of the copyright owner. Further reproduction prohibited without permission.

spectrometer were used for characterizing and identifying the monomers and polymers.

3.3 Procedures

3.3.1 Preparation of Poly vinylbenzylchloride (polyVBC) Microspheres by Suspension Polymerization

Initially we employed conventional suspension polymerization to synthesize the microspheres[1], but we found that we were getting polydispersed microspheres, which were not suitable for our application. Since we needed to prepare monodispersed microspheres, we opted to emulsify VBC and DVB in aqueous solution by the newly introduced SPG technique (Section 2.6).

In this study, the dispersion phase was made up of VBC, DVB, BPO and the porogenic solvents (xylene and dodecane). The complete formulation is shown in Table 3.1. The dispersion phase was transferred to the dispersion phase storage tank, which was then sealed. The continuous phase was made up of 1% wt/wt PVA in water, sodium dodecyl sulfate (SDS) and sodium sulfate (Na_2SO_4). The pressure applied to the sealed apparatus was 0.05 kgf/cm^2 above the critical pressure, which depends on the composition of the two phases. In the present experiment we applied a pressure of 1.85 kgf/cm^2 for a wetted porous membrane with pore sizes of the order of 0.5 μm.

The time taken for the complete emulsification of a 50 ml sample of the dispersion phase was 20-30 minutes. After the emulsification process, the emulsion

Reproduced with permission of the copyright owner. Further reproduction prohibited without permission.

was transferred to a three-necked flask, which we use as the reactor and the polymerization was carried out at 70° C.

Table 3.1 Formulation for the Suspension Polymerization of VBC

Monomer	Vinyl Benzyl Chloride (VBC)	66.7 vol % organic phase
Crosslinker	Divinyl Benzene (DVB)	2.0 mole % monomer
Initiator	Benzoyl Peroxide (BPO)	2.0 mole % monomer
Bulk Solvent	Distilled water	
Stabilizers	Poly (vinyl alcohol) (PVC)	1.0 % (w/w) solvent
	Sodium Sulfate	0.3 % (w/w) solvent
	Sodium Dodecylsulfate	0.7 % (w/w) solvent
Porogenic Solvent	Xylene	20.0 % (v/v) monomer
	Dodecane	13.3 % (v/v) monomer

Reproduced with permission of the copyright owner. Further reproduction prohibited without permission.

A mechanical stirrer, which was equipped with a semi-spherical paddle for efficient mixing, (Figure3.1) was inserted into the middle neck, while the other two were stoppered. We purged the reactor for 20 minutes to remove the dissolved oxygen, after which the reactor was immersed in a water bath in which the temperature had been set at 70 ± 2 °C , the polymerization commenced and was continued for 12 hours.

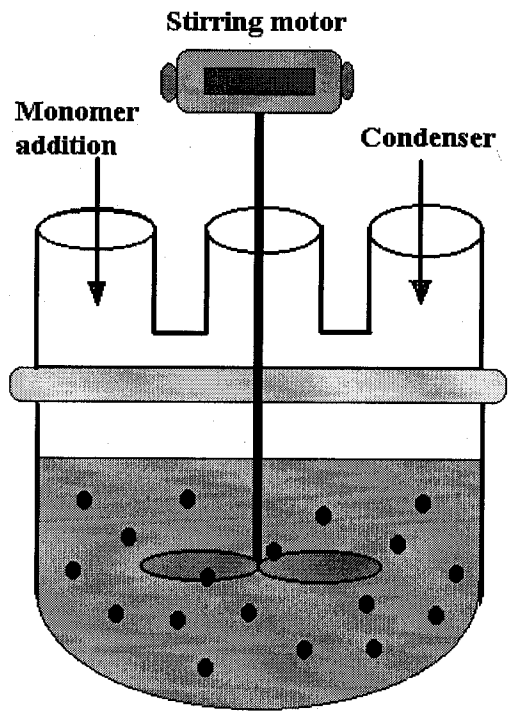

Figure 3.1 Three-neck reactor flask with overhead mechanical stirrer.

Reproduced with permission of the copyright owner. Further reproduction prohibited without permission.

3.3.2 Washing the Microspheres

It is necessary to remove the surfactants and other unreacted solutes before derivatizing the microparticles. SDS, one of the surfactants used in the polymerization process adheres onto the surface of particles imparting a negative charge, increasing colloidal stability. PVA on the other hand stabilizes the microspheres by sterically inhibiting their reactions with the derivatizing reagents.

In our research we chose to use Kraton G1650, an ethylene-butylene-styrene triblock copolymer, as the stabilizer. Its removal after the completion of the polymerization process is essential, because of its hydrophobic nature. In aqueous solution, it may form films on the surface of the beads and clog their surface, thus interfering with their ability to swell and shrink reproducibly.

Therefore we cleaned all the microspheres, by putting them in water, methanol and finally in water again. In between the mentioned steps, we repeatedly centrifuged, decanted and resuspended the microspheres. The microspheres were centrifuged in centrifuge tubes at 3400 rpm. Most of the larger particles (> 1.0 μm) settled to the bottom of the centrifuge tubes. Sub-micron particles however require higher spin rates to effectively settle them. The supernatant, in which the surfactants and other impurities were dissolved, was discarded, before resuspending the microspheres.

It was determined that as the cleaning progresses, it became more difficult to disperse the microspheres as they became more hydrophobic. Ultrasonic sonification was therefore applied to effectively resuspend the microspheres. It was

Reproduced with permission of the copyright owner. Further reproduction prohibited without permission.

found that with 4 to 5 washes, was sufficient to obtain clean and monodispersed microspheres.

3.3.3 Derivatization of Poly (VBC)

After washing the microspheres, they were pre-swollen in 1,4-dioxane for 2 hours. The significance of pre-swelling the microspheres is that in the expanded form, the derivatising agent, NNN- trimethylethylenediamine (TMEN) is able to access the core of the polymer microspheres much more easily. An excess of the TMEN was then added to commence the derivatization reaction as shown in Figure 4.3. The mixture was shaken in the reciprocating water bath for 4 days at 30 ^{o} C. The microspheres were then washed with 0.1 M HCl to remove excess unreacted amine and finally with water as outlined in section 3.3.2

3.3.4 CHN Analysis

It was necessary to perform CHN analysis because it enabled us to know the progress of the derivatization process. With CHN we quantified the extent to which the chloromethyl groups of the Poly (VBC) had been replaced by the amines. The washed beads were first air-dried and then vacuum dried, before being sent for analysis in sealed airtight vials.

Reproduced with permission of the copyright owner. Further reproduction prohibited without permission.

3.3.5 Preparation of Poly (HEMA) Microspheres by Dispersion Polymerization

Hydroxyethylmethacrylate (HEMA) monomer was mixed with AIBN (initiator), Kraton (stabilizer) and EGMA (crosslinker) and dissolved in toluene. A typical formulation is given in Table 3.2.

Table 3.2 Typical recipe for dispersion polymerization of HEMA

Ingredient	Quantity
Monomer - HEMA	5 or 10 g
Stabilizer - Kraton G1650	15 wt % of monomer
Initiator - AIBN	1 wt % of monomer
Crosslinker - EGDMA	2 mol % of monomer
Solvent - Toluene	95 mL

Reproduced with permission of the copyright owner. Further reproduction prohibited without permission.

The mixture was initially degassed and then purged with nitrogen for 20 minutes as is outlined in section 3.3.1. Since the solubility of kraton in toluene is low, we first dissolved it in about 40 ml of toluene, before mixing it with the other reagents and degassing the mixture. The reaction mixture was placed in a 500 mL reactor flask and immersed in a water bath, which was maintained at a temperature of 75 ^{o} C. The polymerization process took 12 hours after which the microspheres were washed as outlined in section 3.3 2

3.3.6 Preparation of N-n-Propylacrylamide Monomer [2]

A solution of propylamine (0.1 mol) was mixed in 300 mL of dichloromethane solvent in a three-neck 500 mL reactor flask (Figure 3.2). The flask was stoppered and immersed in a water bath, whose temperature was maintained at 40 ^{o} C. The solution was then purged with nitrogen to remove oxygen. Acryloyl chloride (0.11 mol) was carefully introduced through a needle and syringe. Introduction of the acryloyl chloride needed to be done slowly because it yielded a highly exothermic reaction with evolution of fumes of HCl.

The reaction mixture was stirred for 2 hours and the cooled to room temperature. It was washed three times each with 0.1 M HCl, brine and saturated solutions of $NaHCO_3$ / NaCl after which it was dried with $MgSO_4$. The solvent was removed in vacuum and the purity of the monomer was confirmed with TLC (using $CHCl_3/CH_3OH$ which showed a single spot). NMR and FT-IR further confirmed the assigned structure of the monomer.

Reproduced with permission of the copyright owner. Further reproduction prohibited without permission.

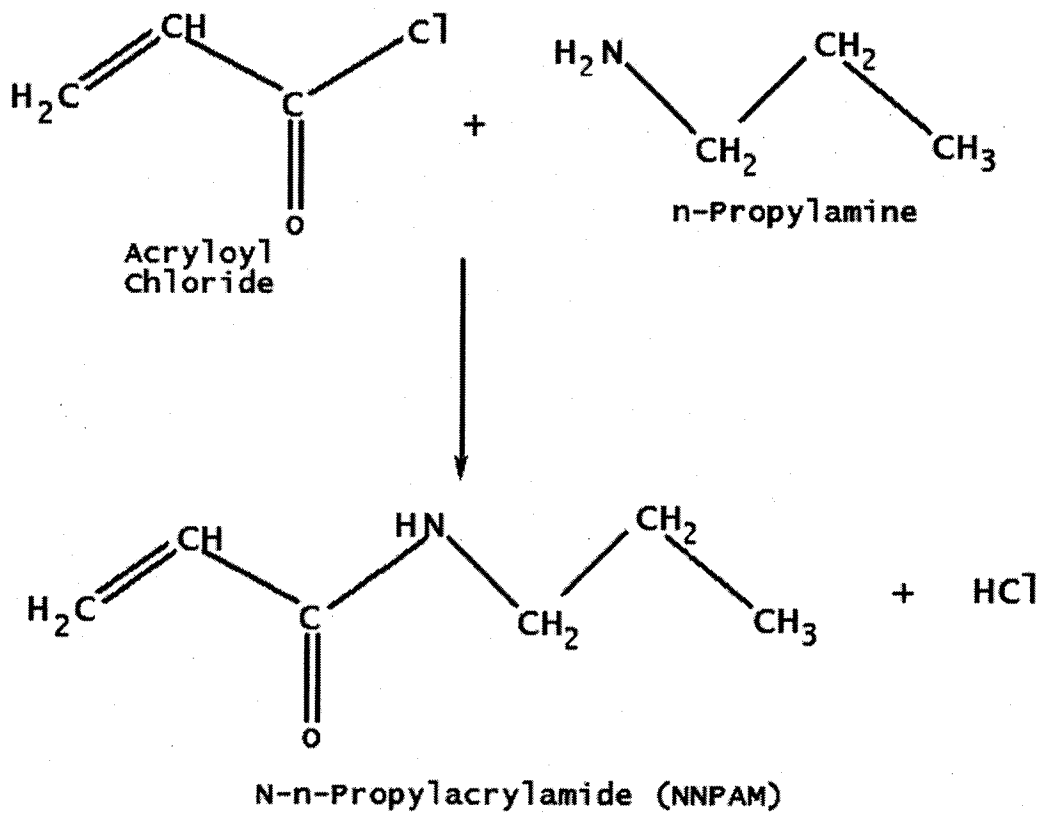

Figure 3.2 Synthesis of N-n-Propylacrylamide from Acryloyl Chloride and n-propylamine.

Reproduced with permission of the copyright owner. Further reproduction prohibited without permission.

3.4 Preparation of the Fluorescent Monomer

3.4.1 Preparation of 4-(6-Hydroxyamino)-7-nitro-2, 1,3-benzoxadiazole

A 100 mg (or 0.50 mmol) portion of 7-Chloro-4-2, 1,3-benzoxadiazole (NBD-Cl) was dissolved in 10 mL of acetonitrile solvent. After addition of 250 mg of 6-amino-1-hexanol, the mixture was stirred at room temperature for 30 minutes. After this the mixture was evaporated to dryness under reduced pressure, and the residue was chromatographed of silica gel using a 2:1 ethyl acetate- n-hexane mixture.

The product obtained was 4-(6-hydroxyhexylamino)-7-nitro-2, 1,3-benzoxadiazole, is shown in Figure 3.3, which appeared as an orange powder, the chemical structure of the product was confirmed with a melting point test, with NMR and FT-IR analysis.

3.4.2 Preparation of 4-(6-Acryloyloxyhexylamino)-7-nitro-2, 1,3-benzoxadiazole (NBD-AE2)

The formulation used for preparing the benzoxadiazole-based fluorophore is shown in Table 3.3. A 38mg (or 0.14 mmol) portion of the product formed above (4-(6-hydroxyamino)-7-nitro-2, 1,3-benzoxadiazole) was dissolved in 10 mL of acetonitrile solvent. 0.6 mL of acryloyl chloride was then added and the mixture was refluxed for 2 hours. This reaction mixture was then refluxed for 2 hours, after which it was evaporated to dryness under reduced pressure.

The residue was chromatographed on silica gel using a 1:2 mixture of ethyl acetate-n-hexane. The product NBD-AE2 (shown in Figure 3.4) appeared as a yellow powder, which was subjected to a melting point test, NMR and FT-IR

Reproduced with permission of the copyright owner. Further reproduction prohibited without permission.

analysis to further confirm its structure. Figure 3.4 shows the preparation of the fluorophore.

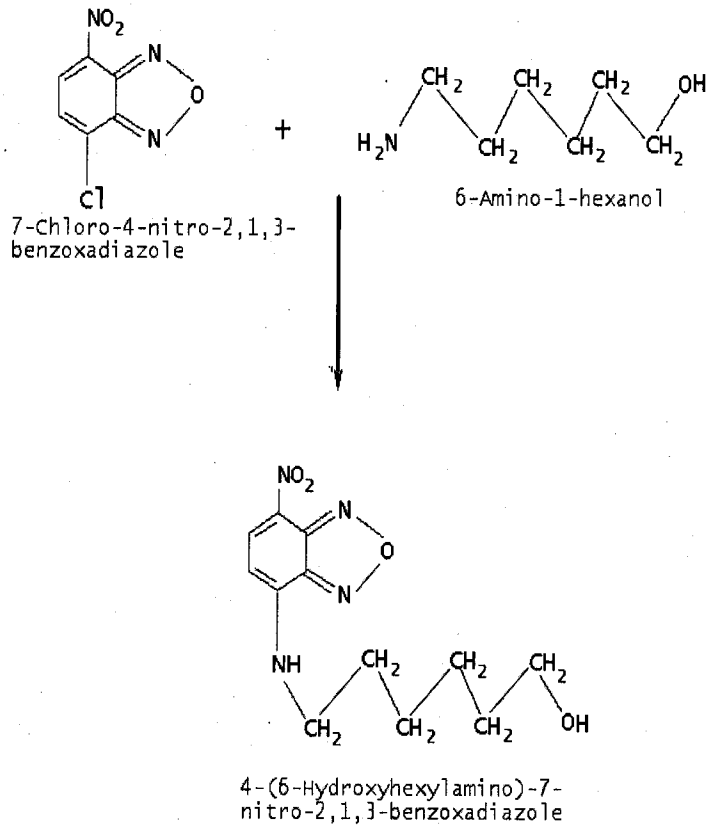

Figure 3.3 Synthesis of 4-(6-Hydroxyamino)-7-nitro-2, 1,3-benzoxadiazole

Reproduced with permission of the copyright owner. Further reproduction prohibited without permission.

Table 3.3 Typical Formulation for the Synthesis of NBD-AE2 Fluorophore.

Ingredient	Quantity
NBD-Cl	100 mg (0.5 mmol)
6-Amino-1-hexanol	250 mg
Acryloyl chloride	0.6 mL
Acetonitrile	20 mL

Reproduced with permission of the copyright owner. Further reproduction prohibited without permission.

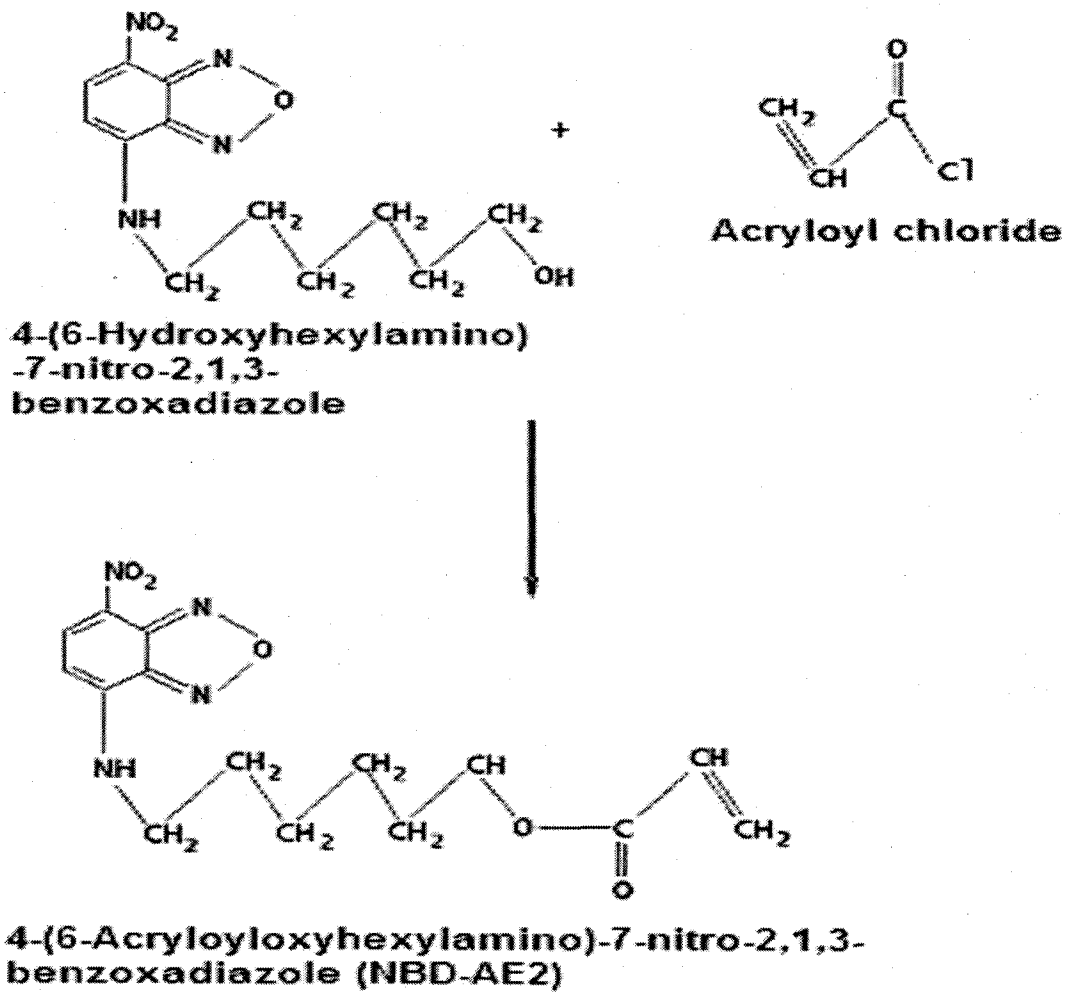

Figure 3.4 Synthesis of 4-(6-acryloyloxyhexylamino)-7-nitro-2, 1,3-benzoxadiazole (NBD-AE2) fluorophore.

Reproduced with permission of the copyright owner. Further reproduction prohibited without permission.

3.5 Preparation of PolyNNPAM-co-AAc-co-NBD-AE2 by Dispersion Polymerization

In this study we prepared uncrosslinked polymer in the presence or absence of the template. Figure 3.5 shows the reactions leading to the synthesis of the untemplated co-polymer. In this case we included the monomer (NNPAM), functional monomer (MAA or AAc), initiator (AIBN), fluorophore (NBD-AE2). These reactants were dissolved in 35 mL of acetonitrile, in a three neck reactor flask .The mixture was degassed in an ultrasonic sonicator for 10 minutes and purged for a further 15 minutes. The flask was stoppered and sealed under nitrogen. Immersing the flask in a water bath set at 70 ^{o} C commenced the polymerization. The reaction mixture was poured in diethyl ether and the polymer was purified by re-precipitation using 1,4-dioxane and diethyl ether.

Reproduced with permission of the copyright owner. Further reproduction prohibited without permission.

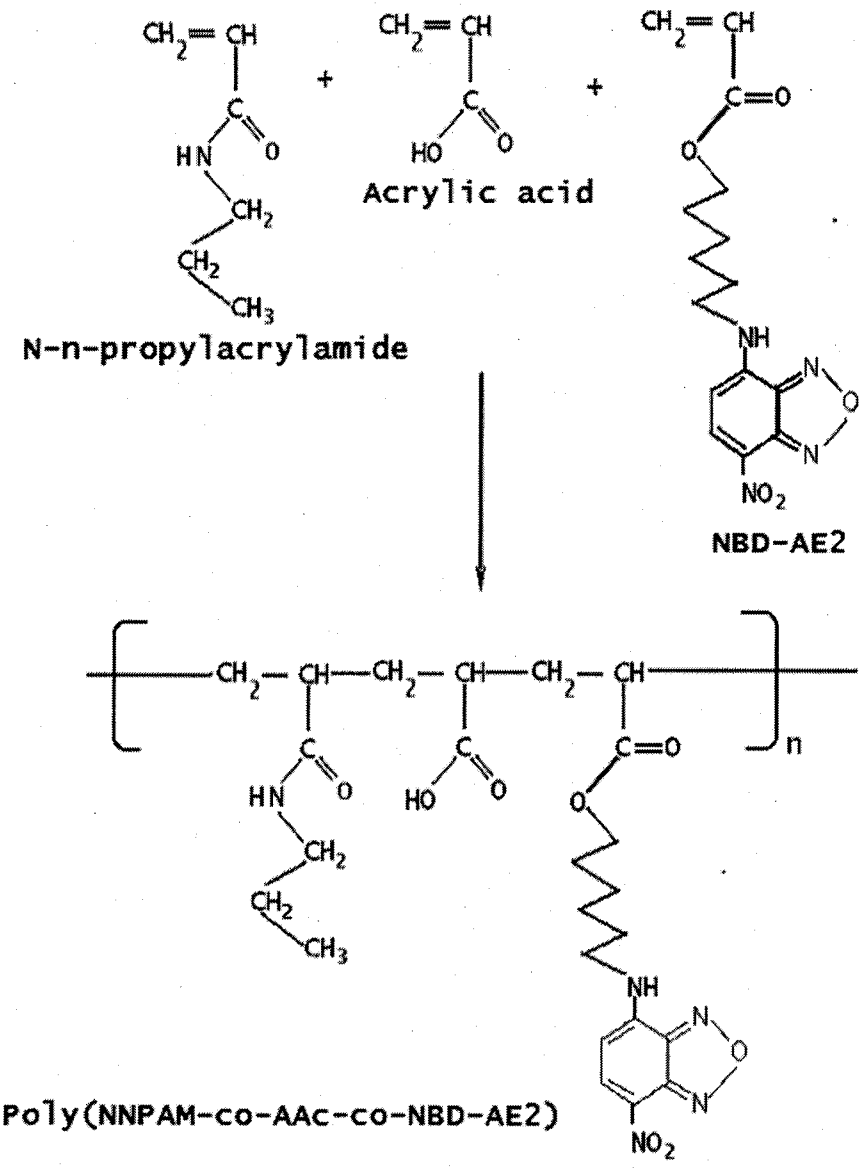

Figure 3.5 Synthesis of uncrosslinked poly (NNPAM-co-AAc-co-NBD-AE2).

To prepare the templated polymer, theophylline was included in the above formulation. It was necessary to first dissolve it completely in acetonitrile. It has a low solubility in this solvent and therefore application of heat was required to enhance the dissolution. After cooling the solution all the other ingredients were

Reproduced with permission of the copyright owner. Further reproduction prohibited without permission.

added and the polymerization effected in the same way as outlined above. Figure 3.6 shows the reactions of this polymerization.

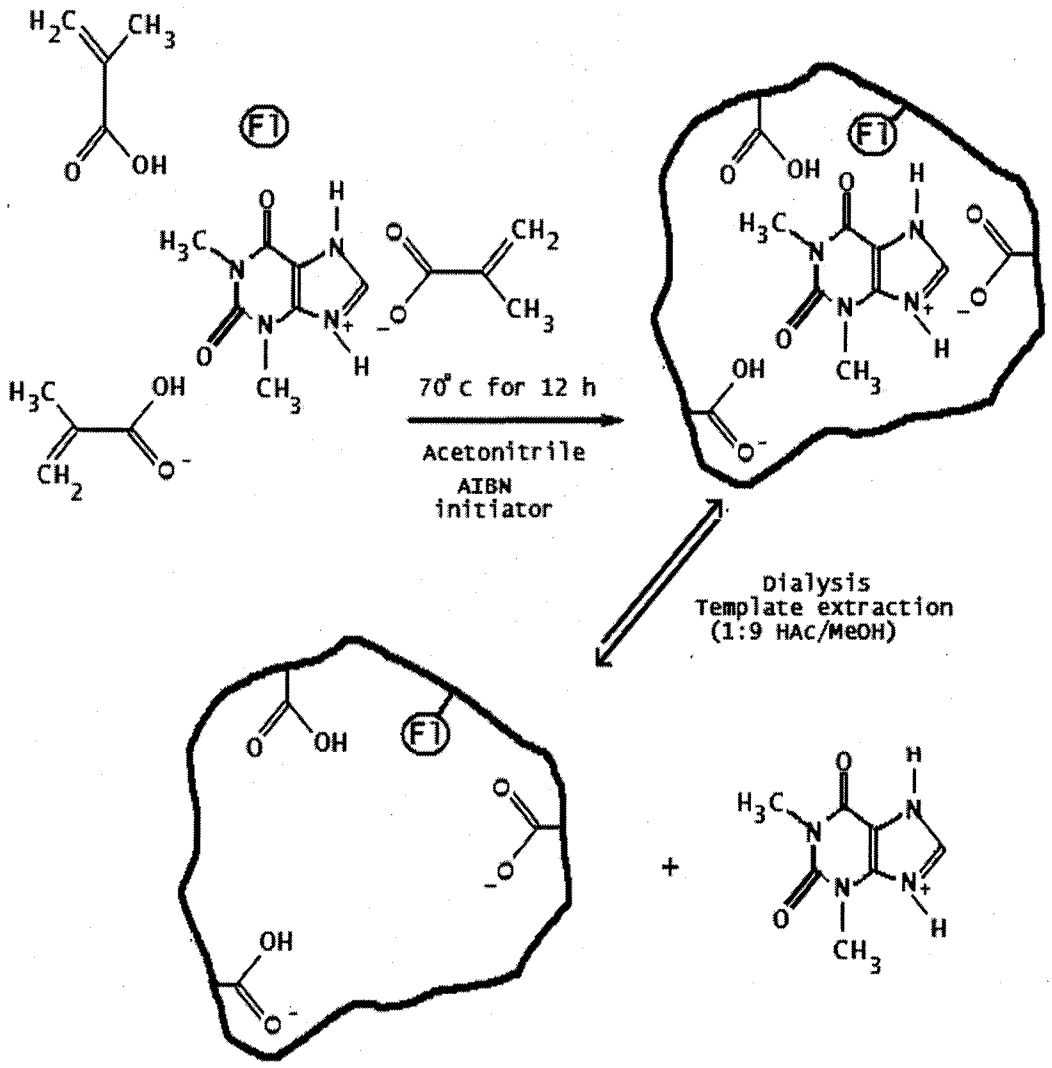

Figure 3.6 Preparation of theophylline selective molecularly imprinted polymers. The Fl represents the 4-(6-acryloyloxyhexylamino)-7-nitro-2,1,3-benzoxadiazole (NBD-AE2) fluorophore.

Reproduced with permission of the copyright owner. Further reproduction prohibited without permission.

3.6 Dialysis for Template Extraction

In conventional procedures, the template is extracted from polymer microspheres by repeated washing with methanol/acetic acid, followed by an acetone wash to remove the stabilizer. However, in the present case the polymer is in solution rather than a separate phase, therefore we could not use this direct kind of washing. Dialysis was applied to separate the template. To do this, the polymer solution was put in a dialysis membrane, which was filled with the polymer and inserted into an external solution of methanol: acetic acid (9:1 v/v). The two ends of the dialysis membrane were sealed with plastic clips and 300 mL of the external solution was used for each extraction.

The solution was allowed to equilibrate for 1 hour, followed by replacement with a new solution. A total of five changes of the external solution were performed before the solution was evaporated and resuspended in aqueous buffer solutions containing the theophylline analyte. Figure 3.7 shows the dialysis apparatus used in this extraction.

Reproduced with permission of the copyright owner. Further reproduction prohibited without permission.

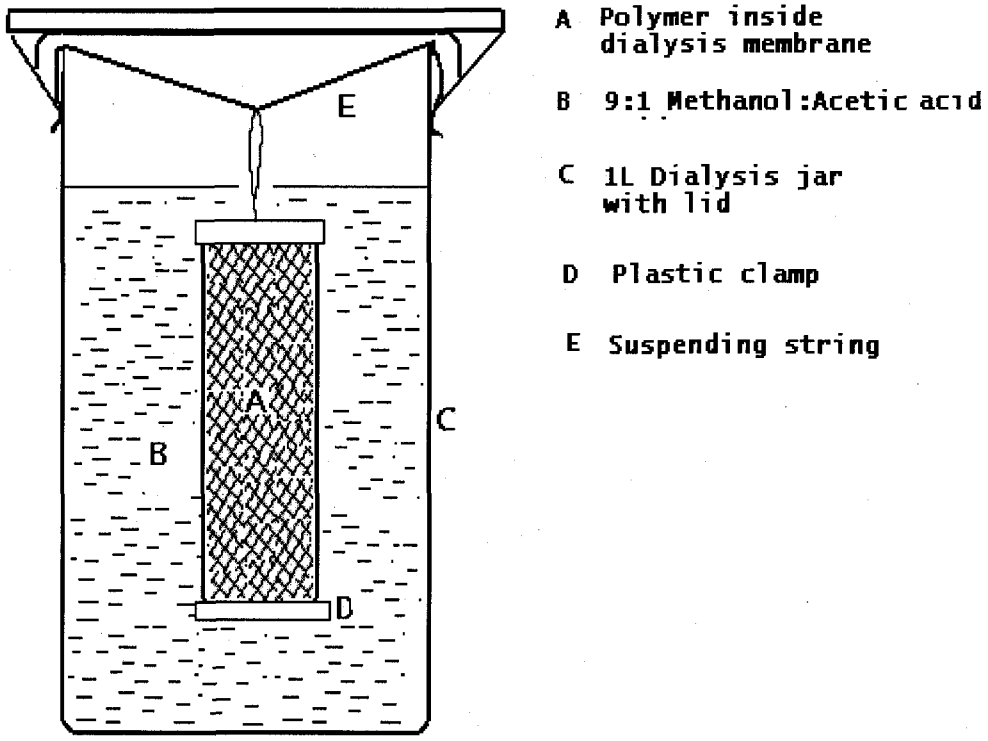

Figure 3.7 Dialysis apparatus used for extracting the template from the polymer.

Reproduced with permission of the copyright owner. Further reproduction prohibited without permission.

Table 3.4 A typical formulation for the dispersion polymerization of theophylline templated polyNNPAM-co-MAA –co-NBD-AE2 copolymer.

Ingredient	Quantity
NNPAM	1.808 g (16 mmol)
MAA (or AAc)	0.344 g (4 mmol)
THO	0.360 g (2 mmol)
AIBN	0.0262 g (0.16 mmol)
NBD-AE2	0.0054 g (16 μmol)
Acetonitrile	35 mL

Reproduced with permission of the copyright owner. Further reproduction prohibited without permission.

3.7 Preparation of Hydrogel Membranes

Hydrogel membranes have been used extensively by our research group for suspending microspheres. Three membranes were used to immobilize microspheres in this study: poly vinyl alcohol (PVA), HYPAN and polyurethane. This is necessary so that turbidity determinations can be done conveniently. The main advantage of using hydrogel membranes is that they allow the polymer microspheres, to swell and shrink in all the three dimensions, in response to different analytes.

They also facilitate easy movement of the analyte molecules into the polymer microspheres. Some factors which we need to consider in choosing a hydrogel membrane to embed microspheres include: its hydrophilicity, its refractive index compared to the refractive index of the microspheres, its mechanical strength, its inertness to analyte (eg Cu^{2+}, pH or template) and optical transparency.

3.7.1 Polyvinyl Alcohol Membranes[4]

Poly vinyl alcohol (PVA) is a hydrophilic, water-soluble polymer, which comes with various degrees of hydration and different molecular weights. PVA of low molecular weights (ca 10,000-30,000) and with high hydration are most suited for hydrogel membrane preparation. A concentration of 10 % (w/w) PVA was found to be ideal in making these membranes. Higher concentrations are difficult to prepare because they are highly viscous and lower concentrations result in membranes with poor mechanical strength and which break easily.

Reproduced with permission of the copyright owner. Further reproduction prohibited without permission.

To prepare a 10 % (w/w) solution of PVA (MW 13,000), 10g of PVA was added to 90 mL distilled water in a beaker and stirred with a magnetic stirrer until all the PVA had dissolved. This solution was stored in a 100 mL plastic bottle.

A 10% gluteraldehyde crosslinker solution was prepared from a 50 % stock solution and stored in a brown bottle, which was kept refrigerated. A 4 M HCl solution was prepared and used as the initiator. A typical preparation procedure for PVA is given below:

I. 0.01 g microspheres were weighed in a small glass vial.
II. 10% PVA was added to bring the mass to 1.00 g.
III. The beads and PVA were mixed by ultrasonication to obtain a homogeneous and cloudy suspension.
IV. 25 μL of 10 % glutaraldehyde solution was added and sonification continued for a further 10 minutes to ensure homogeneous dispersal of the crosslinker.
V. 50 μL of 4M HCl solution was added and sonicated for not more than 1 minute, otherwise the PVA will harden before the membrane can be made.
VI. A portion of the mixture was transferred onto a microscope slide whose edges had been lined with a 76 μm thick Teflon spacer. A second microscope slide is applied on top as a cover and the two slides were tightened together with a clamp. After one hour of gelation the membrane was removed from the slides, washed and stored in distilled water, in readiness for evaluation.

Reproduced with permission of the copyright owner. Further reproduction prohibited without permission.

3.7.2 HYPAN Membranes

HYPAN™ are hydrophilic acrylate polymers, which have a unique multiblock copolymer structure. Individual polymer chains are made up of sequences of units with hydrophilic pendant (soft block) and other sequence units with nitrile pendant (hard block). HYPAN™ polymers come in granular formulation with various water uptake capacities. In this research we used HYPAN HN30, HYPAN HN50, HYPAN HN 68 and HYPAN HN80.The HN number indicated the water uptake capacity (%) of the fully hydrated polymer membrane.

The water content affects the physical properties of these membranes like their mechanical strength and refractive indices. HYPAN crosslinks itself by interactions of the nitrile groups in aqueous solution and therefore unlike the other hydrogels, does not require an external crosslinker and initiator to gelate.

The making of HYPAN membranes begins with preparing 10% HYPAN (w/w) in DMSO. The appropriate amount of MIP microspheres was then added to 2 grams of HYPAN solution. Because of the high viscosity of HYPAN, it needs to be stirred for longer time at elevated temperature (~ 40-50 °C) to obtain homogeneous suspension of the microspheres. It is vital to remove air bubbles, which may be formed during stirring; these are removed by ultrasonication for 15 minutes.

A small portion of the mixture is transferred to a glass slide with a Teflon spacer which is 76 μm thick at the edges. A second glass slide or a cover slide is used as a squeegee to spread the viscous solution down across the slide to form a layer. The slide is placed in a petri dish, which is covered to create a high humidity chamber in order to hydrate the microspheres suspension in the HYPAN solution.

Reproduced with permission of the copyright owner. Further reproduction prohibited without permission.

Upon gelation the slide is placed in water, which extracts the DMSO. The membrane is then removed from the slide and washed with excess water to remove residual DMSO. The cleaned membrane is stored in distilled water.

3.7.3 Polyurethane Membranes

Hydromed D series of polyurethane membranes, which have different water capacities, were purchased from Cardiotech International, Inc. To make the membranes, a 10 % solution of the polyurethane was prepared in 95 % ethanol. The rest of the procedure is similar to the preparation of HYPAN membranes. It was found that it is easy to obtain a uniform suspension of the microspheres in polyurethane. Compared to PVA membranes, polyurethane membranes have good mechanical strength and durability.

3.8 Evaluation of Microparticles

3.8.1 Particle Size and Distribution

Scanning electron micrographs are equipped with a measuring device that is used to indicate the exact dimensions of the microspheres. These measurements (e.g. 1 μm) are usually shown at the bottom of the SEM. In this research a Carl Zeiss microscope, which was coupled with KS200 software and a CCD camera, was used in the determination of particle size.

3.8.2 Optical Microscopy Determinations

The optical microscope was an important tool in the preparation of polymer microspheres. We used a Fisher optical microscope to monitor the formation of

Reproduced with permission of the copyright owner. Further reproduction prohibited without permission.

emulsified droplets in situ and on completion of the process. This helped us to make important decisions regarding the adoption of better experimental strategies and conditions. For example by observing the droplets, information on the efficiency of wetting the porous glass membrane and its effect on the size of microspheres obtained and used to improve the quality of the microspheres prepared.

3.8.3 Refractive Index Measurements

We used an Abbe refractometer to determine the refractive indices of hydrogel membranes in the presence and absence of microspheres. This was important because as is explained in Section 2.7.1, the turbidity of membranes with suspended microparticles depends on the differences between the refractive indices of the microparticles and the membranes.

3.8.4 Fluorescence Intensity Measurements

A Cary Eclipse spectrofluorometer was used to monitor the fluorescence from both the polymer microspheres and in the case of the uncrosslinked polymer, the polymer in solution. Excitation and emission wavelengths of 465 and 480 nm, respectively, were used in these determinations. Most of the fluorescence spectra were collected between the wavelengths of 480 to 650 nm. The fluorescence intensities of the dialyzed polymers in aqueous solution were determined after mixing them with increasing concentrations of theophylline.

Reproduced with permission of the copyright owner. Further reproduction prohibited without permission.

3.8.5 Turbidity Measurement

The membranes were placed in plastic holders which were custom made for us by the University of New Hampshire Machine Shop. The membrane holders were then placed into ordinary 1 cm cuvettes for turbidity measurements (Figure 3.8). For pH determinations, the cuvettes were ¼ filled with pH buffer, which were replaced after each determination. In the case of MIPs the membranes were immersed in cuvettes that were ¼ filled with thophylline solutions.

A sample blank was made up of the membrane without the microspheres; this was used as the reference and immersed in a reference cuvette with the appropriate buffer solution. All turbidity determinations were performed with a UV-Vis-NIR spectrophotometer. The turbidity spectra were obtained by scanning the wavelengths from 400 to 1000 nm.

Reproduced with permission of the copyright owner. Further reproduction prohibited without permission.

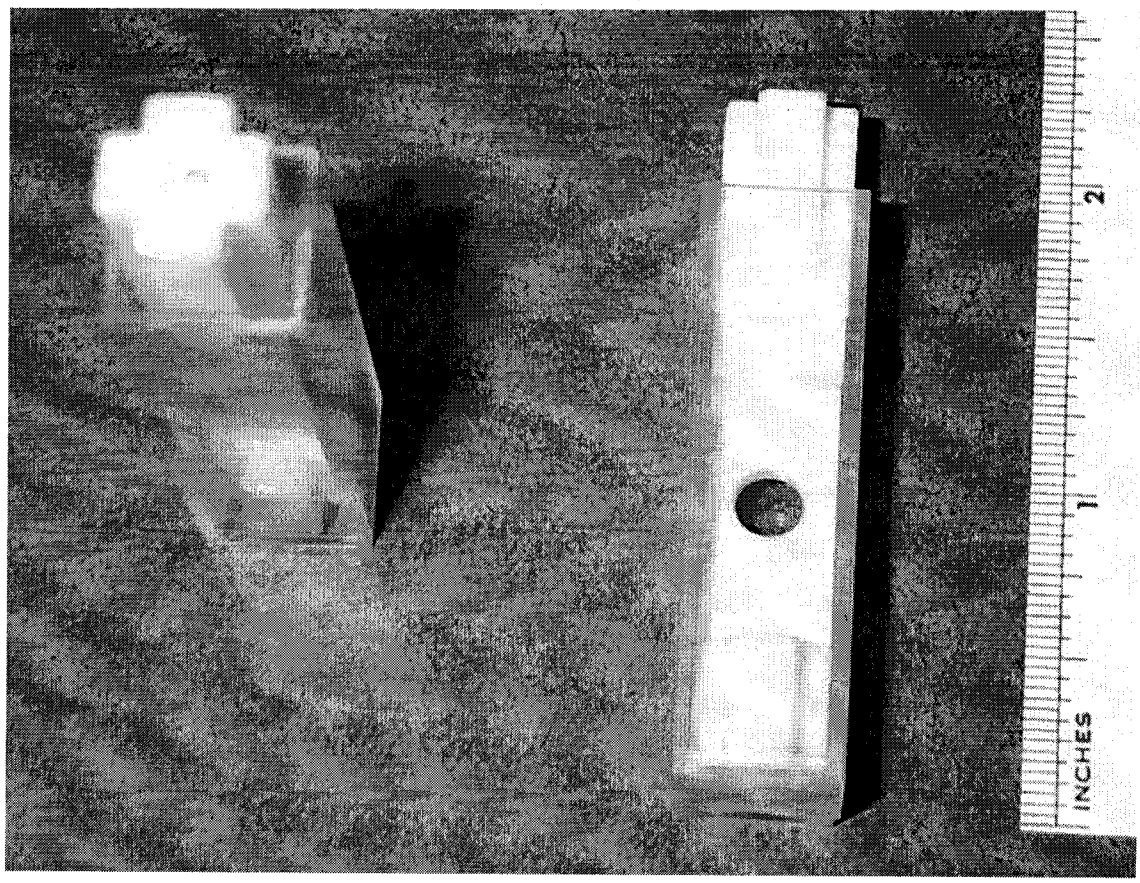

Figure 3.8 Membrane holders for turbidity determinations[94]

Reproduced with permission of the copyright owner. Further reproduction prohibited without permission.

3.8.6 Response Time Measurements

The definition of response time is the time taken for a response signal to reach 90% of the maximum signal. For pH measurements this is the time it takes for the hydrogen ions to interact with the functional groups in the polymer so that 90% of the maximum turbidity is obtained. We determined the response time by measuring the turbidity at a single wavelength (500 nm)

3.8.7 Measurement of Copper Concentration by Atomic Absorption Spectrometry

We prepared membranes in which poly (HEMA) microspheres with immobilized trimethyl ethylenediamine were embedded and immersed them in copper prepared in pH 10 buffer solutions. Starting with the copper solutions of the lowest concentration, we allowed the membrane to equilibrate in the copper solution for 5 minutes, after which the membrane was rinsed with distilled water.

The bound copper was removed from the membrane by treating it with 10 mL of 1 M hydrochloric acid. The membrane was further washed with distilled water to remove the HCl and immersed in the next higher copper solution and the process repeated over again until it had been equilibrated in all the prepared copper solutions. The portions containing the bound copper were further diluted five –fold before analysis with atomic absorption spectrometry. Standards that covered the concentration range of the solutions were made and a calibration plot was constructed. With this we were able to calculate the concentration of copper that was bound in the membrane by the microspheres.

Reproduced with permission of the copyright owner. Further reproduction prohibited without permission.

CHAPTER 4

SUSPENSION POLYMERIZATION SYNTHESIS AND EVALUATION OF AMINATED POLY (VINYLBENZYL CHLORIDE) MICROSPHERES FOR pH OPTICAL SENSING

4.1 Introduction

This chapter explores the synthesis of lightly crosslinked poly vinylbenzylchloride (PolyVBC) microspheres for optical sensing. The goal was to develop a method of preparing Poly VBC microspheres that have a relatively short response time and that swell and shrink reproducibly and reversibly in response to pH.

Since the analytical response to optical sensors is the amount of light reflected by a polymer membrane, development of a working model to describe the response is crucial from a theoretical point of view. The development of such a model has allowed researchers from our research group to optimize and improve the performance of the system.[98] The system was based on the observation of Pan[99] that polymer microspheres synthesized in the presence of Kraton G1652 a styrene-ethylene/butylenes-styrene triblock copolymer, became less opaque on swelling. Zhang and Shaksher[100] also made use of this principle to prepare chemical sensors for pH sensing that was based on changes in reflected light. However the actual mechanism of the optical change was not understood at that time.[100]

Reproduced with permission of the copyright owner. Further reproduction prohibited without permission.

The turbidity of porous amine modified, rubber toughened poly (VBC-co-DVB) microspheres was studied by Rooney.[98] Membranes suitable for sensing were prepared by a more convenient method that uses photoinitiated polymerization and did not require the time consuming pre-polymerization step. One drawback of this method of preparation is that the per unit turbidity ratio these membranes swell more than membranes prepared by the previous method. The response times of these membranes was of the order of an hour. Slow diffusion into the polymer is believed to limit response time.[98]

Based on the work of Conway *et al,*[25] it was established that the presence of a porogen plays a vital role in significantly reducing the response time of the microspheres. In this study a model of the processes involved in the polymerization process was constructed from pore distribution data obtained through mercury porosimetry. Kraton G1652 was added to the reaction mixture so that the polymerization of poly (VBC) would take place in the presence of an elastomer. The morphology of the poly (VBC) matrix is directly affected by the addition of the Kraton G1652 and the porogenic solvents.

When polymerization is complete the porogen was extracted leaving pores in the polymer. A bad solvent for the polymer results in large pores due to the solvent separating into a distinct phase as polymerization progresses. A balance between a good and bad solvent for the polymer is essential for the formation of optimum pores sizes, which lead to uniform and reproducible swelling and shrinking and a relatively fast response time of the polymer. Miele[101] prepared poly

Reproduced with permission of the copyright owner. Further reproduction prohibited without permission.

(VBC) particles by a two-step process, in the first step uniform microparticles were prepared by dispersion polymerization.

A formulation that produced 0.6 μm particles was used to make the seeds which were then dispersed in a reactor with an aqueous surfactant. An emulsified mixture of monomer, crosslinker and porogenic solvents was added slowly to the seeds. The mixture was polymerized for 2 hours at 70°C after initially stirring for 24 hours to allow the seeds to adsorb the monomer. The particles were then derivatized with diethanolamine. These particles produced a large change in turbidity and had fast response time. However, the procedure was tedious and time consuming. It is with this view that we investigated the Shirazu porous glass method. Using this method Kaval[94] produced fairly monodispersed poly (VBC) microparticles with diameters of a few micrometers. The microparticles were then derivatized with diethylamine to impart the pH sensitive functionality. They were observed to swell and shrink very rapidly with a 'switch-like action' and thus were unsuitable for pH sensing.

The porogenic solvents used in this study are a mixture of xylene and dodecane used in a ratio of 2:1 respectively. In this research a new method known as the Shirazu Porous glass method was employed. It results in the formation of uniform microspheres in the emulsion and helps in overcoming some of the disadvantages of using the traditional method of emulsion polymerizations. A key advantage of the porous glass method is that unlike dispersion polymerization this method can be applied with porogens that make the polymer porous and thus, can

Reproduced with permission of the copyright owner. Further reproduction prohibited without permission.

be easily permeated by the analytes of interest. Observing the change in turbidity with pH at constant ionic strength tested the response of the aminated microspheres.

Two different membranes were used to suspend the particles. These are PVA and hydrogels of the HYPAN polymer series, details of which are discussed in Section 3.7. The pH 2.0 buffers were made from chloroacetic acid while those between pH 3.0 to 5.0 were made from acetic acid. Buffers from pH 6.0 to 8.0 were made with N- (-2-acetamido)-2-aminothanesulphonic acid (ACES) while those between pH 9.0-10.0 were made with ammonium hydroxide. The ionic strengths of all the buffers were adjusted to 0.1 M with NaCl.

4.2 Preparation of Poly (VBC) Microspheres by Suspension Polymerization.

Poly (VBC) microspheres were synthesized by employing a new method of emulsion polymerization known as the Shirazu Porous Glass (SPG) method using a membrane with 0.5 μm size pores. We opted to use this method over the traditional suspension polymerization methods because it can produce larger porous particles.

The method does not require vigorous stirring to break up larger droplets for optimum size distribution. The initial experiments done on the system led to the preparation of very large beads, (Figure 4.1). This was due to incomplete wetting of the membrane and application of higher than optimum pressure. It showed that we were applying too much pressure which resulted in the larger non-uniform drops being extruded from the pores of the membrane.

Reproduced with permission of the copyright owner. Further reproduction prohibited without permission.

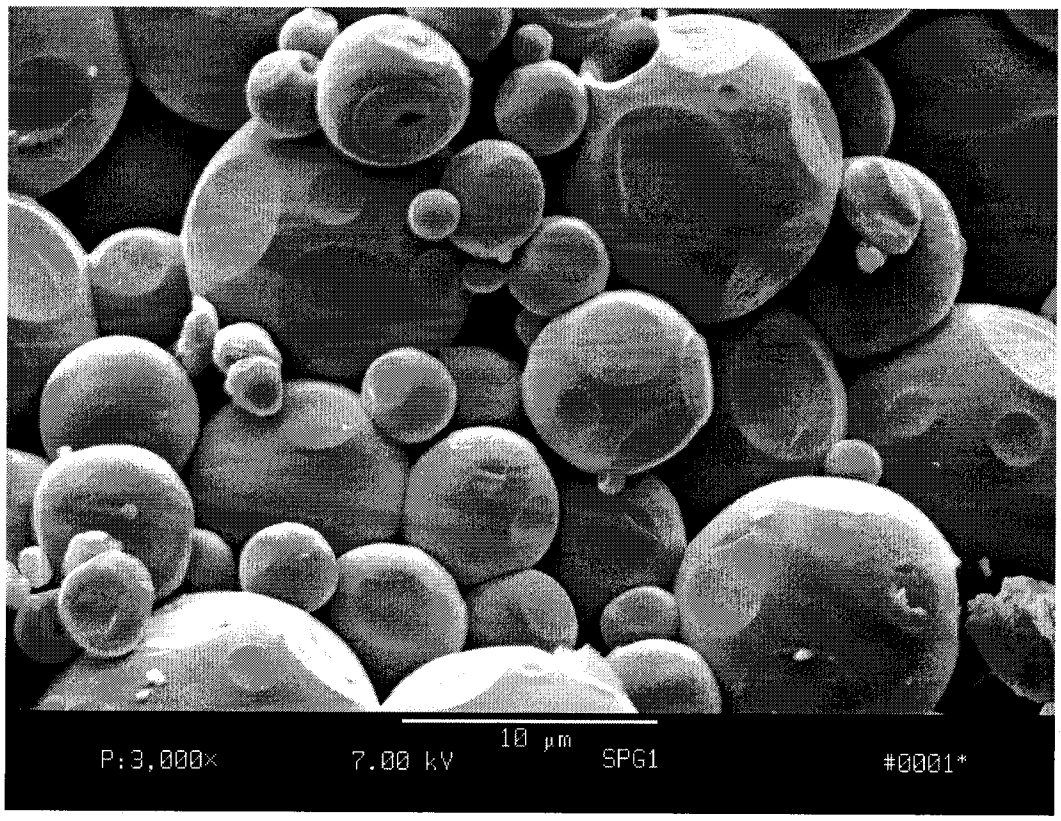

Figure 4.1 Non-uniform and large Poly (VBC) particles prepared initially.

Reproduced with permission of the copyright owner. Further reproduction prohibited without permission.

We were able to synthesize particles of narrower size distribution after some practice, which are shown in Figure 4.2. The particles had an average diameter of the order of 3 μm. To prepare the emulsion, 30 ml of the dispersion phase consisting of the VBC monomer, EGDMA crosslinker, benzoyl peroxide initiator and the porogenic solvent were place in the dispersion phase tank (Section 3.3). This phase was then allowed to permeate through the porous membrane, into the continuous phase, which was circulated by a pump, while maintaining the appropriate pressure, (Section 2.6). The droplets are then transferred to a three-necked flask to commence the suspension polymerization.

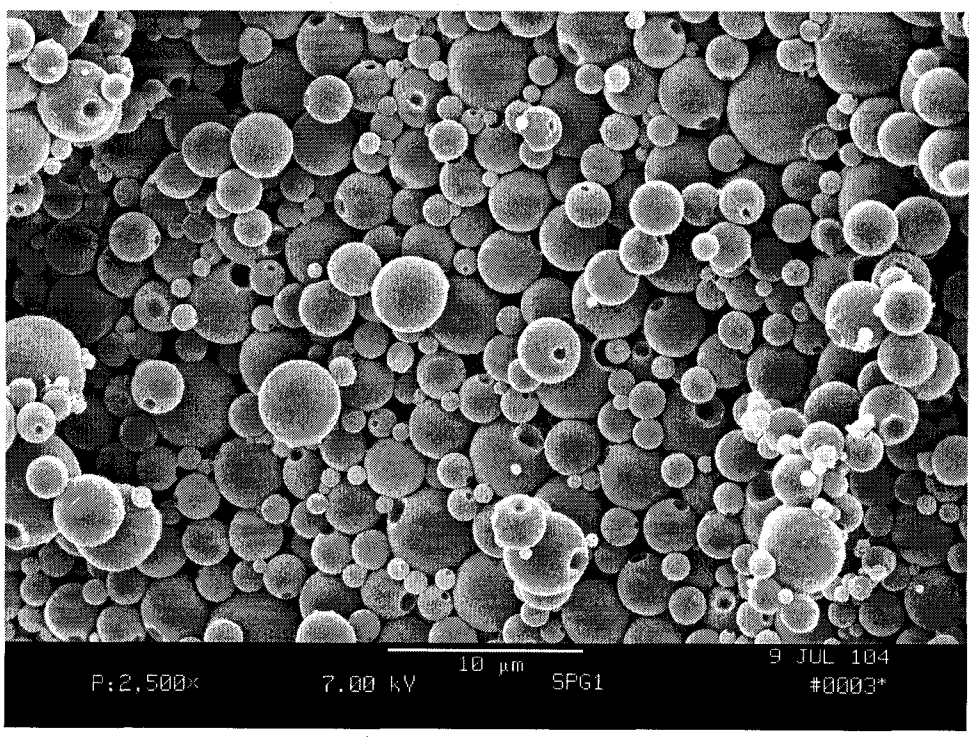

Figure 4.2 Uniform and monodisperse polyVBC microspheres prepared after some practice with the SPG apparatus.

Reproduced with permission of the copyright owner. Further reproduction prohibited without permission.

4.3 Derivatization of Poly (VBC) Microspheres with NNN'-Trimethyl ethylenediamine (Tmen)

After the polymerization process is complete, the particles need to be functionalized so that they can be sensitive and respond to different pH conditions and also the concentration of metal ions. Figure 4.3 shows the amination of polyVBC with NNN'-trimethlethylenediamine (TMEN). The procedure is described in Section 3.3.2.

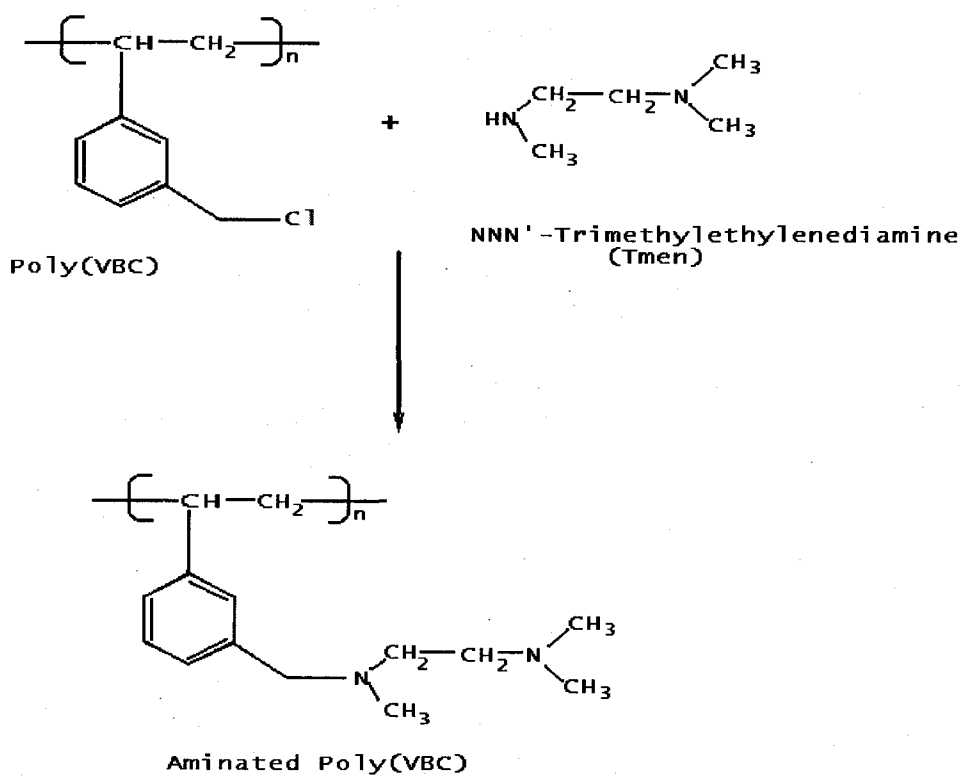

Reproduced with permission of the copyright owner. Further reproduction prohibited without permission.

Figure 4.3 Derivatization of poly (VBC) microspheres

4.4 Results and Discussion

4.4.1 Potentiometric Titration

The microspheres were titrated against 0.1 M NaOH after first acidifying them with acid to protonate the amino groups on the polymer. The progress of the titration was followed by using a pH electrode to monitor the change in pH with addition of the NaOH. This experiment confirmed the binding capacity and showed that the derivatized microspheres have an apparent pK_a of 5.4 (Figure 4.4).

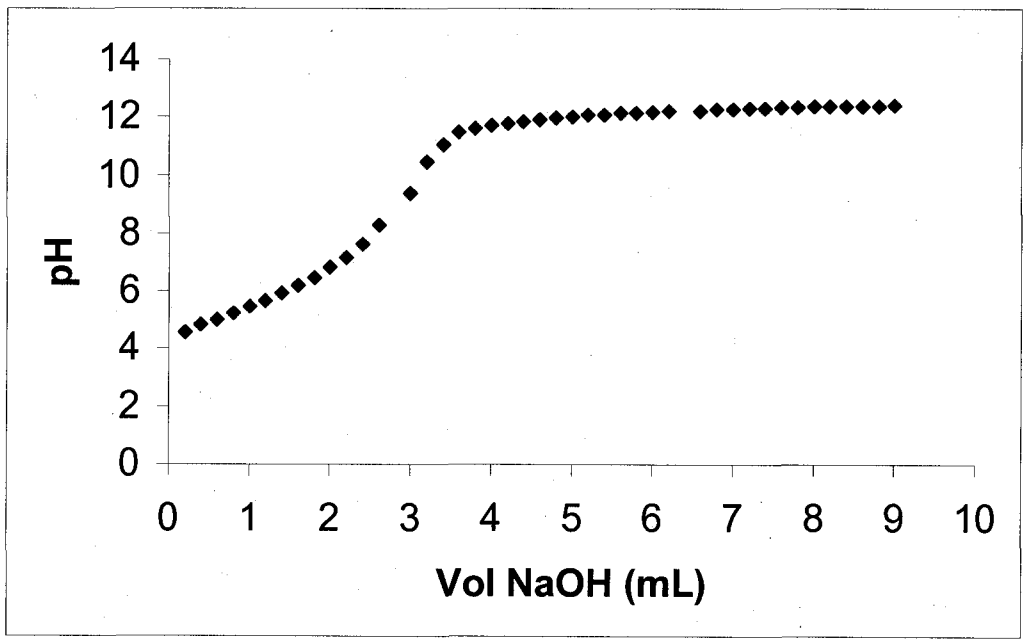

Figure 4.4 pH titration of NNN'-trimethylenediamine derivatized poly (VBC) with 0.1 M NaOH solution.

Reproduced with permission of the copyright owner. Further reproduction prohibited without permission.

The turbidity spectra of the membranes containing poly (VBC) microspheres of the order of 3 microns and with a nitrogen content of 5.2 % are shown in figure 4.5. The concentration of the microspheres in the membrane was 0.1 wt %. In this experiment aminated polyVBC microspheres were embedded in a polyurethane membrane and immersed in pH buffer solutions.

The wavelengths were scanned from 400-1000 nm at 25 ^{o} C while monitoring turbidity values. Figure 4.6 shows the turbidity vs. pH plot taken at a wavelength of 500 nm. There is a large change in turbidity in at pH 5.4. This investigation suggests that it may be possible to estimate the apparent pK_a of aminated microspheres by monitoring the change in turbidity. However this possibility needs to be explored further because there may be other factors that contribute to these changes.

The refractive index of polyurethane used in the study (Figures 4.6) was 1.56. This is higher than that of the microspheres (RI = 1.47) and therefore in high pH buffer the microspheres had the lowest reflectance. This is because the refractive index of the microspheres increased in high pH buffers and became closer to the refractive index of the membrane. This made the membrane to appear more transparent. The opposite effect was observed when PVA membrane (R.I = 1.34) was used (Figures 4.8-4.10). In this case the refractive index of the membrane was lower than that of the microspheres. In high pH buffer the microspheres become less transparent as the difference between the refractive indices of the two media becomes bigger.

Reproduced with permission of the copyright owner. Further reproduction prohibited without permission.

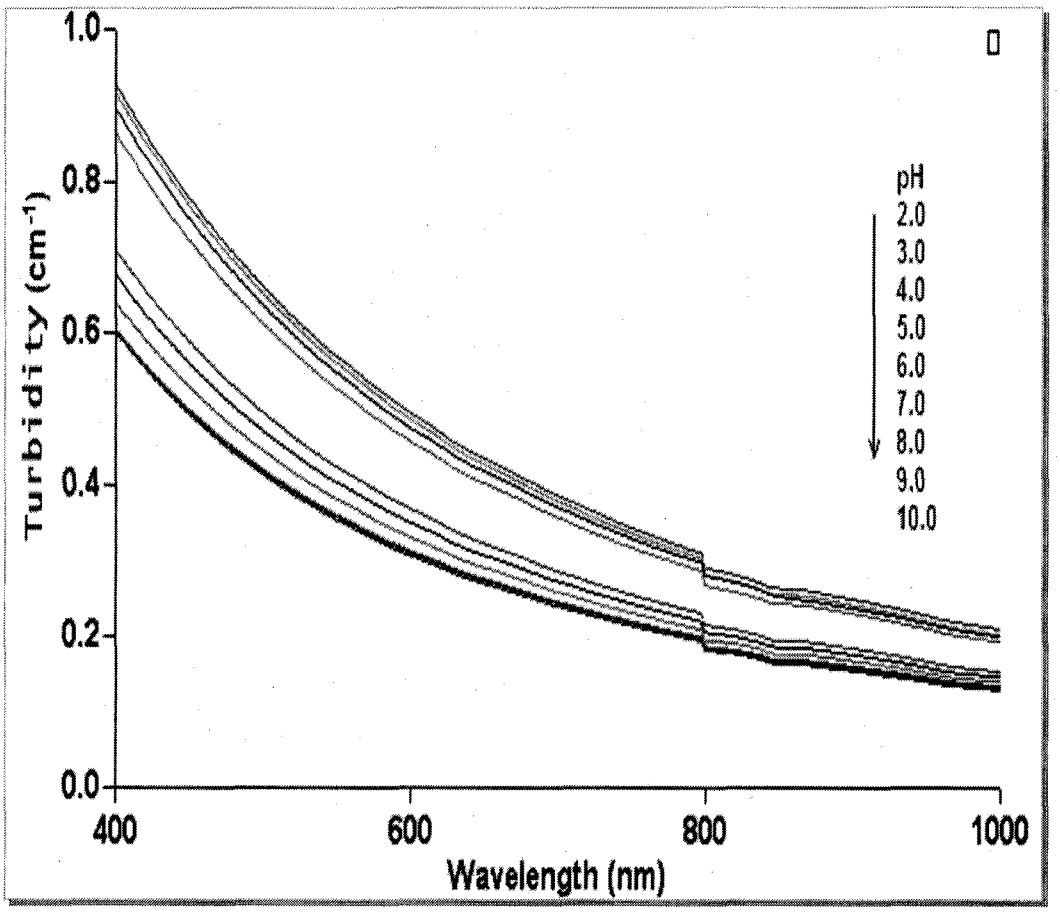

Figure 4.5 Turbidity vs. wavelength spectra of NNN`trimethylenediamine derivatized poly (VBC) microspheres suspended in PVA membrane. The membrane was immersed in buffers of different pH values and the turbidity determined.

Reproduced with permission of the copyright owner. Further reproduction prohibited without permission.

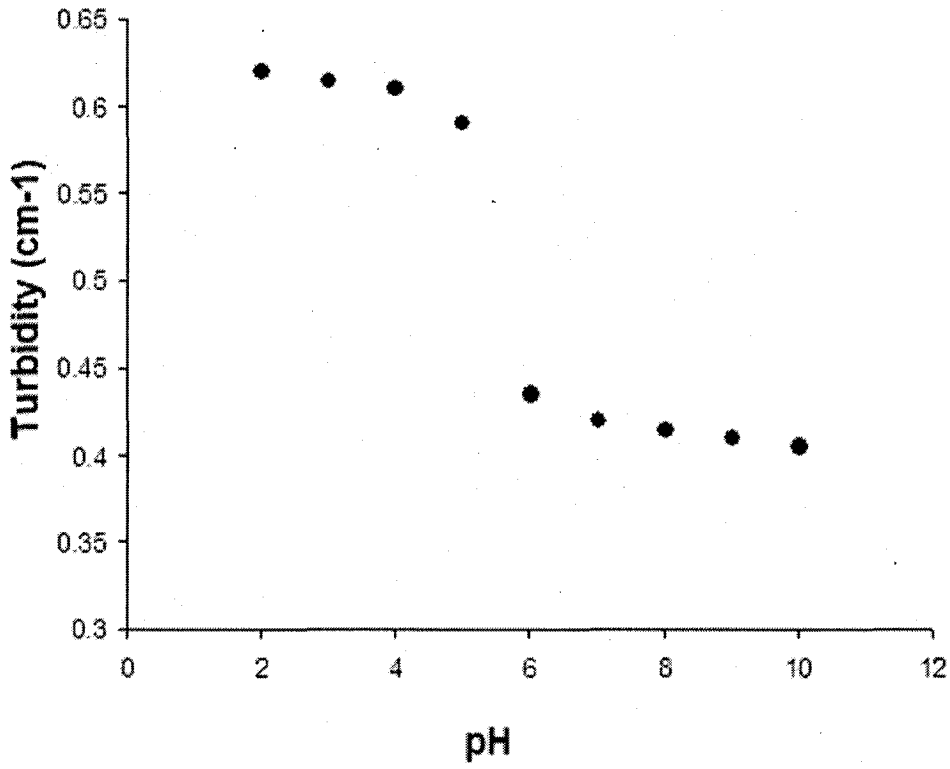

Figure 4.6. Turbidity vs. pH of NNN`trimethylenediamine derivatized poly (VBC) microspheres suspended in polyurethane membrane. The turbidity values were monitored at a wavelength 500nm.

Reproduced with permission of the copyright owner. Further reproduction prohibited without permission.

Figures 4.7 to 4.9 illustrate the change in turbidity of aminated poly (VBC) microspheres in pH 4 and pH 10 buffer solutions. The percentage of nitrogen derivatized onto the polymer was 3.38 %, 5.78% and 11.27 % respectively. The spectra show that a bigger response is obtained for the polymer with a higher amount of nitrogen.

Figure 4.9 shows a change of 0.084 turbidity units (cm^{-1}) at 600 nm when the membrane is first immersed in pH 4 buffer and then transferred to the higher pH 10 buffer. This is a six-fold increase over the 0.013 cm^{-1} observed in Figure 4.7 at 600 nm. Figure 4.8 showed an intermediate change of 0.059 cm^{-1} for the same buffer solutions. These data suggest that the degree of amination may be an important aspect in the synthesis of these polymers.

We therefore undertook to explore the temperature conditions that favor a greater percentage of nitrogen being incorporated into the polymer. Poly (VBC) microspheres were derivatized from the same batch using the method outlined in Section 3.3.3. The experimental conditions were the same for all of the experiments with temperature being the only variable. The nitrogen content of the polymer microspheres was determined by CHN analysis and is shown in Table 4.1.

The theoretical masses of carbon, hydrogen and nitrogen were calculated assuming complete substitution of the chloromethyl group of the poly (VBC) with diethylenetriamine. These were 76.06 %, 10.09 % and 12.84 % for C, H and N respectively. The results of this experiment indicate that it is desirable to carry out the derivatization reaction at elevated temperature to obtain a higher yield of the aminated polymer. The percentage of nitrogen obtained at 50° C is quite close to

Reproduced with permission of the copyright owner. Further reproduction prohibited without permission.

the theoretically calculated value showing almost complete reaction at this temperature.

Table 4.1 Results from CHN analysis for amination of poly (VBC) microspheres at different temperatures

Temperature ^{o} C	N mass % **Expt**
25	1.25
30	2.20
35	4.60
40	5.91
45	8.80
50	11.27

Reproduced with permission of the copyright owner. Further reproduction prohibited without permission.

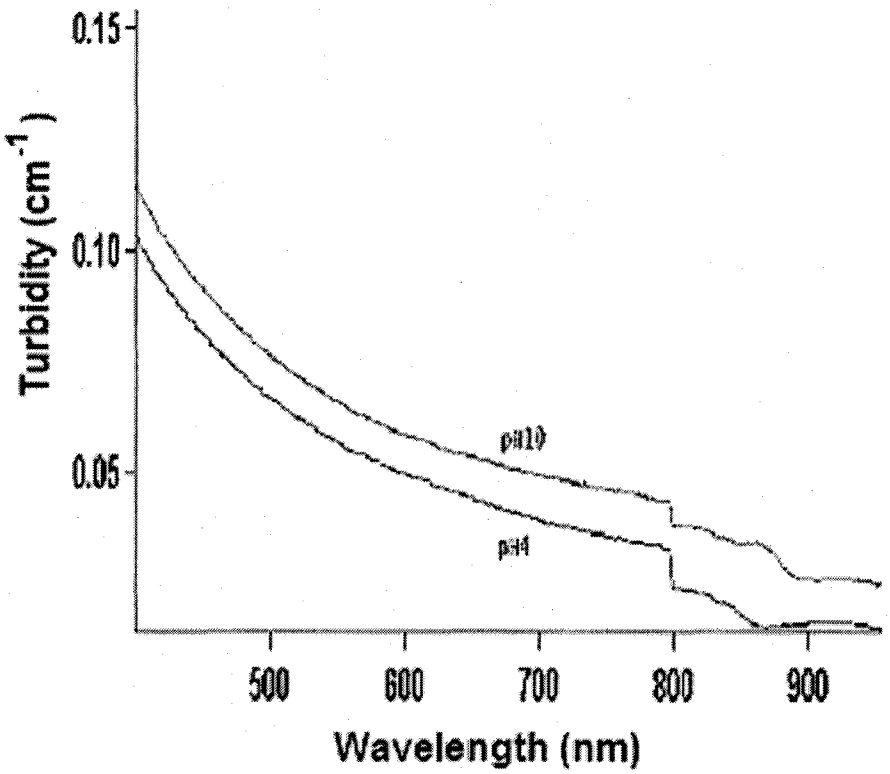

Figure 4.7 Turbidity spectra for aminated polyVBC microspheres in pH 4 and pH 10 buffers. The amount of N derivatized on the microspheres was 3.38%

Reproduced with permission of the copyright owner. Further reproduction prohibited without permission.

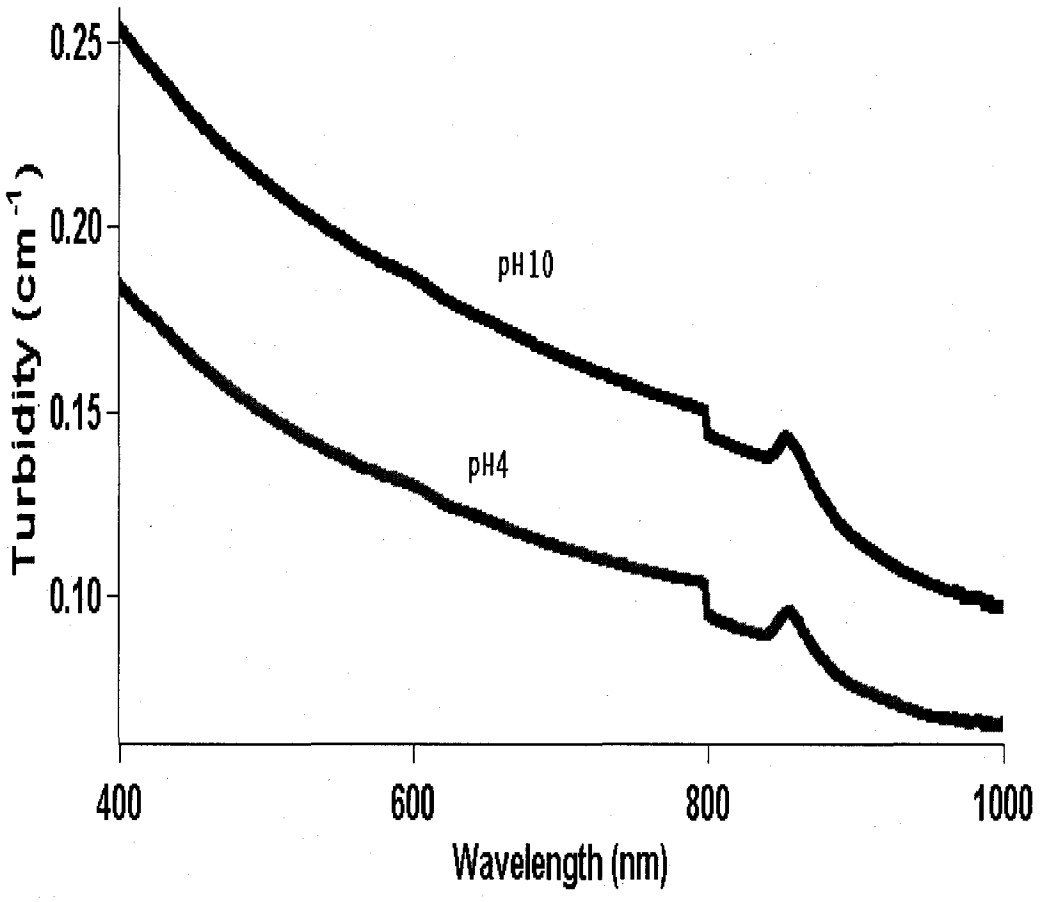

Figure 4.8 Turbidity spectra for aminated polyVBC microspheres in pH 4 and pH 10 buffers. The amount of N derivatized on the microspheres was 5.91%

Reproduced with permission of the copyright owner. Further reproduction prohibited without permission.

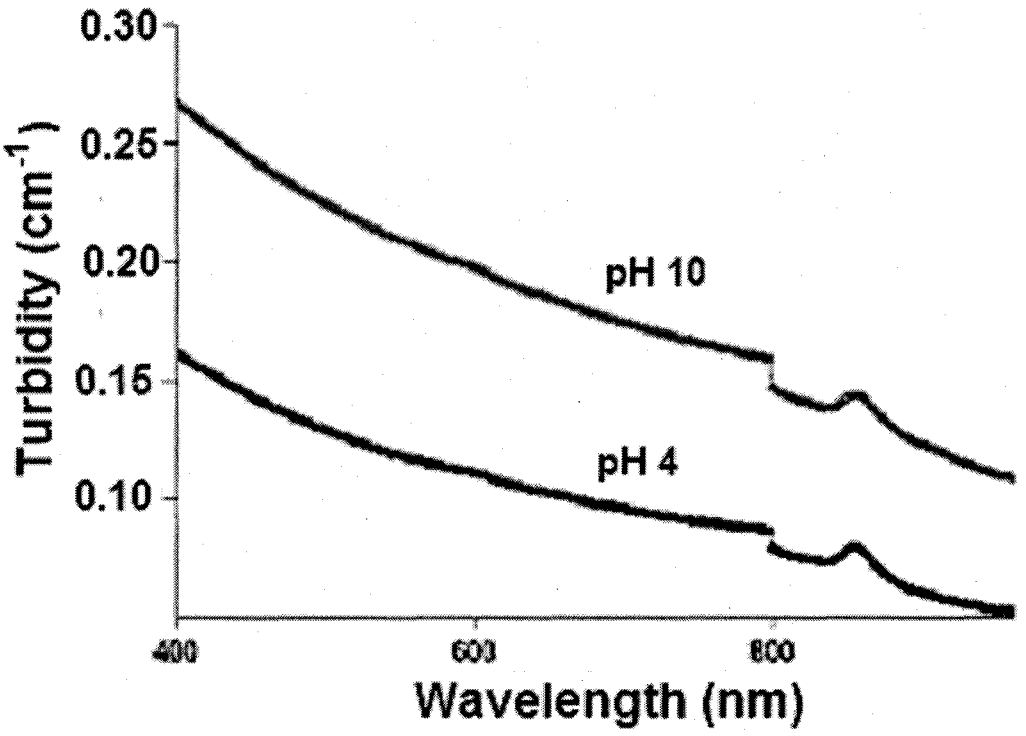

Figure 4.9 Turbidity spectra for aminated polyVBC microspheres in pH 4 and pH 10 buffers. The amount of N derivatized on the microspheres was 11.27%

Reproduced with permission of the copyright owner. Further reproduction prohibited without permission.

Figure 4.10 shows the shrinking and swelling response time of poly (VBC) that was derivatized with NNN'-diethylenetriamine. The carbon, hydrogen and nitrogen content of this aminated polymer was determined to be 76.85%, 8.04% and 5.91% respectively by CHN analysis.

The response times of the aminated poly (VBC) microspheres were measured by monitoring the change in turbidity as function of time. There was an increase of 0.06 turbidity units (cm^{-1}) within the first 4 seconds. At pH 4, the turbidity of the membrane also took about 6 seconds to reduce to about 70 % of the maximum turbidity. A possible reason for this more gradual reduction in turbidity may be due to the force required to displace solvent molecules. These empirical finding show that there is need for further investigation to relate the changes in microspheres turbidity with size.

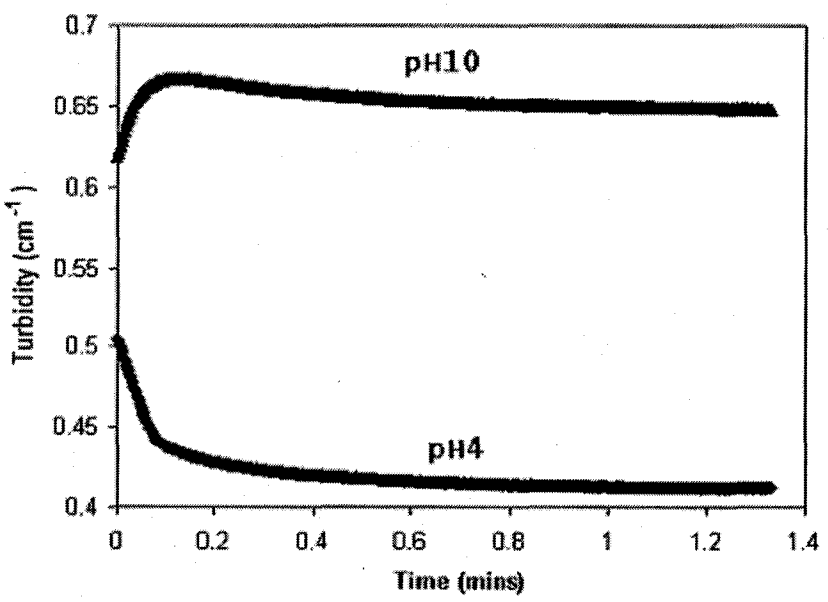

Figure 4.10 Response time of NNN'-trimethylenediamine derivatized poly (HEMA) in pH 4 and pH 10 buffer solutions.

Reproduced with permission of the copyright owner. Further reproduction prohibited without permission.

4.5 Conclusions

The SPG method is an effective method of synthesizing small particles that have uniform distribution in size.[61] It has been demonstrated that using a 0.5 –1μm porous membrane which has been thoroughly wetted and with the application of optimum pressure, we can synthesize fairly monodisperse microspheres.

The condition under which the derivatization reaction is carried out was found to be of great importance. From the experiments reported in this chapter, it was determined that generally higher temperatures applied during the derivatization process, result in higher yields of the aminated product. It was shown that at 50° C, the nitrogen derivatized onto the polymer was close to the theoretically calculated value. This observation was important because in subsequent experiments it was determined that higher percentages of amination led to stronger responses to the hydrogen ions.

The microspheres generated by the SPG method have been found to respond to pH buffers by changing turbidity as the polymer becomes protonated and deprotonated respectively. The particles have been found to respond fast with typical response times of the order of 6 seconds. Potentiometric titration of the derivatized microspheres with NaOH, using a pH electrode showed that they have an apparent pK_a of 5.4.

Reproduced with permission of the copyright owner. Further reproduction prohibited without permission.

CHAPTER 5

DISPERSION POLYMERIZATION SYNTHESIS AND EVALUATION OF AMINATED POLYMER MICROSPHERES FOR pH AND Cu^{2+} SENSING

5.1 Introduction

This chapter explores the synthesis and evaluation of poly (HEMA) micro particles for pH and Cu^{2+} ion sensing. The work presented here is an extension of work previously conducted in our group.

Kaval[94] reported in his research on dispersion polymerization of poly (HEMA), that one of the most convenient ways of controlling microsphere size is by changing the monomer concentration. He found that as the monomer concentration increased from 0.5 μm to 0.8 μm at the 10 % monomer level and 1.03 μm at the 15 % monomer concentration. However polydispersity became an issue at higher monomer concentrations. Therefore a 10 % monomer concentration was used in this study. Dispersion polymerization was used to synthesize particles in this research. The main drawback in this method is that unlike in suspension polymerization, it is impossible to introduce pores in the polymer by incorporating a porogen. This causes the response of these beads to be slow to the targeted analytes.

The choice of poly (HEMA) microspheres for chemical sensing stems from the hydrophilic properties of these polymers. They have a high capacity for holding water, which is advantageous for chemical sensing, as they create fine pores within

Reproduced with permission of the copyright owner. Further reproduction prohibited without permission.

the polymer network that facilitate transport of the analytes to the cores of the polymers.

Two types of hydrogel membranes were used in this study. These are HYPAN 68 (a hydrophilic acrylate multiblock copolymer) and a polyurethane membrane. The behavior of these two membranes, when immersed in the analytes, was different due to differences in their refractive indices. When the microspheres are dispersed in HYPAN membrane and the membrane immersed in an acidic buffer solution, it becomes transparent, while in a basic buffer solution, the membrane becomes cloudy. This is due to the swelling and shrinking the microspheres in the two media.

Most of the work done in this area has focused on developing the technique of making small and highly monodisperse beads. This study will concentrate more on the evaluation of the prepared and derivatized microspheres with particular emphasis on the interaction between protons and copper ions with the amino groups on the polymer. We will investigate the ratio of copper that binds to the nitrogen groups because this will lead to a better understanding of the magnitude of the interaction. It will also be useful in designing an aminated polymer that gives a big response on binding to copper.

5.1 Activation and Derivatization of PolyHEMA Microspheres.

The amination of polyHEMA microspheres is a two-step process. In the first step shown in Figure 5.1, 2.0g of the polyHEMA particles are washed and suspended in 30 mL of 1,4-doixane. To this suspension 2.5 g of 1,1-carbonyldiimidazole (CDI)

Reproduced with permission of the copyright owner. Further reproduction prohibited without permission.

are added and dispersed for ca.15 seconds. The suspension is then shaken at room temperature for 12 hours to complete the activation.

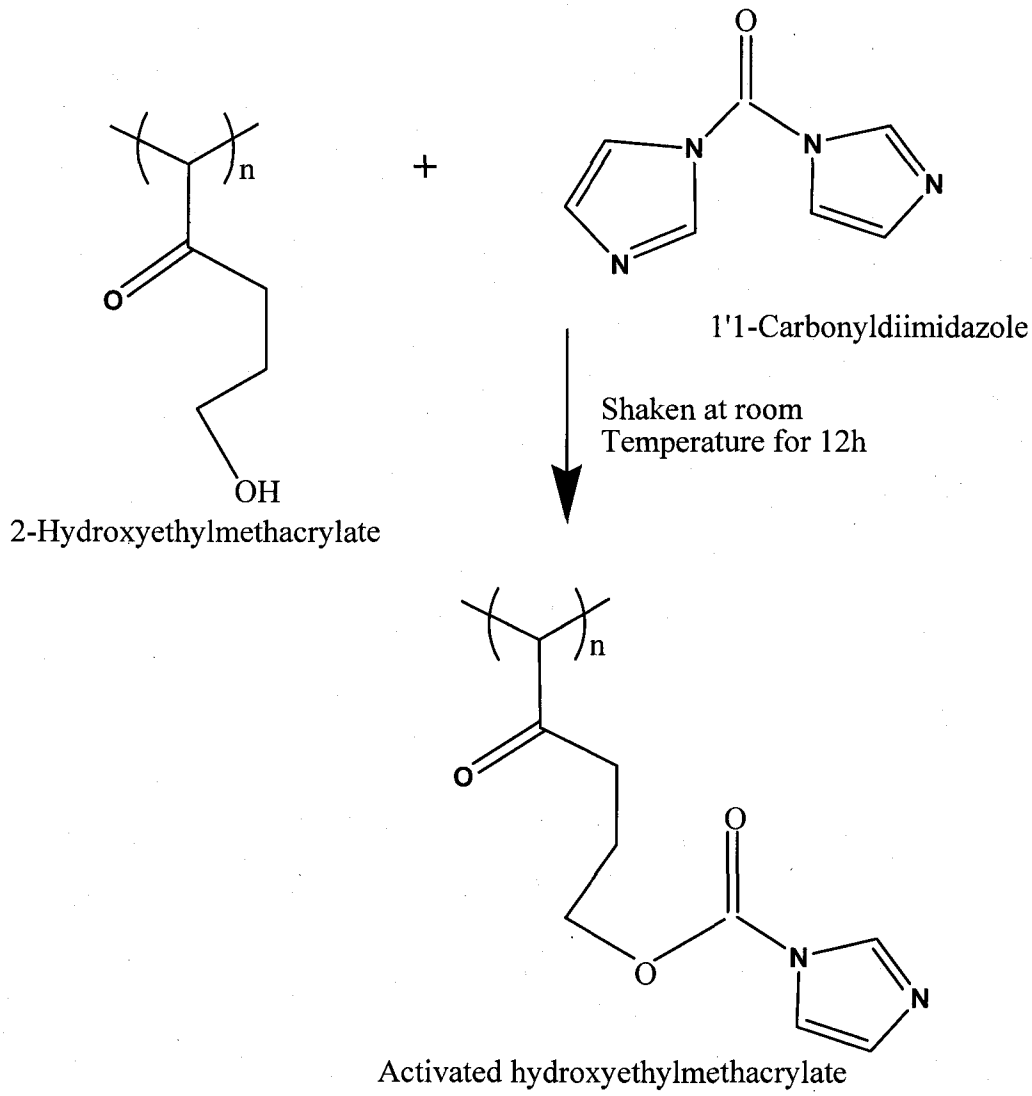

Figure 5.1 Activation of poly (HEMA) to introduce the imidazolyl carbamate group, which is susceptible to nucleophilic attack by amines in organic solutions.

Reproduced with permission of the copyright owner. Further reproduction prohibited without permission.

In the second step, ethylenediamine is derivatized on the polyHEMA microspheres as shown in Figure 5.2. In this step, 5g of the microspheres, suspended in 30mL of 1,4-dioxane was transferred to a flask containing 20 mL ethylenediamine and 10 mL 1,4-dioxane. The mixture is shaken for 4-5 days at a temperature of 30-40 °C to complete the amination.

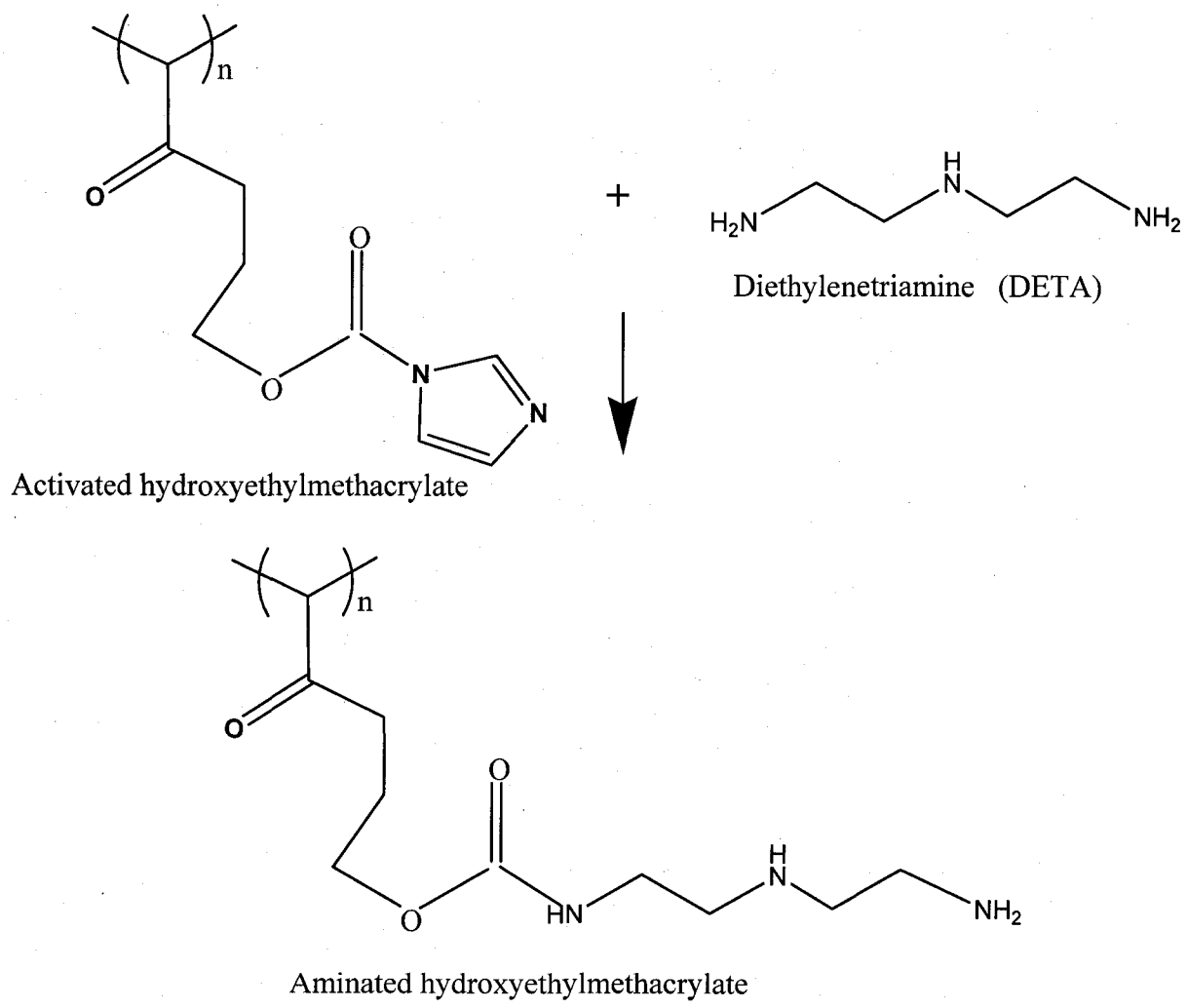

Figure 5.2 Coupling the activated poly (HEMA) matrix with diethylenetriamine to introduce the pH and metal sensing functionality.

Reproduced with permission of the copyright owner. Further reproduction prohibited without permission.

Results and Discussion

5.2 Light Microscope Images of the Swelling and Shrinking of Aminated PolyHEMA Microspheres

Aminated polyHEMA microspheres were immobilized on a microscope slide and observed with a Zeiss light microscope. Figure 5.3 shows that the microspheres increase in size as the pH buffer was changed from pH 11 to pH 2. The four highlighted microspheres have a diameter of 5 μm at pH 11. They swell to a diameter of 8.5μm in pH 2 buffer. This change represents a swelling of more than 40 %. It can also be seen that as the particles swell they became more transparent as they take in buffer, scattering less light and thus becoming less visible. In this experiment the buffer was cycled from low to high pH repeatedly in order to condition the microspheres. They were allowed to equilibrate in the buffers for a few minutes before observing the shrinking and swelling properties.

Reproduced with permission of the copyright owner. Further reproduction prohibited without permission.

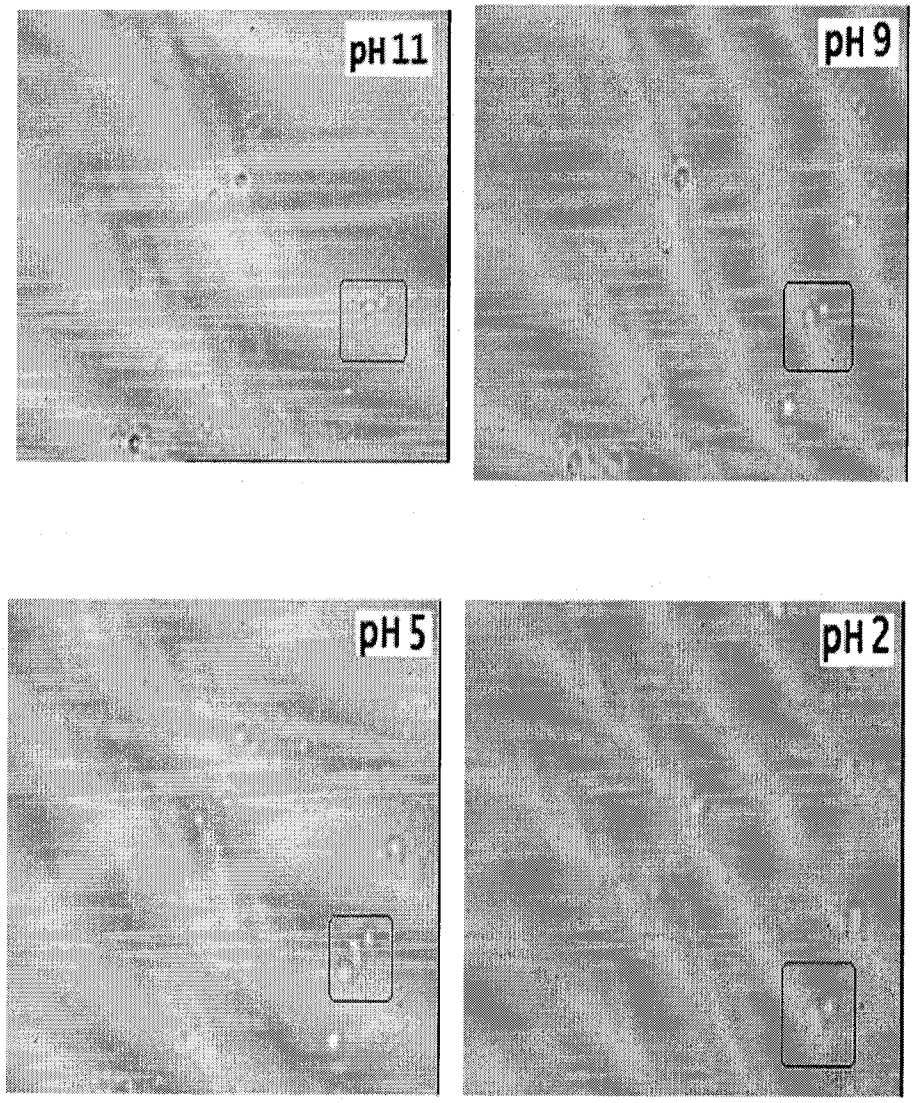

Figure 5.3 Light micrograph images of aminated poly (HEMA) in the swelling process when immersed in buffers from pH 11 to pH 2.The groups of four particles have been highlighted for clarity.

Reproduced with permission of the copyright owner. Further reproduction prohibited without permission.

5.3 Evaluation of Aminated Poly (HEMA) for pH Sensing

The evaluation was done by suspending diethylenetriamine derivatized poly (HEMA) microspheres in PVA and polyurethane membranes. Figure 5.4 shows a typical spectrum in which 1 % (wt/wt) of these microspheres were suspended in a 75 μm -thick polyurethane membrane. The membrane was immersed in different pH buffers and the turbidities were measured with a UV/Vis spectrophotometer.

An interesting feature of this system is observed for the polyurethane membrane, which consists of 68% water. The turbidity of the membrane decreased from pH 2 to pH 10.2 at 25 °C as shown in Figures 5.4 and 5.5. This change is opposite to the trend usually observed during the swelling process. The refractive index of polyurethane at 1.56 is higher that of the microspheres which was determined to be 1.38 in the swollen state. When the microspheres swell, their refractive index decreases. This increases the difference in the refractive indices between the particles and the membrane. According to the Fresnel equation, this will cause the membrane to become less transparent.

On the other hand when the particles are placed in high pH buffer, they become smaller in size. This causes their refractive index to increase. The difference between the two refractive indices decreases, reversing the observation seen earlier. The membrane therefore appears more transparent.

Reproduced with permission of the copyright owner. Further reproduction prohibited without permission.

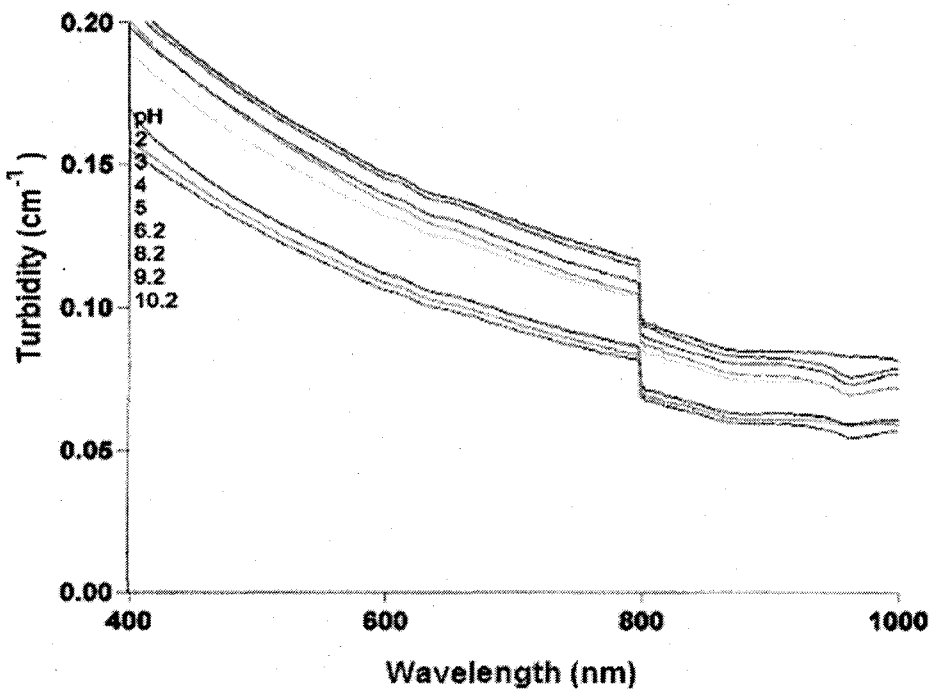

Figure 5.4 Turbidity vs. pH of 1 % diethylenetriamine derivatized poly (HEMA) particles at 25 °C suspended in 76 μm thick polyurethane membrane.

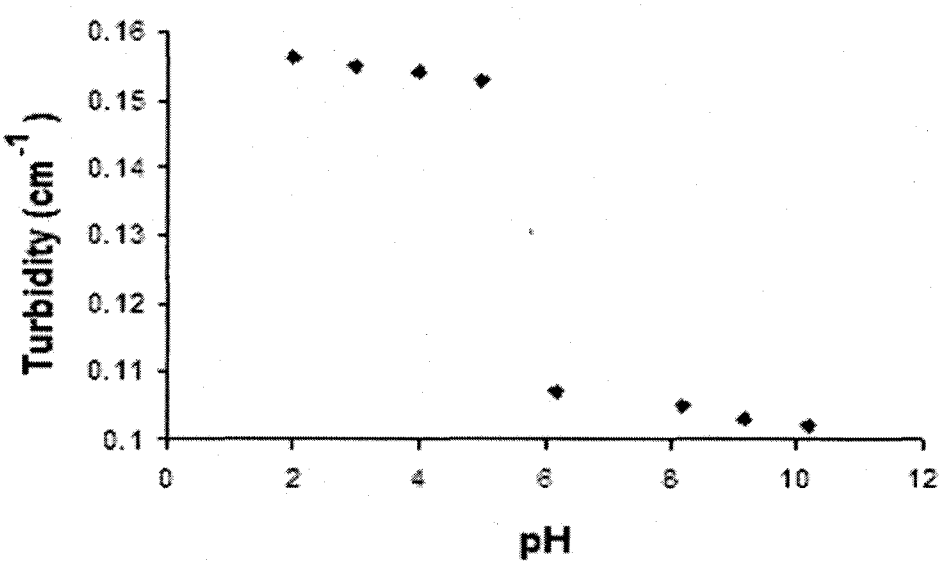

Figure 5.5 Turbidity vs. pH of 1 % diethylenetriamine derivatized poly (HEMA) monitored at 500nm.

Reproduced with permission of the copyright owner. Further reproduction prohibited without permission.

Figure 5.6 shows a typical plot of the turbidity versus pH of the microspheres in a polyurethane membrane, which was cycled between pH 10 to pH 4 and vice-versa. The sensitive pH range is approximately 5 to 7.5. This experiment shows a slight hysteresis effect at higher pH, this may be due to inadequate equilibration. This effect was nevertheless quite small and reduced by allowing the membrane to equilibrate longer in the buffer solutions.

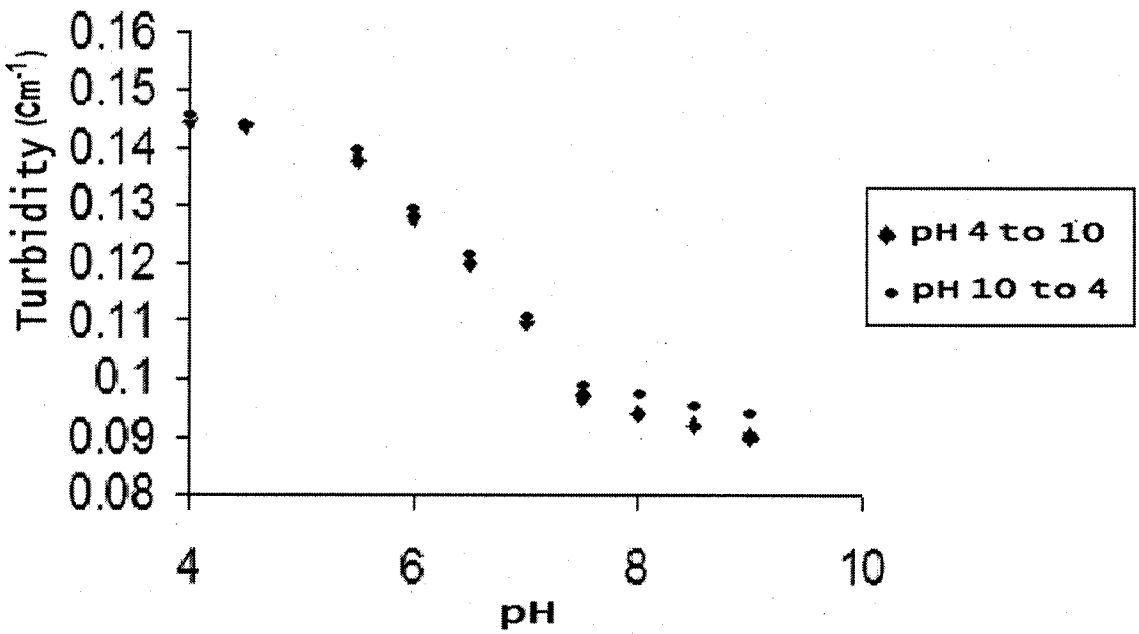

Figure 5.6 The pH response curve of CDI-activated Poly (HEMA) microspheres derivatized with diethlenetriamine. The beads (1% w/w) were in immobilized in a polyurethane membrane and monitored at 600nm.

Reproduced with permission of the copyright owner. Further reproduction prohibited without permission.

Figures 5.7 and 5.8 show that when the aminated poly (HEMA) microspheres are suspended in a PVA membrane the trend of change in turbidity is reversed when compared to polyurethane membrane. Figure 5.8 shows the change in turbidity as function of pH at 500 nm.

In this case the highest turbidity was observed when the microspheres were immersed in pH 10 buffer. This is because the hydrated PVA membrane in which the microspheres were embedded has refractive index of 1.34, which is lower than that of the microspheres at 1.38. These values were determined at 25 ^{o} C and in pH 6 buffer. The change in turbidity is therefore opposite to that observed when using the polyurethane membrane.

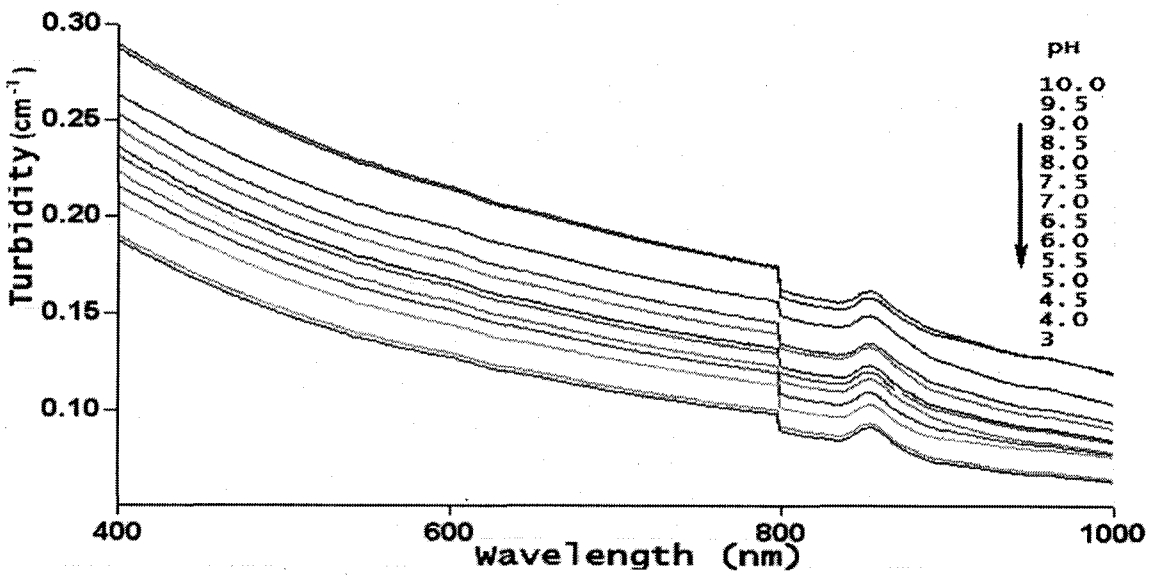

Figure 5.7 0.2 % Diethylenetriamine derivatized poly (HEMA) microspheres suspended in Poly (Vinyl alcohol) membrane.

Reproduced with permission of the copyright owner. Further reproduction prohibited without permission.

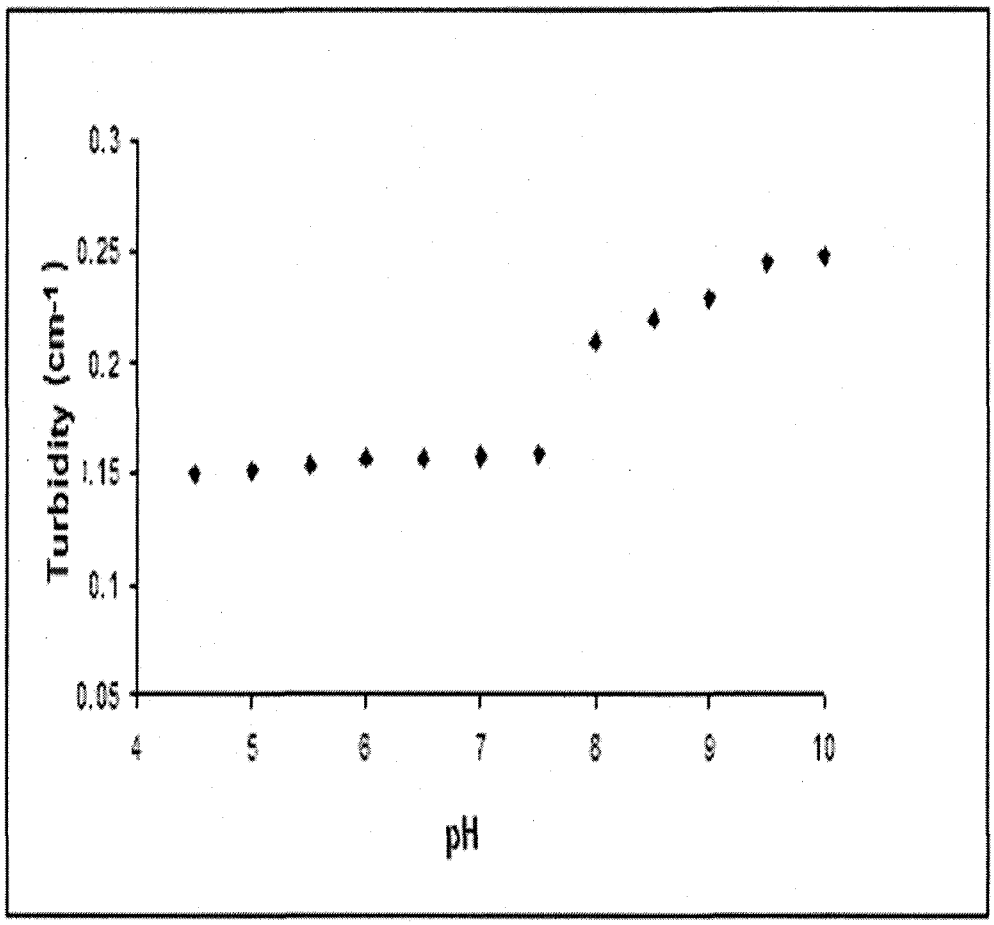

Figure 5.8 0.2 % Diethylenetriamine derivatized poly (HEMA) microspheres suspended in Poly (Vinyl alcohol) membrane. The turbidity was monitored at 500nm.

Reproduced with permission of the copyright owner. Further reproduction prohibited without permission.

5.4 Titration of Aminated Poly (HEMA) Microspheres with Cu^{2+}

Titration experiments were done with the aminated poly (HEMA) microspheres in order to determine the complexation ratio of copper to the amine nitrogen. A cupric ion selective electrode that was first calibrated against standard solutions was used in this determination.

In this experiment, the aminated polymer microspheres were titrated against a 0.02 M Cu^{2+} solution, which was buffered at pH 3.8 and maintained at a constant ionic strength of 0.1 M. The addition of 15 mL of the Cu^{2+} solution saturated the binding sites on the derivatized microspheres, after this volume was added; there was an increase in the amount of detected Cu^{2+}. Figure 5.9 shows that, at the beginning of the titration there was no copper detected by the electrode. This was because the available copper was bound to the ligands of the derivatized polymer. However after these binding sites were saturated further addition of copper showed was reflected by an increase in the concentration of Cu^{2+} in solution.

We used the molarity and volume of the copper solution, the mass percentage of nitrogen determined from CHN analysis and the mass of aminated polymer used in the titration (4.6 %) to calculate the ratio of moles of nitrogen to moles of copper in the complex.

This ratio of copper to nitrogen in the complex was found to be 0.5, indicating that every Cu^{2+} was coordinated in an environment between two nitrogen atoms of the diethylenetriamine functional group of the polymer microspheres. There was no evidence of the formation of 2:1 complexes between two ethylenediamine molecules per one of copper.

Reproduced with permission of the copyright owner. Further reproduction prohibited without permission.

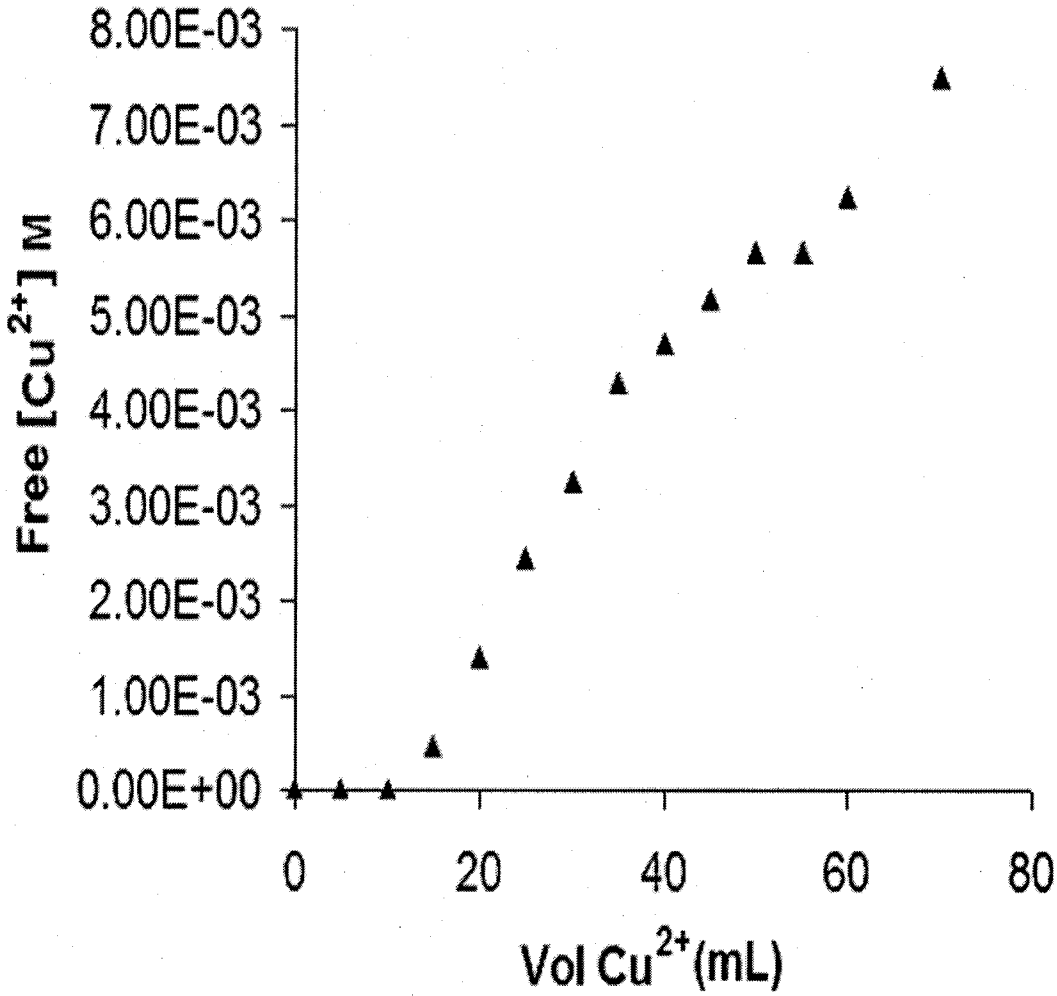

Figure 5.9 Potentiometric titration of Poly (HEMA)-CDI-Diethylenetriamine Derivatized beads with 0.02M $Cu.^{2+}$

Reproduced with permission of the copyright owner. Further reproduction prohibited without permission.

In order to determine the response time of the polymer to copper, we added 20 mL of 0.05 M Cu^{2+} solution to 2.5 g of the aminated poly (HEMA) dissolved in 20 mL of pH 5.8 buffer. Figure 5.10 shows the progressive reduction in free copper, as the copper was continuously removed from solution and being complexed to the aminated polymer. It takes about 3 hours for the concentration of copper to fall to zero. The process is slow especially when it takes place in solution. This may be because surface adhered copper may cause repulsion preventing the bulk of the copper ions from accessing the polymer core.

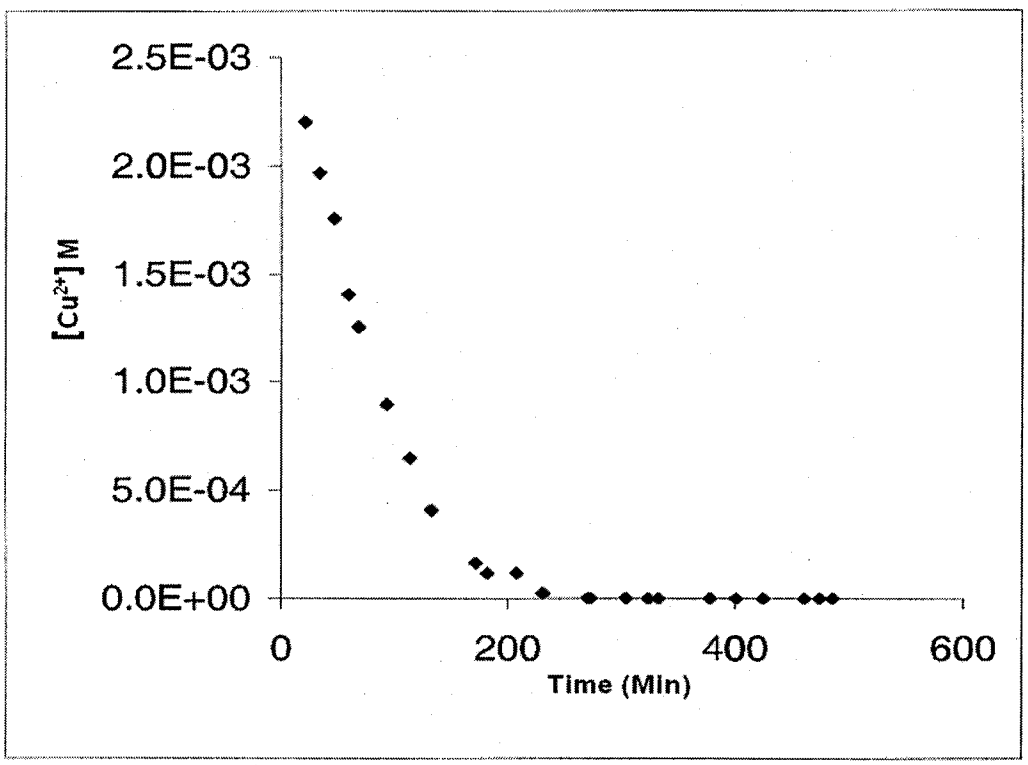

Figure 5.10 Response time of poly HEMA-CDI-Dithylenetriamine to Cu^{2+}. The polymer and copper were mixed and the response time monitored potentiometrically with a cupric ion elective electrode.

Reproduced with permission of the copyright owner. Further reproduction prohibited without permission.

5.5 Copper Turbidity Spectra for diethylenetriamine Derivatized Microspheres.

Diethylenetriamine derivatized microspheres were embedded in a hydrogel membrane and turbidity spectra were obtained. The amount of nitrogen derivatized on the polymer was determined to be 2.5 % by mass from CHN analysis. Figure 5.11 shows the spectra obtained with 3% by mass of the microspheres embedded in polyurethane membrane. The membrane was immersed in copper solutions of increasing concentration from 1 x 10^{-4} M to 1 x 10^{-2} M. The copper solution was buffered at pH 5. As the concentration of copper increased the turbidity also increased showing that complexes were being formed between the copper and the nitrogen atoms of the amine ligands.

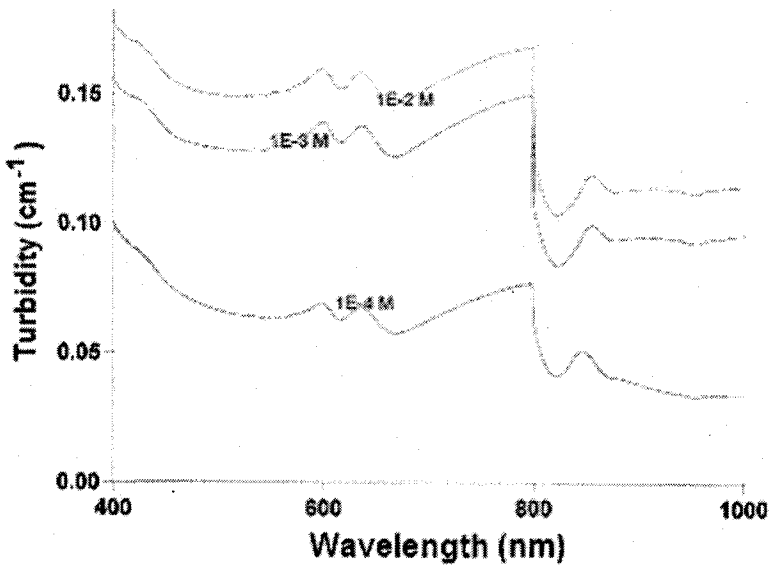

Figure 5.11 Turbidity response of PolyHEMA-CDI-Diethylenetriamine beads to Cu(II) at pH 5.5 The glitch at 800 nm is due to the spectrophotometer changing detectors.

Reproduced with permission of the copyright owner. Further reproduction prohibited without permission.

Figure 5.12 shows the turbidity spectra of polyHEMA-CDI-Diethylenetriamine microspheres 3% by mass in polyurethane membrane and how they respond to Cu^{2+} concentration. The nitrogen from the amine groups was 4.6% by mass. This experiment was performed with a narrow range in copper concentrations from 1.5 x 10^{-2} M to 7 x 10^{-2} M. The copper solution was made in pH 10 ammonia buffer. The response observed in this spectrum was better than in the previous spectrum. This better response may be attributed to two reasons, first the higher percentage of nitrogen provides more sites for copper to complex and second, because the pH of the copper solution was maintained at pH 10, most of the copper was kept in solution and available to complex with the nitrogen groups on the polymer.

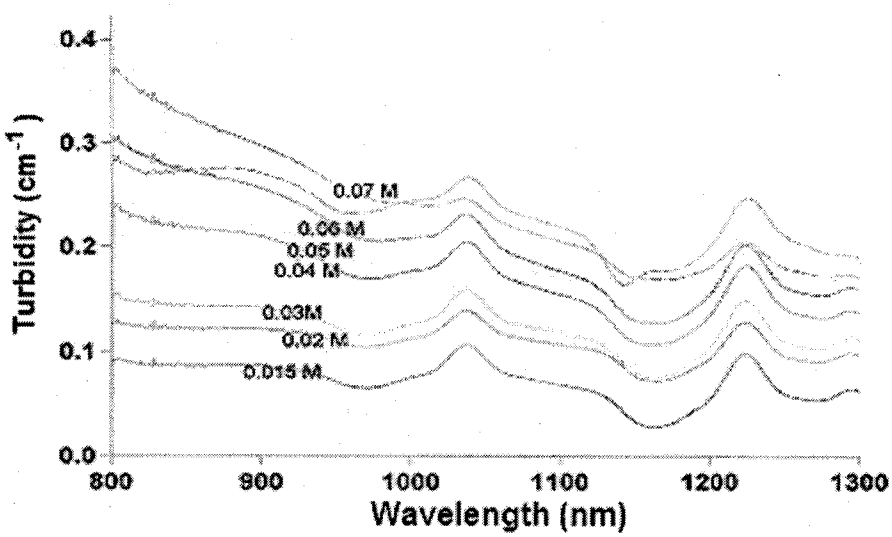

Figure 5.12 PolyHEMA-CDI-Diethylenetriamine 3% embedded in polyurethane membrane. Response to Cu^{2+} in pH 10 buffer.

Reproduced with permission of the copyright owner. Further reproduction prohibited without permission.

5.6 Determination of Copper to Nitrogen Complexation Ratio

In this experiment, the mole ratio of Cu^{2+} to nitrogen in the complex was determined. In order to do this, it was necessary to determine the total Cu^{2+} in the membrane. Aminated poly (HEMA) microspheres were suspended on a polyurethane membrane and the membrane immersed in copper solutions of increasing concentration, which were buffered at pH 10. The membrane was then treated with 1 M HCl to extract the Cu^{2+}, the amount of copper extracted was quantified by atomic absorption spectrometry. Since the percentage of nitrogen in the polymer had been determined from elemental analysis, it was now possible to calculate its complexation ratio with copper.

Figure 5.13 shows that there was a continuous increase of the mole ratio of Cu^{2+} : N as the membrane was immersed in the copper solutions of higher concentrations. This trend continued until the membrane was immersed in copper solutions greater than 0.1 M at which point it leveled off and became steady. This corresponds to a Cu^{2+} : N mole ratio of 0.5 suggesting that each copper ion is complexed with two nitrogen atoms, which supports the earlier determination, which had been performed potentiometrically.

Reproduced with permission of the copyright owner. Further reproduction prohibited without permission.

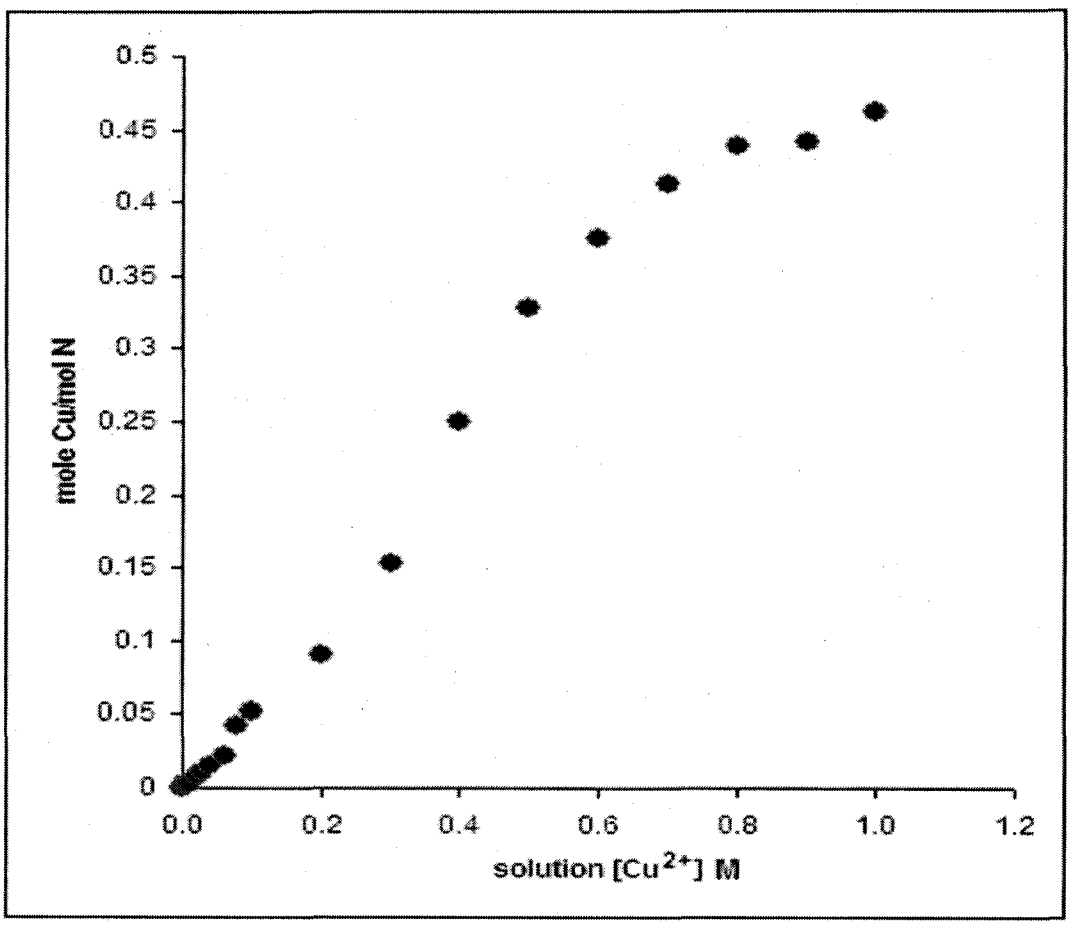

Figure 5.13 Copper complexation of Poly(HEMA-CDI-Diethylenetriamine) derivatized microspheres 3% by mass suspended in polyurethane membrane.

The percentage of suspended polymer microspheres in the polyurethane hydrogel membrane was decreased to 1 % w/w and the result of the copper

Reproduced with permission of the copyright owner. Further reproduction prohibited without permission.

complexed by the microspheres is shown in Figure 5.14. It can be seen that the mole ratio of copper to nitrogen becomes constant when the membrane is immersed in copper solutions of greater that 0.3 M Cu^{2+}, a much lower concentration than the last experiment. The mole ratio is however close to that observed when higher amounts of the microspheres were used.

These results show that although Cu^{2+} has a strong tendency to form four-coordinate complexation with ligands, it coordinates with two nitrogen groups in this polymer. The fact that the mole ratio observed in Figure 5.14 is less than 0.5 suggests that some amino groups in the polymer may only be partially coordinated to the copper. Both figures 5.13 and 5.14 show an initial steep slope, which then gradually flattens out before becoming constant at high copper concentrations. This is because at the beginning of the complexation process, when there is a large excess of the nitrogen atoms over the copper, all the available copper is well complexed, with many other amino groups still available for complexation.

As the membrane is immersed in higher concentrations of copper solutions, the nitrogen groups become saturated and repulsion begins to come into play. This may prevent more copper from interacting with the polymer. When all the amino groups have been occupied, a constant mole ratio is obtained which indicates the capacity of the polymer microspheres for copper ions.

Reproduced with permission of the copyright owner. Further reproduction prohibited without permission.

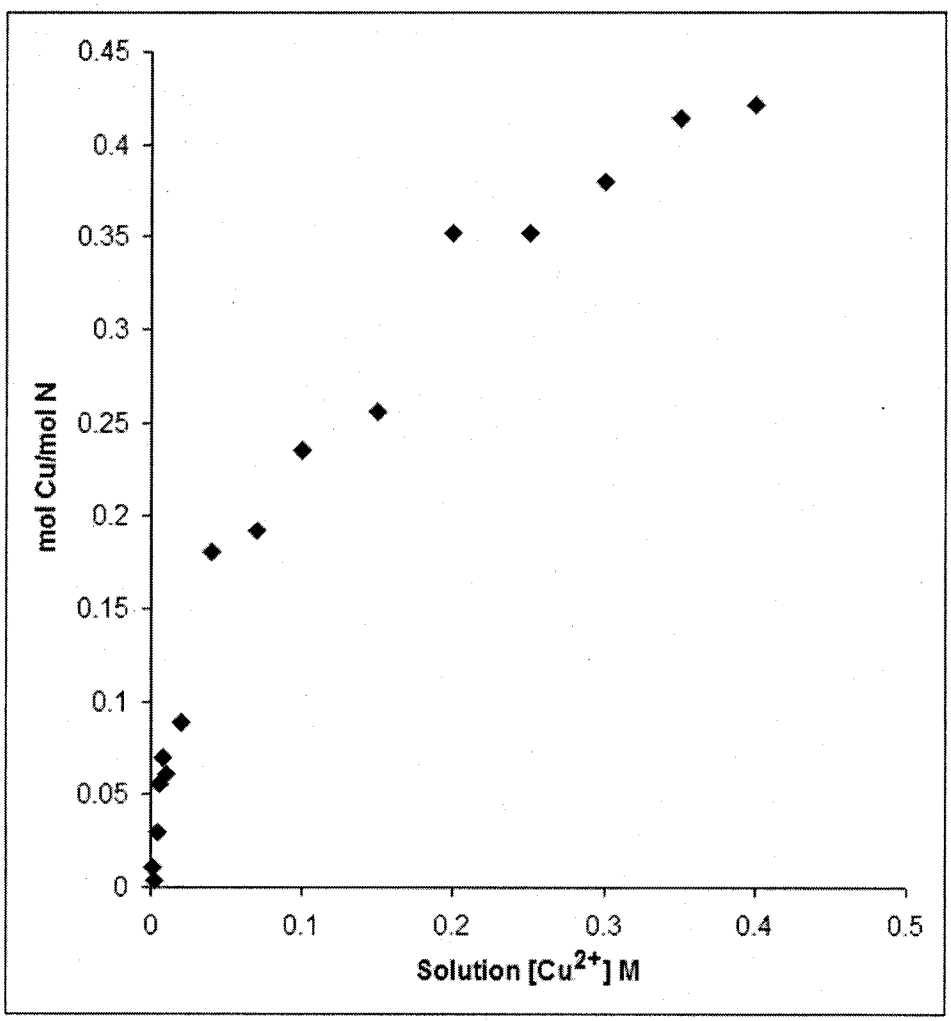

Figure 5.14 Copper complexation of poly (HEMA-CDI-Diethylenetriamine) derivatized microspheres 1% by mass suspended in Polyurethane membrane.

Reproduced with permission of the copyright owner. Further reproduction prohibited without permission.

5.7 Electron Paramagnetic Spectra

EPR (Electron Paramagnetic Resonance) or ESR (Electron Spin Resonance) is a magnetic resonance method formally related to NMR (nuclear magnetic resonance). It is a well-established method that has been used for the investigation of the structure of complexes. The basis of this method is the interaction of unpaired electrons in the sample with an external magnetic field produced by the EPR spectrometer.

The interactions of Cu^{2+} ions with amino groups of various ligands have been the subject of many investigations.[95,96] Transition metals like copper normally have a wide range spectrum (several hundred gauss). The g-factor and the hyperfine (hf) interaction are very sensitive to the environment that is the kind of coordination, of the metal ions. From the analysis of the g and hf tensors, it is possible to determine the kind of coordination. In this study the results have been interpreted by comparing the aminated poly (HEMA)- Cu^{2+} complexes with a series of models, which were made up of ethylenediamine complexed with Cu (II) at different mole ratios.

Figures 5.15 A-D show the EPR spectra of the model ligand, ethylenediamine that had been complexed with Cu^{2+} at different mole ratios. Figures 5.16 and 5.17 show the spectra of the aminated poly (HEMA) polymer complexed with copper. By comparing these spectra we arrived at the conclusion that the EPR spectra of the polymer most closely resembled that of Figure 5.15 B, where the mole ratio of amine to copper was 0.5:1, because of the highlighted features.

Reproduced with permission of the copyright owner. Further reproduction prohibited without permission.

EPR Spectra

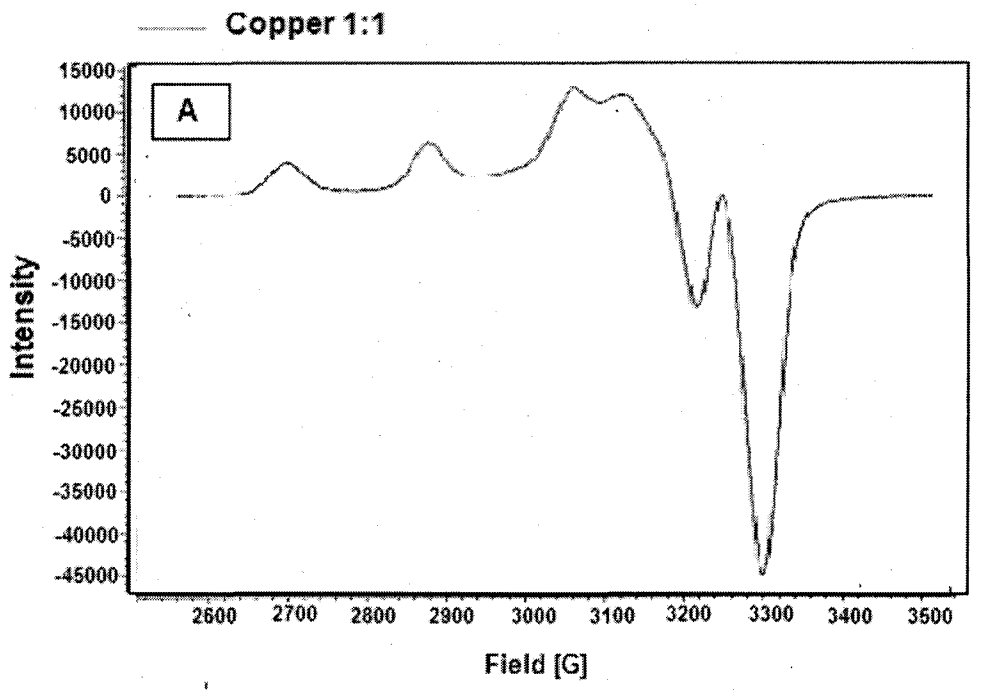

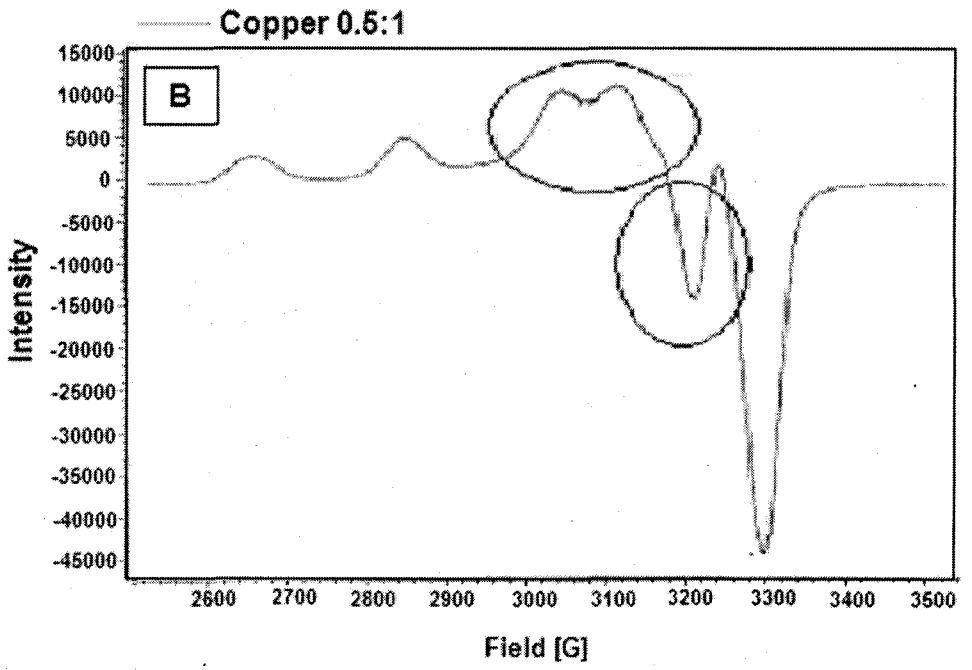

Figure 5.15 **A and B** electron paramagnetic spectra of the complexes of Cu^{2+} with the model ligand Ethylenediamine. The ratios refer to the mole ratio of copper to Ethylenediamine in the complex.

Reproduced with permission of the copyright owner. Further reproduction prohibited without permission.

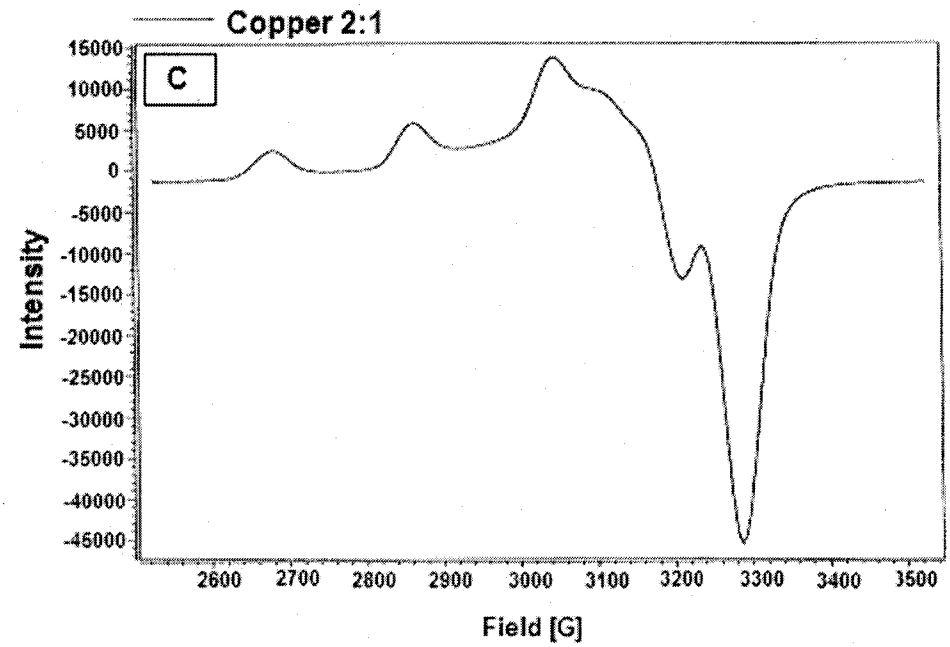

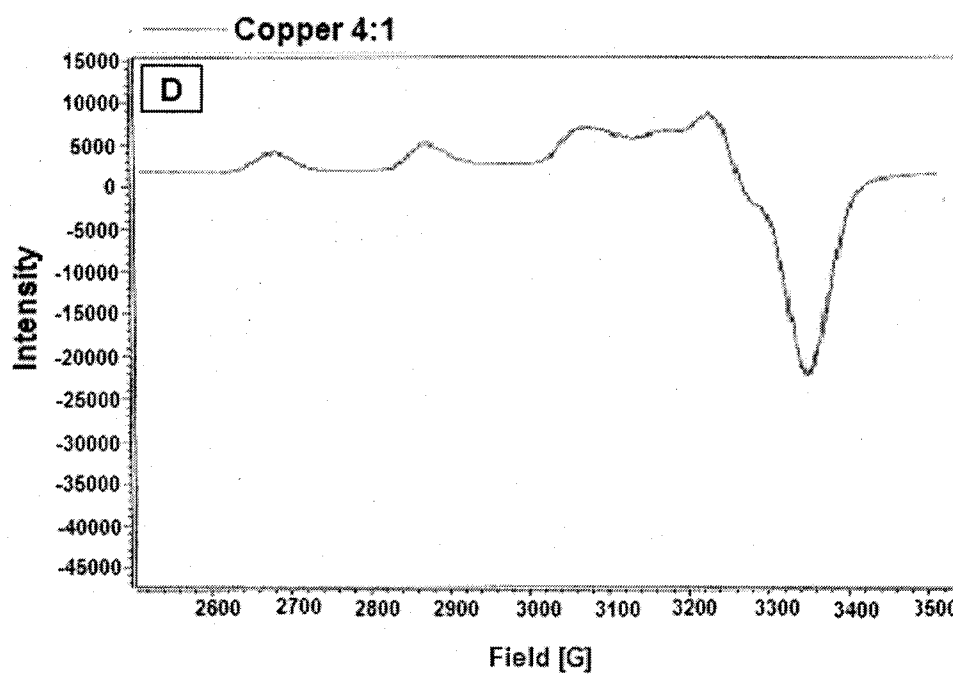

Figure 5.15 C and D Electron paramagnetic spectra of the complexes of Cu^{2+} with the model ligand Ethylenediamine. The ratios refer to the mole ratio of copper to Ethylenediamine in the complex.

Reproduced with permission of the copyright owner. Further reproduction prohibited without permission.

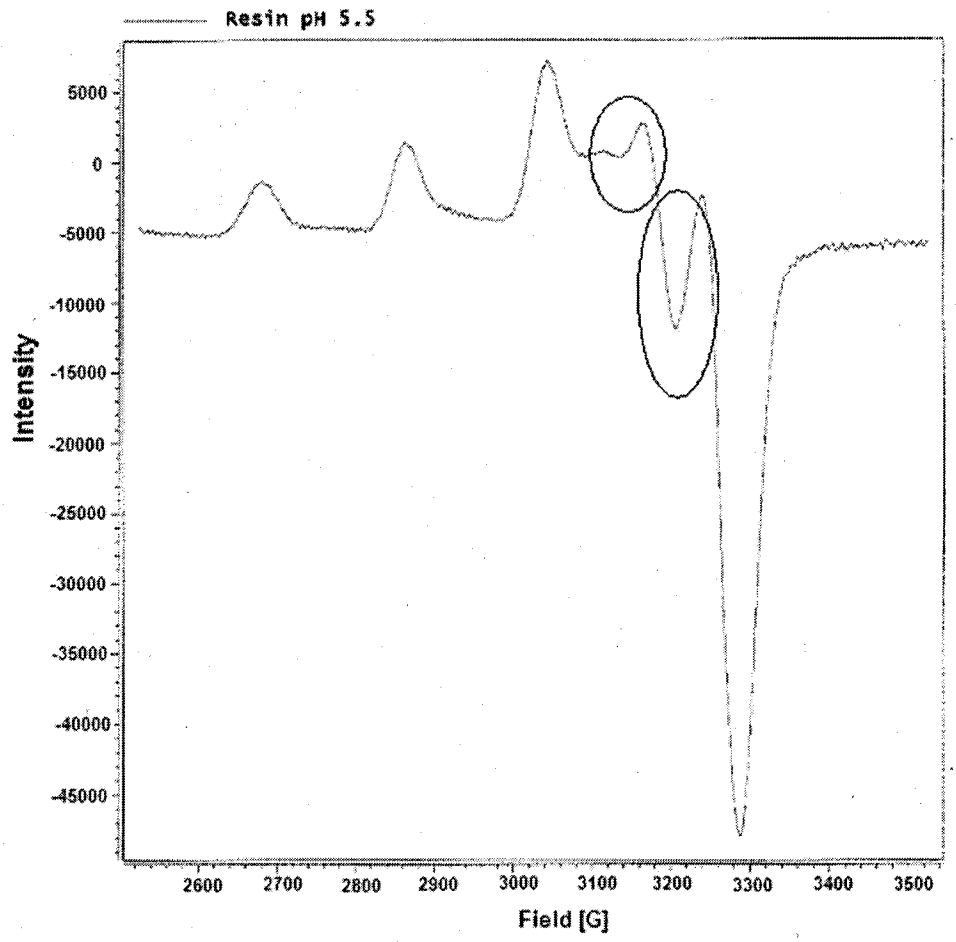

Figure 5.16 EPR spectrum of diethylenetriamine derivatized poly (HEMA). The solution was buffered at pH 5.5.

Reproduced with permission of the copyright owner. Further reproduction prohibited without permission.

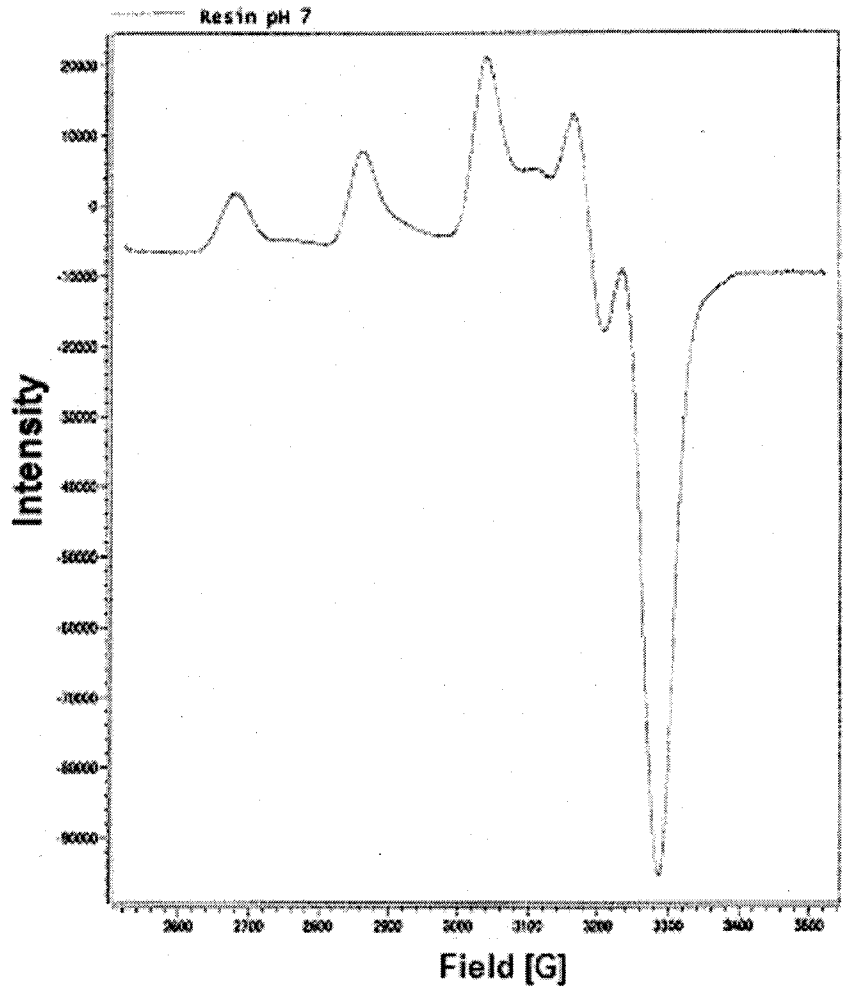

Figure 5.17 EPR spectrum of diethylenetriamine derivatized poly (HEMA). The solution was buffered at pH 7.0.

Reproduced with permission of the copyright owner. Further reproduction prohibited without permission.

This result may be explained by considering the kind of complex formed between the nitrogen of the amino acids and copper. At low pH the protons compete effectively with the Cu^{2+} to complex with the ligand atoms, the predominant species in solution at this pH is $Cu(H_2O)_6{}^{2+}$, at higher pH the Cu^{2+} is able to compete with the protons for the lone pair of electrons on the nitrogen of the amine. This results in substitution of the water molecules by the nitrogen atoms of the polymer amino groups. The EPR spectra were obtained at pH 5.5 and 7.0.

The EPR spectra obtained from the aminated poly (HEMA) was typical of tetragonally elongated octahedrally coordinated Cu^{2+}, in which the Cu^{2+}, two nitrogen atoms and two water molecules form an approximately planar geometry. The axial water molecules are coordinated less strongly because of the Jahn-Teller distortion effect[95], which is a common feature in all Cu^{2+} species.

Reproduced with permission of the copyright owner. Further reproduction prohibited without permission.

5.8 Conclusions

The aim of the work described in this chapter was to synthesize microspheres that can be used for chemical sensing. The microspheres swell and shrink in response to specific analytes of interest. The research focused mainly on the sensing of pH and copper ions in aqueous solution.

The preparation and derivatization of polyHEMA microspheres was discussed in the first part of this chapter. The microspheres were prepared by dispersion polymerization and were of the order of 1-3 μm. Polyurethane, PVA and HYPAN hydrogels were used to suspend the microspheres before evaluating them with UV-Vis spectrophotometry.

Results obtained with the last two types of membranes were different from those obtained with the initial ones. This difference was due to the differences between the refractive indices of the microspheres and that of the hydrogel. When a polyurethane membrane was used, the swelling cycle showed an increase in turbidity while the shrinking of the microspheres exhibited less turbidity. A slight hysteresis effect was observed on moving from the low to the high pH buffer. This may be attributed to the incomplete equilibration. Allowing enough time for the membrane to equilibrate was necessary to reduce this effect.

The second part of this chapter discussed how the stoichiometry of the Cu^{2+}, complexes with derivatized polyHEMA was established. This was done using three different methods. A titration experiment was first performed in which the concentration of nitrogen groups present in the derivatized polymer microspheres was estimated by elemental analysis. Titration of the microspheres against copper

Reproduced with permission of the copyright owner. Further reproduction prohibited without permission.

solution using a cupric ion selective electrode showed that the ratio of Cu^{2+}:N in the complex was 1:2.

The second method involved suspending the derivatized microspheres in a hydrogel membrane and immersing the membrane in copper solutions of increasing concentrations. The complexed copper was then removed from the membrane by putting it in a 1M HCl solution and quantifying the copper by atomic absorption spectrometry. This method also indicates a 1:2 complex between copper and nitrogen. The above two results were finally confirmed by investigating the complex, using electron paramagnetic resonance spectrometry. A series of model complexes were first run and by comparing their spectra with that obtained in this experiment, this suggested that the ratio of copper to nitrogen in the complex was 1:2. This information is required to relate the response of the derivatized microspheres to Cu^{2+}.

Reproduced with permission of the copyright owner. Further reproduction prohibited without permission.

CHAPTER 6

MOLECULARLY IMPRINTED POLYMER MICROSPHERES FOR ROOM TEMPERATURE THEOPHYLLINE SENSING

6.1 Introduction

Our research on molecular imprinted polymers was inspired by a study done by Watanabe *et al*[83] in which it was shown that synthetic polymer gels can undergo large swelling change, but still retain molecular recognition ability in the shrunken states. In these experiments, thermosensitive copolymer gels were made of NIPA (8 mmols), acrylic acid (2 mmols) and 0.5 mmols NN'-methylenebis(acrylamide). The gels were prepared in the presence of guest molecules like *dl*-norephedrine hydrochloride or *dl*-adrenaline hydrochloride (templates) and in the absence of them (for reference gels).

The polymerization was carried out in glass capillaries so that the gels appeared as thin strands. The volume of the strands was measured as a function of temperature by observing the change in length. It was found that volume decreased with increasing temperature. Crosslinking and the presence of the acrylic acid functional group caused the polyNIPA transition temperature to occur over a wide temperature range. The decrease in volume at elevated temperature was less in the presence of template. Untemplated copolymers did not show any effect and the adrenaline templated polymers reacted only to adrenaline and never to norephedrine, and vice-versa.

Reproduced with permission of the copyright owner. Further reproduction prohibited without permission.

These observations encouraged us to pursue the possibility of templated microspheres for chemical sensing. Our choice of using theophylline as the template was based on a literature report[82] which described the preparation of molecularly imprinted sorbents using dispersion polymerization with theophylline and estradiol as the templates. Theophylline is one of the most commonly used medications for the treatment of the symptoms of chronic asthma. Its most important actions are to prevent the signs and symptoms of asthma and reduce the need for cortisone type medication. It is a bronchodilator, relaxing muscles around the airway, allowing air to travel more freely in and out of the lungs.

Different individuals require different amounts of theophylline in order to achieve the desired results of the medication. One person may require a dosage of 4 or 5 times higher than another. It is therefore important to measure the amount of theophylline circulating in the blood system and to determine if the right amount is being taken. Accumulation of theophylline in the plasma can also lead to fatal toxicity, thus it is crucial to monitor the concentrations of this drug in the body as frequently as possible.

Various analytical methods have been employed for theophylline detection and quantification. These include HPLC,[3] immunoassays,[4,5] spectrophotometric,[6]CE,[7] GC[8] and GC-MS.[9] Most of these methods have the distinct disadvantage of requiring elaborate and time consuming pre-treatment steps prior to introduction into the analytical systems. HPLC demands that the samples first undergo filtration[10] or extraction.[11]

Reproduced with permission of the copyright owner. Further reproduction prohibited without permission.

Fan[92] prepared molecularly imprinted poly NIPA-MAA microspheres by dispersion polymerization in acetonitrile. 20 % poly (acrylonitrile-co-styrene) was used as the stabilizer and the resulting microspheres were fairly uniform and spherical with diameter ca. 1.0 μm. The most important factors affecting polymer swelling, the percentages of NIPA and crosslinker were investigated in this study. Increased NIPA level and decreased crosslinker level led to larger swelling and shrinking. However it was found that decreased NIPA (increased functional monomer, MAA) and increased crosslinker resulted in increased selectivity.

A high ratio of template to functional monomer resulted in more recognition sites in the polymer but a large amount of template was shown to affect the polymerization. The NIPA-MAA microspheres were embedded in a PVA membrane and evaluated for response and selectivity, they were found to be suitable for sensing theophylline in water at temperatures up to 50 ^{o} C at concentrations as low as 1.0 x 10^{-8} M theophylline. There was no response to caffeine up to 1 x 10^{-3} M showing high selectivity. In order to use the sensor at room temperature in water, work was done to shift the phase transition to low temperature by replacing part of the NIPA with N-tert-butylacrylamide (NTBA) or all of the NIPA with N-n-propylacrylamide (NNPAM).

It was found that the optimum formulation for poly NIPA-NTBA-MAA microspheres was 60% NIPA, 15 % NTBA, 20 % MAA, 5% MBA and 2/1 of MAA to theophylline (THO). The phase transition was brought down to ~ 12 ^{o} C. The optimum concentrations of reactants for polyNNPAM-MAA was found to be 75 % NNPA, 20 % MAA, 5% MBA and 2/1 MAA to THO.

Reproduced with permission of the copyright owner. Further reproduction prohibited without permission.

In other studies,[92] the effect of pH on turbidity and transition of PolyNIPA-MAA was investigated. The carboxyl group of MAA on the polymer backbone can be deprotonated at high pH. MAA which has a pK_a of ~4.7 is protonated at low pH and there is no charge on the polymer backbone.

6.2 Results and Discussion

In the present study, molecularly imprinted polymers for sensing theophylline at room temperature were prepared and investigated. Based on an earlier study[92] it was determined that particles with a 2:1 ratio of recognition monomer to template showed a larger turbidity change at higher concentrations. This observation is important because it indicates that we have some control over the binding population by varying the ratio of recognition monomer.

Figure 6.1 shows the turbidity of polyNIPA copolymerized with methacrylic acid at pH 7. A formulation of 0.5 mmols MBA crosslinker, 2 mmol MAA functional monomer, 9 mmols NIPA and 0.2 mmols theophylline were used. The formulation for Figure 6.3 is the same except that it has 1 mmol MAA and 8 mmol NIPA. Both figures show that turbidity increases with increase in theophylline concentration. This may be because at pH 7 the MAA groups on the polymer are deprotonated and are negatively charged. Increasing the concentration of theophylline neutralizes this charge. The polymer therefore shows an increase in turbidity as more of the deprotonated sites on the polymer are neutralized. Figure 6.2 shows the results when data from figure 6.1 was monitored at a single wavelength (500nm). Figure 6.3 shows that there was no big change in turbidity when the concentration of the functional monomer was reduced by 50%.

Reproduced with permission of the copyright owner. Further reproduction prohibited without permission.

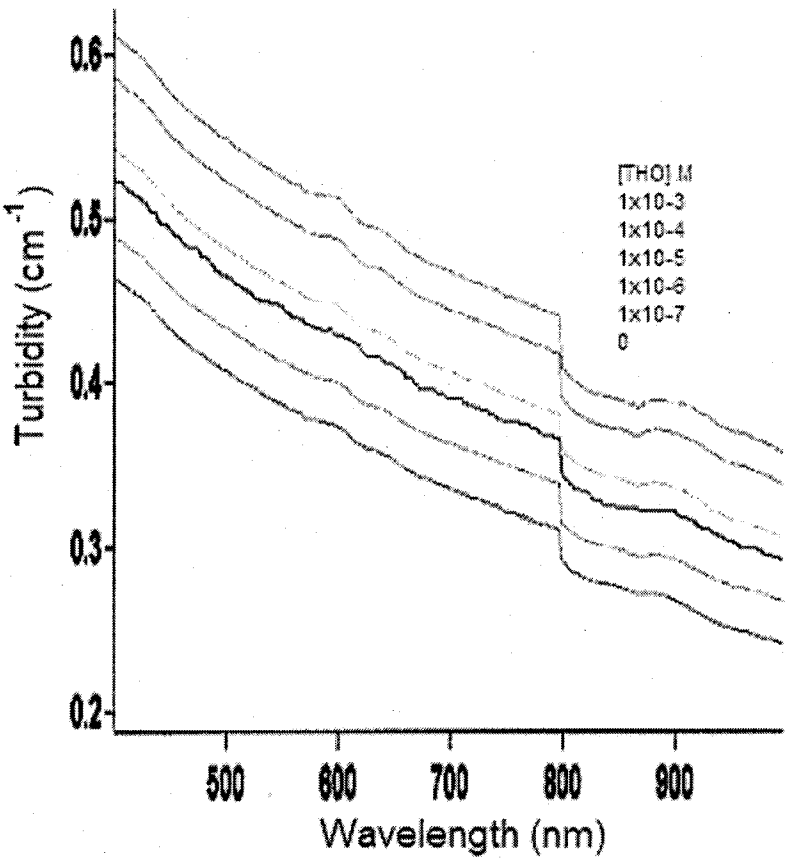

Figure 6.1 Response of templated PolyNIPA-co- MAA to theophylline concentration at room temperature and pH 7. 20 % of MAA was used in this formulation

Reproduced with permission of the copyright owner. Further reproduction prohibited without permission.

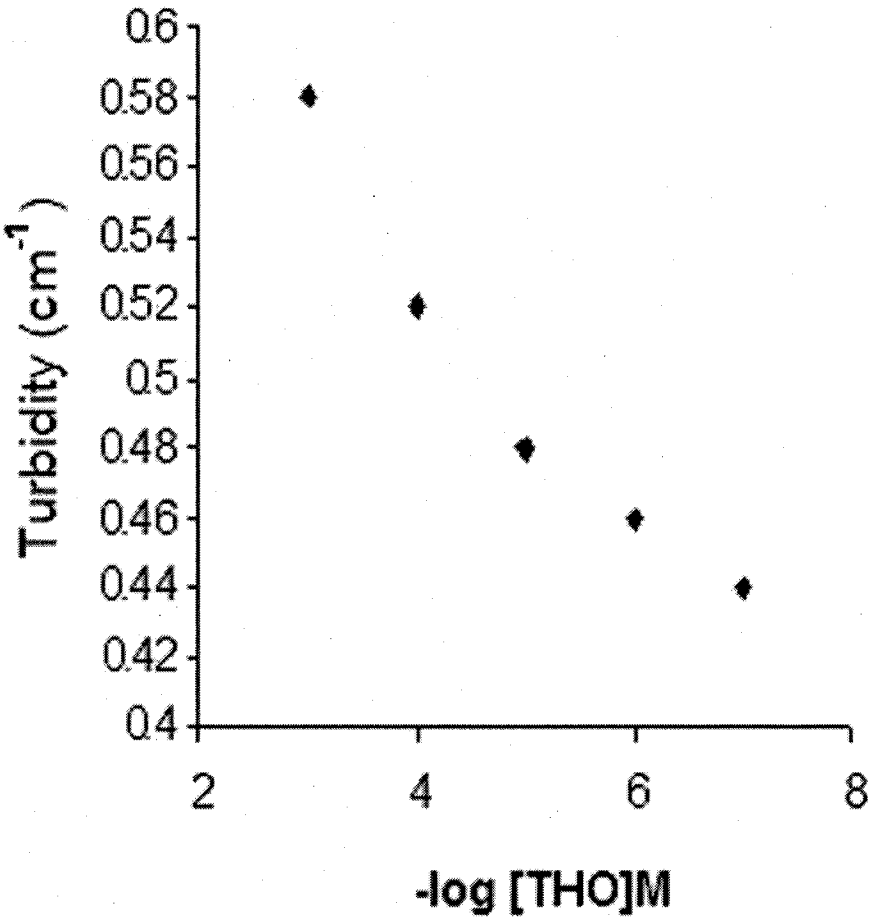

Figure 6.2 Response of templated PolyNIPA-co- MAA to theophylline concentration at room temperature and pH 7.The spectrum was taken at 500nm.

Reproduced with permission of the copyright owner. Further reproduction prohibited without permission.

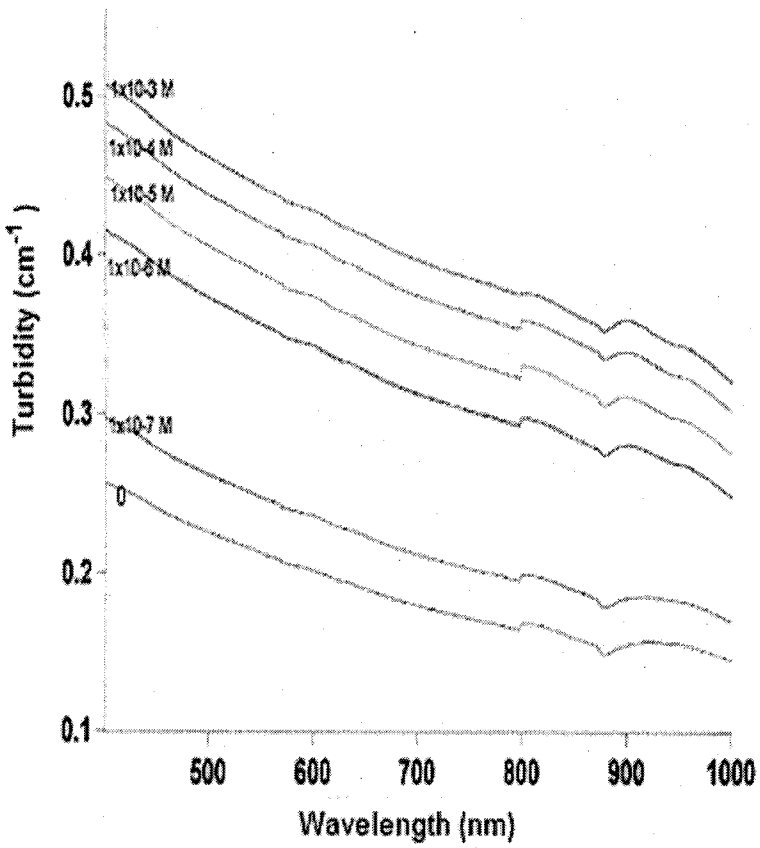

Figure 6.3 Response of templated PolyNIPA-co- MAA to theophylline concentration at room temperature and pH 7. 10 % of MAA was used in this formulation

Reproduced with permission of the copyright owner. Further reproduction prohibited without permission.

6.3 Conclusion

Theophylline templated, swellable molecularly imprinted polymer microspheres were prepared by dispersion polymerization. Particles of the order of 1.0 μm were obtained. The main formulation reagents that affect the swelling properties of the microspheres were the percentages of principal monomer NIPA, crosslinker and functional monomer. A 50 % reduction in the concentration of the MAA functional monomer was found to enhance the turbidity of the microspheres at pH 7. The microspheres were evaluated for selectivity and response to theophylline at room temperature. PVA membranes were used for suspending the microspheres before evaluating the turbidity changes with a Cary 5 UV spectrophotometer. This was only an empirical study and further investigation should be undertaken to better understand the properties of the molecularly imprinted polymers.

Reproduced with permission of the copyright owner. Further reproduction prohibited without permission.

CHAPTER 7

MOLECULAR IMPRINTED POLYMERS BASED ON UNCROSSLINKED AND FLUORESCENTLY LABELLED POLYMERS

7.1 Introduction

Fluorescent chemical sensors have received a lot of attention due to their ability to detect analytes at low concentrations.[104-107] The main advantage of fluorescence detection compared to absorption measurements is the greater sensitivity. This is achievable because the fluorescence signal has, in principle, a zero background. Hydrogen bonding plays an important role in the interaction between polymers and solvents. At low temperatures it enhances solubility of the polymer, but because hydrogen bonds are thermally labile an increase in temperature reduces the number of bonds which eventually causes phase separation.[54]

This study was inspired by research done by Uchiyama *et al,*[62] in which five fluorescent monomers having a benzofurazan skeleton were synthesized and the co-polymers of NIPA and small quantities of the fluorescent monomers were investigated for their fluorescence properties. These fluorophores fluoresce efficiently only in non-polar environments and are quenched in water and other polar solvents.[62]

Reproduced with permission of the copyright owner. Further reproduction prohibited without permission.

Fluorescence spectra and quantum yields are more dependent on the environment than absorption spectra and extinction coefficients. There are many environmental factors that exert influence on fluorescent properties. The three most common are:

- Solvent polarity
- Proximity and concentrations of quenching species
- pH of the aqueous medium

Fluorescence spectra strongly depend on the solvent especially with fluorophores that have large excited-state dipole moments, which result in spectral shifts to longer wavelengths in polar solvents. Representative fluorophores of this type include dansyl, and benzoxadiazole, which was used in the present study. These fluorophores have been found to be effective probes of environmental polarity, for example in a protein interior.[104]

Binding of a probe to its target may dramatically affect its fluorescence quantum yield. Some probes exhibit high quantum yields when bound to a particular target but are otherwise effectively non-fluorescent when unbound. Fluorescence quenching can be defined as a bimolecular process that reduces the fluorescent quantum yield without changing the fluorescent spectrum. It may be caused by transient excited state interactions (collisional quenching) or from formation of ground state species. Extrinsic quenchers like oxygen and heavy ions such as iodide, reduce fluorescence quantum yields in a concentration dependent manner.

Reproduced with permission of the copyright owner. Further reproduction prohibited without permission.

Many fluorophores are quenched by water.[105] Examples are NBD (used in this research), and fluorescein. Acrylamide polymers undergo a temperature dependant phase transition. They can be used to sense temperature changes. The polymer is labeled with a fluorophore that is affected by the change in environment that accompanies the phase transition.[62]

Co-polymers of NIPA and the fluorescent monomers dissolve at low temperature and very low fluorescence is observed. When the fluorophore is exposed to an aqueous environment, the fluorescence is quenched. When the temperature is increased, the phase transition occurs and there is a large increase in the fluorescence of the polyNIPA as it comes out of solution. The polyNIPA collapses around the fluorophore displacing water. The fluorescence increases due to the formation of an increased non-polar environment around the fluorophore. It was seen that with an increase in temperature the co-polymer had a phase transition at ~ 32° C. The fluorescene of the co-polymers increased at this temperature. These results inspired us to pursue the possibility of developing theophylline templated polymers that change fluorescence characteristics upon binding with the template.

We started by synthesizing a fluorescent monomer with a benzofurazan skeleton. Derivatizing agents based on the benzofurazan (2,1,3-benzoxadiazole) backbone have found widespread application for bioanalytical and environmental purposes.[62] A copolymer of this benzofurazan monomer and NNPAM was then prepared. The starting level of the fluorescent monomer was set at 0.1 mol % of the NNPAM because a larger percentage of fluorescent groups in the copolymer has

Reproduced with permission of the copyright owner. Further reproduction prohibited without permission.

been shown to affect the temperature induced phase transition due to the NNPAM units.[62]

We determined the fluorescent spectra of the synthesized copolymers at different temperatures. In these experiments we used NNPAM rather than NIPA, because it has a lower phase transition. This allows us to observe template binding at lower temperatures. At low temperatures, both NNPAM and NIPA based polymers are soluble in water. At high temperature they come out of solution. This process causes a change in the fluorescence intensity when the polymer is copolymerized with an environment sensitive fluorophore.

NNPAM, methacrylic acid (or acrylic acid), and benzofurazan copolymers were prepared in the presence of theophylline template. The complete procedure is outlined in Section 3.5. The polymer was evaluated by spectrofluorimetry for selectivity for theophylline and compared to caffeine both of which have the same structure, but for the methyl group in caffeine, instead of hydrogen (Figure 7.1)

Reproduced with permission of the copyright owner. Further reproduction prohibited without permission.

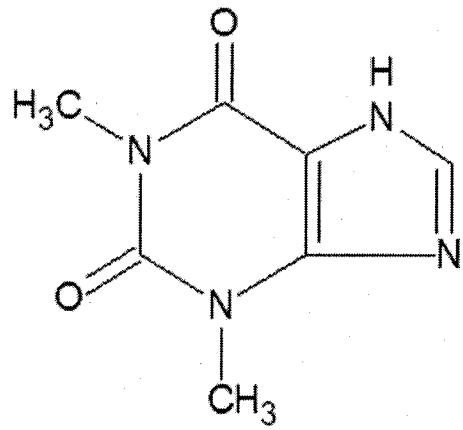

Theophylline

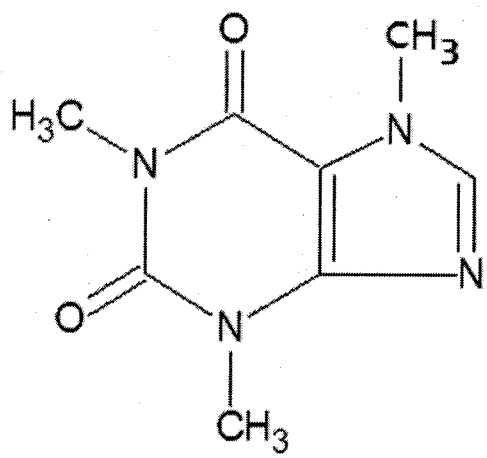

Caffeine

Figure 7.1 The structures of Theophylline and Caffeine.

Reproduced with permission of the copyright owner. Further reproduction prohibited without permission.

7.2 Temperature Response of Uncrosslinked Templated PolyNNPAM

Figure 7.2 shows the change in fluorescence as function of temperature for polyNNPAM-co-AAC-co-NBDAE2. It can be seen that this molecularly imprinted polymer is more suited for sensing in room temperature conditions because the phase transition takes place between 22-26 ° C. The effect of adding NTBA to NIPA and acrylic acid is shown in Fig 7.3, where the phase transition takes place between 25- 30 ° C. Adding NTBA to NIPA is an alternate way of lowering the response temperature to room temperature. The results indicate that although NTBA shifts the phase transition temperature to lower temperatures, pure polyNNPAM may be better suited for room temperature sensing applications.

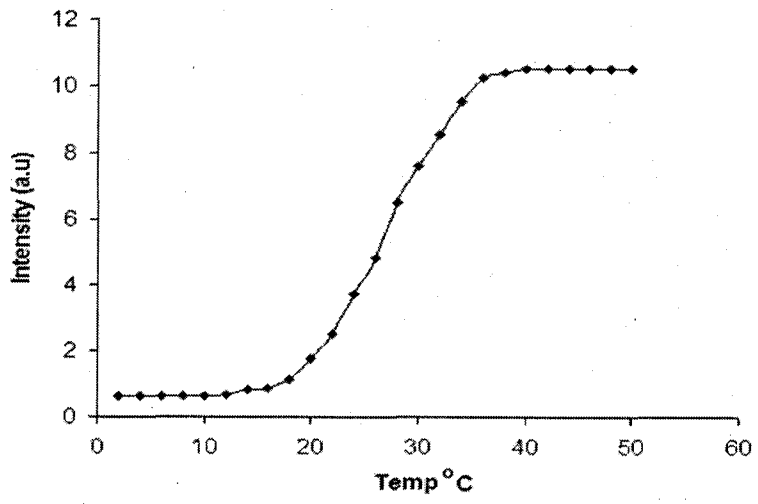

Figure 7.2 Temperature response of uncrosslinked and templated poly NNPAM-co-AAc-co-AE2.

Reproduced with permission of the copyright owner. Further reproduction prohibited without permission.

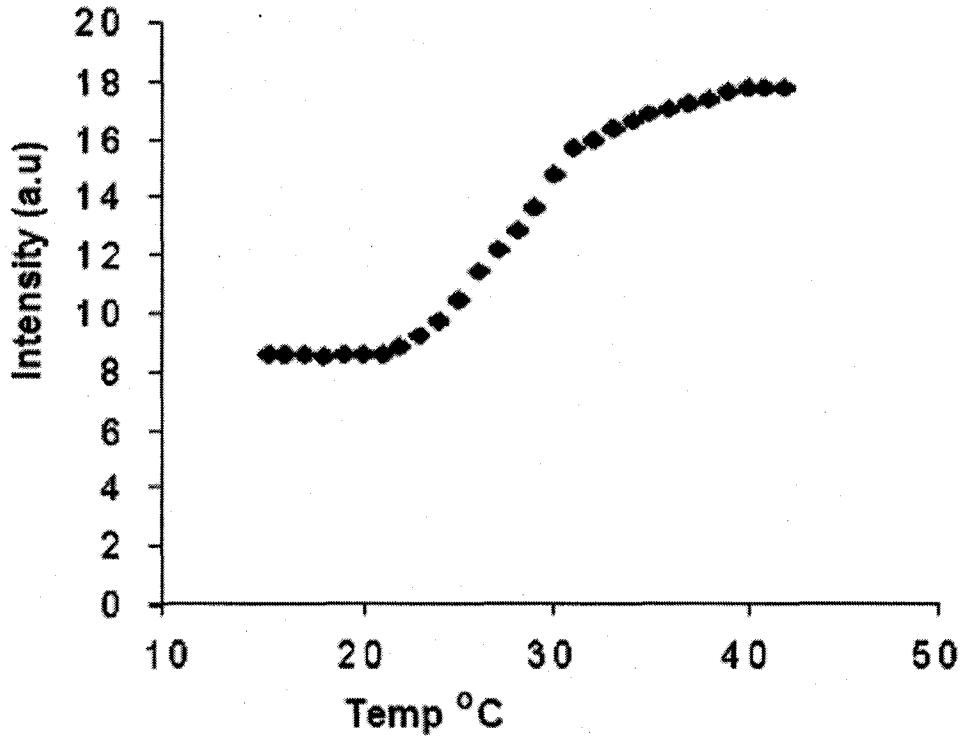

Figure 7.3 Temperature response of uncrosslinked polyNIPA-co-AAc-co-NTBA-co-AE2. The formulation was 60% NIPA, 15% NTBA.

Reproduced with permission of the copyright owner. Further reproduction prohibited without permission.

7.3 Selectivity of PolyNNPAM-co-AAc-co-NDB-AE2 in Buffer at Constant Temperature.

During the process of molecular imprinting, the template the template (theophylline in the present investigation) occupies the complementary binding sites[108] of the molecularly imprinted co-polymer in its neutral form. After the extraction of the template, as shown in chapter 3, Figure 3.6 at pH 7, the carboxylic acid groups are deprotonated. There is electrostatic repulsion between the negatively charged groups and the polymer remains in an expanded form. Since the polymer is immersed in aqueous buffer, there may be a polymer solvent interaction taking place and the water will gain access the inside of the polymer and quench the fluorescence intensity from the benzoxadiazole fluorophore.

In this experiment NNPAM was co-polymerized with a fluorophore and methacrylic acid in the presence of the theophylline template. The experiment was performed as described previously (Section 3.5), except that the crosslinker was not included in the formulation. Figure 7.4 shows the fluorescence intensity of uncrosslinked and templated polyNNPAM- co-AAc-co-AE2 as a function of wavelength and theophylline concentration at pH 4. We see that there was increase in fluorescence with small increases in the theophylline concentration. For instance on increasing theophylline concentration from 2×10^{-5} M to 4×10^{-5} M, there was an increase of 20 intensity units. At pH 4.0 the carboxylate groups on the polymer are partially deprotonated. The resulting charge enhances the solubility of the polymer so that it is in an extended conformation. It is suggested that theophylline binds to charged functional groups and neutralizes them and reduces the copolymer solubility. This may cause the increase in fluorescence, as the fluorophores are in

Reproduced with permission of the copyright owner. Further reproduction prohibited without permission.

now in a non-polar environment. These results are preliminary and more work needs to be done to confirm the changes.

Figure 7.5 shows fluorescence intensity of uncrosslinked and templated PolyNNPAM-co-AAc-co-AE2 as a function of wavelength and caffeine concentration at pH 4. It can be seen that there is absolutely no increase of fluorescence intensity with caffeine concentration. The spectrum shows that even at the highest concentration of 1 x 10^{-3} M there was no change in the fluorescence intensity. This may indicate that of this co-polymer is selective to theophylline.

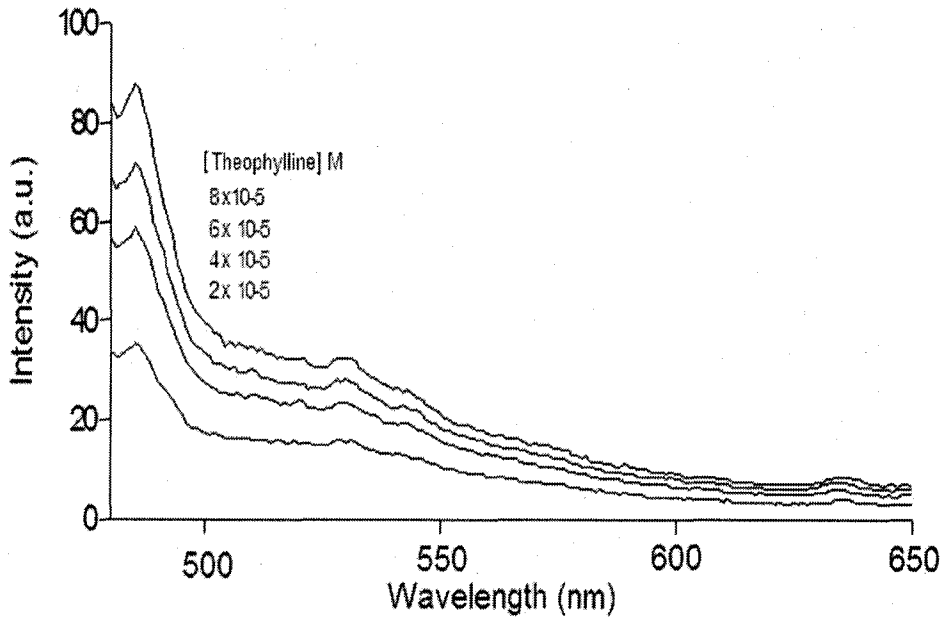

Figure 7.4 Fluorescence intensity of uncrosslinked and templated polyNNPAM- co-AAc-co-AE2 as a function of wavelength and theophylline concentration at pH 4.

Reproduced with permission of the copyright owner. Further reproduction prohibited without permission.

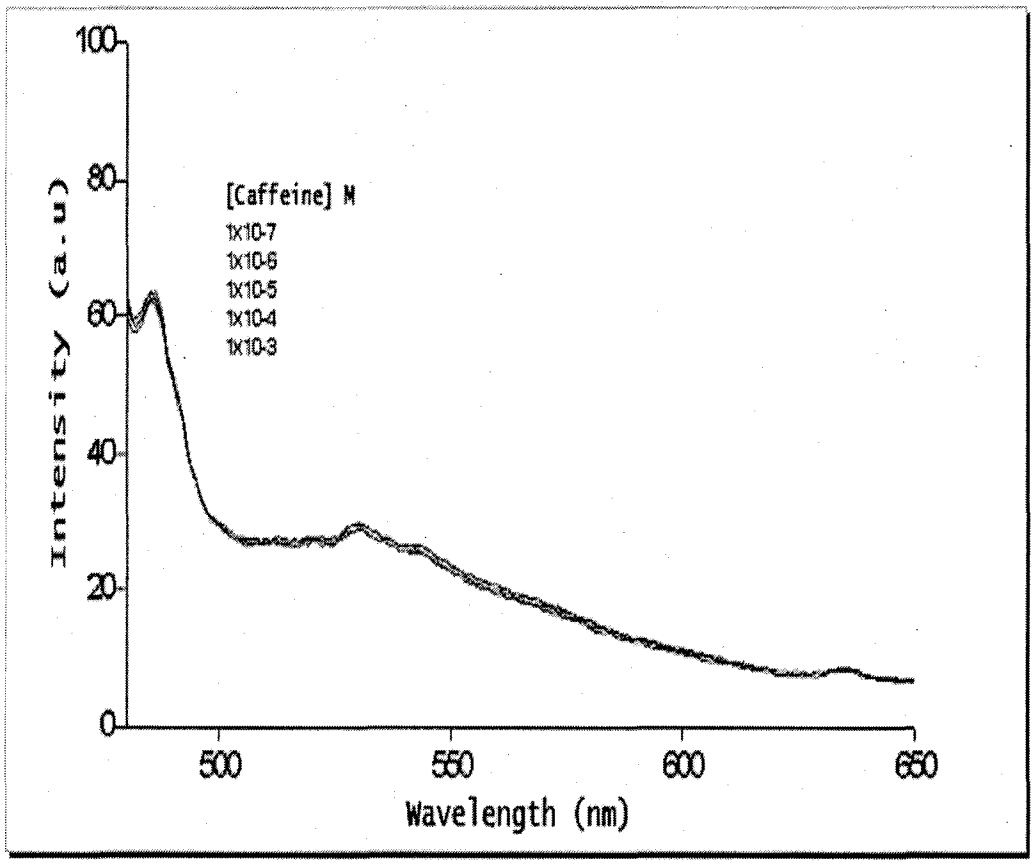

Figure 7.5 Fluorescence intensity of uncrosslinked and templated polyNNPAM- co-AAc-co-AE2 as a function of wavelength and caffeine concentration at pH 4.

Reproduced with permission of the copyright owner. Further reproduction prohibited without permission.

7.5 Response of Uncrosslinked, Fluorescently Labeled, PolyNNPAM Co-polymer to Theophylline Concentration

Figure 7.6 shows the fluorescence intensity of uncrosslinked and templated polyNNPAM- co-MAA-co-AE2 as a function of wavelength and theophylline concentration at 25 ^{o}C in pH 2.0 buffer. In this spectrum we can see that the copolymer responds to theophylline concentration, but in this case, the theophylline of lower concentration produces the higher intensity and vice-versa. This may be because the theophylline, which was prepared in a pH 2.0 buffer, is protonated, when it takes up position inside the cavities; there is a physical effect that keeps the polymer from collapsing in on itself.

As more theophylline molecules take position inside these cavities the copolymer expands and as it swells, it takes in the aqueous buffer, which reduces the fluorescence. It is also possible that the carboxylic acid groups deprotonate and form ion pairs with the protonated theophylline, resulting in no net charge in the polymer. The greater the reduction of charge in the polymer the more it takes up water and quenches the fluorescence. In these spectra we can see that for the highest concentration of theophylline, 1 x 10^{-4} M, the lowest fluorescence intensity of 10 a.u. was obtained, showing that at this concentration there is more theophylline interacting with the polymer and causing quenching of the fluorescence. However the total decrease was small. This modest response may be attributed to the template preventing the contraction of the copolymer at high temperature. The polymer-solvent interaction may also be reduced at high temperature due to the disruption of hydrogen bonds between the polymer and water molecules.

Reproduced with permission of the copyright owner. Further reproduction prohibited without permission.

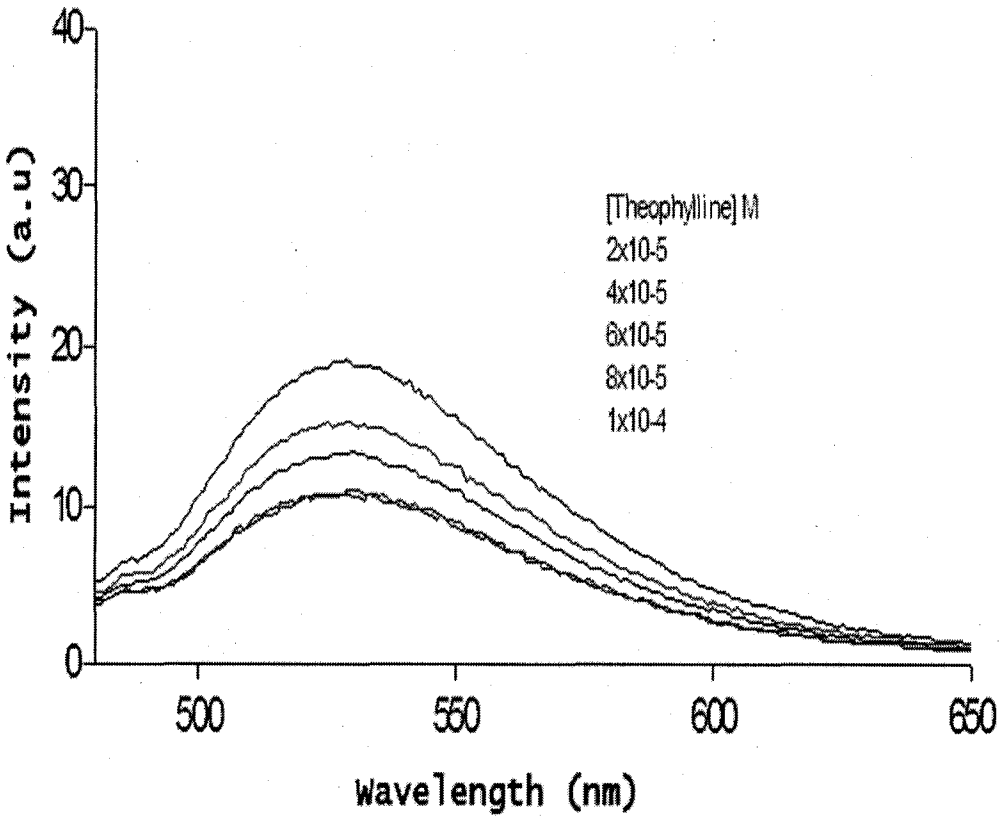

Figure 7.6 Fluorescence intensity of uncrosslinked and templated polyNNPAM- co-MAA-co-AE2 as a function of wavelength and theophylline concentration at pH 2.

Reproduced with permission of the copyright owner. Further reproduction prohibited without permission.

In order to determine the effect of the template, we repeated the experiment but this time we did not include the template in the polymer system. Figure 7.7 shows the fluorescence intensity of uncrosslinked and untemplated polyNNPAM-co-AAc-co-NBD-AE2 as a function of wavelength and theophylline concentration. It is clear from this spectrum that there was no response, when increasing concentrations of theophylline were applied to the co-polymer. This suggests that for recognition to take place it is essential to co-polymerize the template with the polymer before extracting it, to create complementary recognition sites for the analyte.

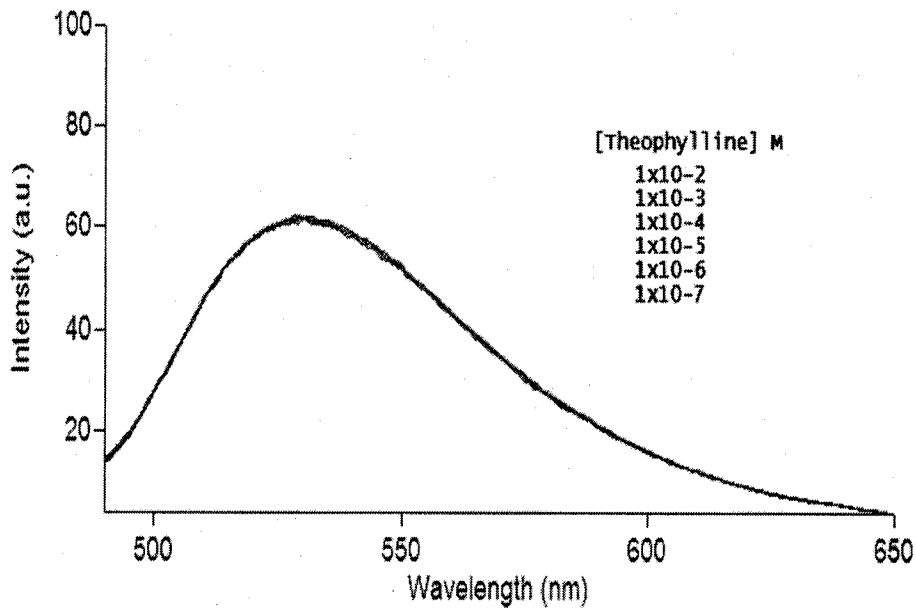

Figure 7.7 Fluorescence intensity of uncrosslinked and untemplated PolyNNPAM- co-MAA-co-AE2 as a function of wavelength and THO concentration.

Reproduced with permission of the copyright owner. Further reproduction prohibited without permission.

7.6 Response Time

Injecting theophylline into an aqueous solution of the co-polymer, and measuring the fluorescence intensity determined the response time of this polymer to theophylline. All measurements were performed at a temperature of 24 ± 1°C. Figure 7.8 shows the data obtained in this experiment. We observed that about 40 % of the response occurs in the first minute. The response however takes about five minutes to level out. Further research on different functional monomers that may interact better with the template may lead to an improvement of the response time.

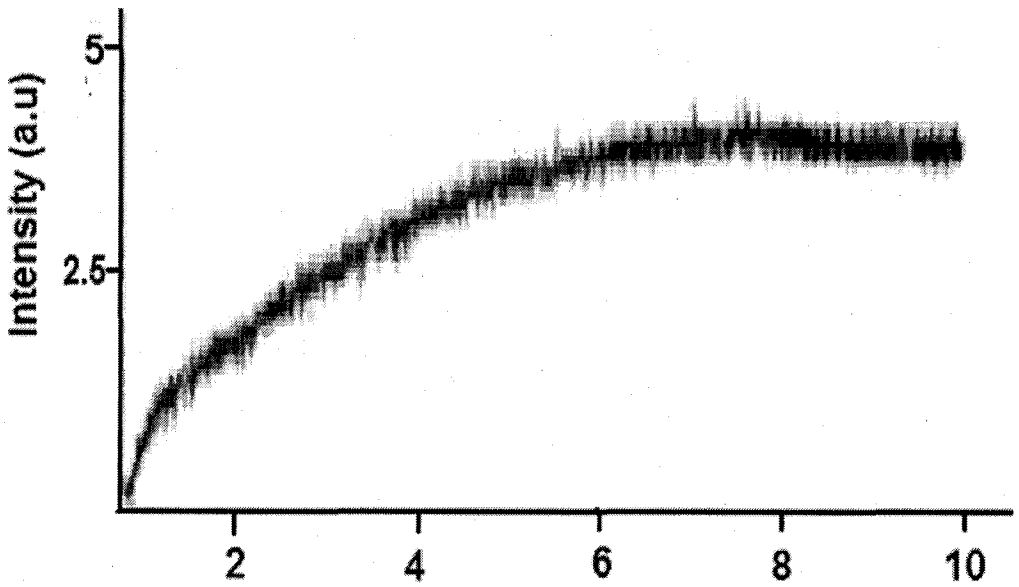

Figure 7.8 Response time of uncrosslinked polyNNPAM-co-AAc-co-AE2.

Reproduced with permission of the copyright owner. Further reproduction prohibited without permission.

7.7 Conclusions

Initial experiments on molecularly imprinted polymers were all performed with N-isopropylacrylamide as the thermally sensitive monomer. This monomer however has a high thermal transition temperature, which may be unsuitable in many applications. It was shown that it was possible to lower this thermal phase transition temperature by substituting part of the NIPA with a more hydrophilic monomer like N-t-butylacrylamide. However this had the disadvantage of broadening the temperature range of the thermal transition temperature.

In this empirical study, N-n-propylacrylamide was used as the thermally sensitive monomer because it has a lower transition temperature than NIPA, which takes place within a narrow range of 2-3 degrees C. The polymerization was conducted in the conventional manner except that the crosslinker was excluded from the formulation. Dialysis was performed to extract the template, with 9:1 methanol: acetic acid solution. Experiments were then performed to investigate the response to this co-polymer to theophylline.

It was shown in these studies that the uncrosslinked, templated co-polymer responds selectively to theophylline. There was no change in the fluorescence intensity when caffeine was used in place of theophylline, even at the relatively high concentration of 10^{-3} M. This investigation suggests that it is either possible to prepare uncrosslinked "molecularly imprinted polymer" or one in which the crosslinks are entirely, intermolecular and non-covalent, made up by the compounds included in the formulation. Further investigation is needed in order elucidate the exact mechanism of reaction and possible interfering agents.

Reproduced with permission of the copyright owner. Further reproduction prohibited without permission.

CHAPTER 8

CONCLUSIONS

An optical chemical sensor based on polymer swelling has been developed and studied. Derivatized and lightly crosslinked poly (VBC) microspheres of between 1-3 μm diameters were prepared by suspension polymerization by the Shirazu porous glass method. Porogenic solvents consisting of xylene and dodecane were used to introduce porosity in order to allow analyte access to the interior of the microspheres.

After dispersing the microspheres in a hydrogel membrane the absorbance was measured versus wavelength on immersing the modified membrane in buffer solutions of varying pH (2.0-10.0). When PVA membrane was used to suspend the microspheres, at low pH (2.0), the turbidity had the lowest value (0.12).It increased when the pH was increased to pH 10. The time taken for the aminated polymer to attain its maximum turbidity on moving from low to high pH was established to be of the order of 8 seconds. The swelling process was faster as it took only 1 second to reach 95 % of its maximum turbidity. A Potentiometric titration performed on the poly (VBC) microspheres showed an apparent pK_a of 5.4, the documented pKa of ethylenediamine, the aminating reagent used in the polymer formulation is 6.4. This indicates that the apparent pKa of the polymer was probably erroneous and further investigation is therefore necessary to determine this value.

Reproduced with permission of the copyright owner. Further reproduction prohibited without permission.

Aminated Poly (HEMA) dispersed in a polyurethane membrane was used to bind copper. The complex formation between the amine groups in the polymer caused the polymer to shrink, resulting in an increase in absorbance over a concentration range from 1.0×10^{-3} to 1.0×10^{-2} M. Potentiometric titration of the aminated poly (HEMA) microspheres indicated that the ratio of nitrogen to copper in the complex was 2:1. This observation was confirmed with electron paramagnetic resonance (EPR) and through the determination of membrane complexed copper using atomic absorption spectrometry.

A new method for the synthesis of templated co-polymers that change fluorescence on binding to the template was developed. The fluorescent monomer, 4-(2-acroyloyloxyethylamino)-7-nitro-2, 1,3-benzoxadiazole was co-polymerized with N-isopropylacrylamide and it was verified that, as the temperature was elevated there was a large increase in fluorescence. It was established that the lower critical solution temperature (LCST) of polyNIPA is ~34 °C. The fluorescent monomer was then co-polymerized with methacrylic acid (MAA) as the functional monomer and N-n-propylacrylamide (NNPAM) was used as the principal monomer instead of NIPA. NNPAM has a lower transition temperature than NIPA, which makes it suitable for observing template binding at low temperature.

The response of the templated polymer was tested against increasing concentrations of theophylline at different pH values. At pH 2.0, when the MAA recognition monomer is fully protonated, there was a strong increase in fluorescence. This fluorescence decreased with increase in template concentration. The total decrease however was only about 20% at the highest template concentration. This was attributed to the interference of the template on the polymer's ability to collapse on itself at elevated temperatures.

Reproduced with permission of the copyright owner. Further reproduction prohibited without permission.

Experiments were conducted where uncrosslinked theophylline templated NNPAM was investigated for response to theophylline concentration. The experiment was conducted in the same way as before except that no crosslinker was used in the formulation prior to polymerization. It was found that the uncrosslinked polymer responds to selectively to theophylline. In pH 4.0 buffer, the polymer showed a large increase in fluorescence with increasing theophylline concentration. This is probably because at this pH there is partial deprotonation of the polymer and the binding of theophylline to the charged sites neutralizes them. This may have caused the polymer to undergo a thermal phase transition, which in turn altered the polarity in the environment of the fluorophores and increased the fluorescence.

There was no change in fluorescence when caffeine was used in place of theophylline, even at caffeine concentrations as high as 10^{-3} M. Determination of response versus time of the uncrosslinked fluorescent co-polymer showed that about 40% of the response occurred in the first minute. Nevertheless, it took 5 minutes for the response to level out.

Reproduced with permission of the copyright owner. Further reproduction prohibited without permission.

REFERENCES

1. Chemical Sensors and Microinstrumentation, Murray, R. W.; Dessy, R. E.; Heineman, W. R.; Janata, J.; Seitz, W. R.; Ed.; American Chemical Society, Washington D. C.: **1989**

2. Principles of Chemical and Biological Sensors, Diamond, D.; Wiley-Interscience, New York: **1998**

3. Principles of Chemical Sensors, Janata, J.; Ed., Plenum Press, New York: **1989**

4. Lambeck., P.V.; *Sensors and Actuators,* B, **1992**, 103.

5. Chemical Sensors in Oceanography, Mark, S.V.; Ed., Gordon and Breach Science Publishers, Amsterdam: **2000**

6. Janata. J.; *Anal. Chem.* **1998**, 70, 179R.

7. Pollak-Diener. G.; Obermeier. E.; *Sens. Actuators*. B. **1993**, 13, 345.

8. Rumpler.W.; Leiss.H.D.; *Ferroelectronics*. **1995**, 165, 205.

9. Grate, J. W.; Martin, S.J.; *Anal. Chem.* **1993**, 65, 940A.

10. Brett, C. M. A.; *Pure Appl. Chem.* **2001**, 73, 1969.

11. Chudyak, W., et al.; *Anal. Chem.* **1985**, 57, 1237.

12. Peterson J.I.; Goldstein, S. R.; Fitzgerald R. V.; *Anal. Chem.* **1980**, 52, 864.

13. Saari, L. A.; Seitz, W.R .; *Anal. Chem.* **1982**, 54, 821.

14. Christine, M.; David, R.W.; *Anal. Chem.* **1986**, 58, 1427.

15. St, John, P. M.; Davis, R.; Cady, N.; Czajka, J.; Batt, C. A.; Craighead, H.G; *Anal. Chem.* **1998**, 70, 1108.

16. Seiler, K.; Simon W.; *Anal. Chim. Acta*. **1992**, 266, 3.

17. Bakker, E.; Simon W.; *Anal. Chem.* **1992**, 64, 1805.

18. Michael, K. L.; Laura, C. T.; Sandra, L.S.; David R.W.; *Anal. Chem.* **1998**, 70, 1242.

Reproduced with permission of the copyright owner. Further reproduction prohibited without permission.

19. Arnold, M. A.; *Anal. Chem.* **1985**, 57, 585.

20. Kulp, T.J.; Camins, I.; Angel S.M.; *Anal. Chem.***1987**, 59, 2849.

21. Chemical Sensors in Oceanography., Mark, S.V.: Ed., Gordon and Breach Science Publishers, Amsterdam: **2000.**

22. Rosenzeig. Z., Kopelman R. In *Analytical Properties of Miniaturized Oxygen and Glucose Fiber Optic Fibers*, The 6th International meeting on Chemical Sensors, NIST, Gaithersburg, MD, **1996**.

23. Zhujun, Z.; Zhang, Y.; Wangbai, M.; Russel, R.; Shakhsher, Z. M.; Grant, C. L.; Seitz, W. R.; *Anal. Chem.* **1989**, 61, 202.

24. Conway, V. L.; Hassen, K.P.; Zhang, L.; Seitz, W.R.; Gross, T.S.; *Sensors and Actuators B.* **1997**, 45, 1.

25. Shakhsher, Z.; Seitz, W. R.; *Anal. Chem.* **1994**, 66, 1731.

26. McCurley, M. F.; Ph.D. Dissertation, University of New Hampshire, Durham, NH, 1990.

27. Shakhsher, Z. M.; Odeh, I.; Jabr, S.; Seitz, W. R.; *Microchim. Acta.* **2004**, 144, 147.

28. Civiello, M. D.; Ph.D. Dissertation, University of New Hampshire, **1997**.

29. Dickey F. H.; *Proc. Natl. Acad. Sci.* **1949**, 35, 227.

30. Peters, E.C.; Petro, F.; Svec, F.; Frechet, J. M. J.; *Anal. Chem.* **1997**, 69, 3646.

31. Palm, A.; Novotny, M. V.; *Anal. Chem.* **1997**, 69, 581.

32. Matsumi, J.; Akamatsu, K.; Nishiguchi, S.; Miyoshi, D.; Nawafume, H.; Tamaki, K.; Sugimoto, N.; *Anal. Chem.* **2004**, 76, 1310.

33. Chemical Instrumentation: A Systematic Approach, Strobel, H. A.; Heineman W. R .; John Wiley & Sons, NY: **1989**.

34. Sellergren, B.; Ekberg, B.; Mosbach, K.; *J. Chromatogr.* **1990**, 1, 347.

35. O'Shannessy, D.J.; Ekberg, B.; Mosbach, K.; Anderson, L. I.; *J. Chromatogr.* **1989**, 470, 391.

36. Mosbach, K.; Anderson, L. I.; *J. Chromatogr.* **1990**, 516, 313.

Reproduced with permission of the copyright owner. Further reproduction prohibited without permission.

37. Kempe, M.; Mosbach, K.; *J. Chromatogr.* **1994**, 664, 276.

38. Romstrom, O.; Nicholls, I.A.; Mosbach, K.; *Tetrahedron.* **1994**, 5, 649.

39. Siemann, M.; Anderson, L.I.; Mosbach, K.; *J. Antibiot.* **1997**, 50, 349.

40. Shea, K.J.; *Trends in Polymer Sci.* **1994**, 2, 166.

41. Kriz, D.; Mosbach, K.; *Anal. Chim. Acta.* **1994**, 300, 71.

42. Piletsky, S.A.; Butovich, A.; Kukhar, V.P.; *Zh. Anal. Khim.* **1992**, 47, 1661.

43. Owens, P.K.; Karlsson, L.; Lutz, E.S.M.; Anderson, L.I.; *Trends in Analytical Chemistry.* **1999**, 18, 3, 146.

44. Liao, Y.; Wang, W.; Wang, B. H.; *Bioorg.Chem.***1999**, 27, 6, 463.

45. Rathbone, D. L.; Su, D.; Wang, Y.; Billington, D. C.; *Tetrahedron Lett.* **2000**, 41, 123.

46. Wang, W.; Gao, S. H.; Wang, B. H.; *Org. Lett.* **1999**, 8,1209.

47. Turkewitsch, P.; Wandelt, B.; Darling, G.D.; Powel, W.S.; *Anal. Chem.* **1998**, 70, 2025.

48. Rathbone, D.L.; Ge, Y.; *Anal. Chim. Acta.* **2001**, 435, 129.

49. Kriz, D.; Ramstrom, O.; Svensson, A.; Mosbach, K.; *Anal. Chem.* **1995,** 67, 2142.

50. Piletsky, S.A.; Piltetskaya, E.V.; Elskaya, A.V.; Levi, R.; Yano, K., Karube, I.; *Anal. Lett.* **1997**, 30, 445.

51. Rachkov, A.; Mc Niven, S.; El'skaya, A.; Yano, K.; Karube, I.; *Anal. Chim. Acta.* **2000**, 405, 23.

52. Nguyen, T. K. T.; Rathbone, D. L.; Billington, C. B.; Nicholas, A. H.; *Anal. Lett.* **2002**, 35, 2499.

53. Sellergren, B.; *Mikromol.Chem.* **1989**, 190, 2703.

54. Polymers: Chemistry and Physics of Modern Materials, J. M. G. Cowie; Intext Educational Publishers, NY: **1973.**

Reproduced with permission of the copyright owner. Further reproduction prohibited without permission.

55. Introduction to Polymer Chemistry, J. W. Stille; John Wiley and Sons, NY:**1962.**

56. Textbook of Polymer Science, Billmeyer, F. W.; Interscience Publishers, NY:**1962.**

57. Organic Chemistry of Synthetic High Polymers, Robert W. L.; Darrel C. F.; Interscience Publishers, NY: **1967.**

58. Emulsion Polymerization and Emulsion Polymers, Lovell, P. A .; El-Aasser, M.S; John Wiley & Sons Ltd., Chichester, England: **1997.**

59. Paine, A.J.; *J. Coll. Int. Sci.* **1990**, 138, 157.

60. Principles of Polymer Science, Flory, P. J.; Cornell University Press: Ithaca NY: **1953.**

61. "Membrane Emulsification Operation Manual", 1st Ed., Nakashima ,T.; Shimizu, M.; Kukizaki, M. Department of Chemistry Industrial research of Miyazaki Prefecture, Miyazaki-City 880, Japan, **1991.**

62. Uchiyama, S.; Matsumura, Y.; de Silva, A. P.; Iwai, K.; *Anal. Chem.* **2003**, 75, 5926.

63. Eeckman, F.; Moes, A. J.; Amighi, K.; *Int. J. Pharm.* **2002**, 241, 113.

64. Schild, H. G.; *Prog. Polym. Sci.* **1992**, 17, 163.

65. Choi, H. S .; Kim, J. M .; Lee, K. J.; Bae, Y. C.; *J. Appl. Polym. Sci.* **1998**, 69, 799.

66. Katayama, S.; Hirokawa, Y.; Tanaka, T.; *Macromolecules.* **1983**, 16, 887.

67. Muller, K.F.; *Polymer.* **1992**, 33, 3470.

68. Jin, M. R.; Wu, C. F.; Lin, P.Y.; Hou, W.; *J. Appl. Polym. Sci.* **1994,** 56, 285.

69. Yeh, P. Y.; Koeckova, P.; Kopecek, J.; *J. Appl. Polym. Sci.* **1994,** 32, 1627.

70. Inomata, H.; Saito, S.; *Macromolecules.* **1990**, 23, 4887.

71. Yi, Y.D.; Oh., K.S.; Bae, Y.C.; *Polymer.* **1997**, 38, 3471.

72. Whitten, D.; Johnes, R.; Bergdtedt, T.; Chen, L.;Heeger,P.; *Optical sensors and switches,* **2001**, 1, 189.

Reproduced with permission of the copyright owner. Further reproduction prohibited without permission.

73. Ensing, K.; Berggren ,C.; Majors R.E.; *LC.GC int.,*2-8, January **2002**

74. Polyakov, M.W.; *Zh. Fiz. Khimii.* **1931**, 2, 799.

75. Wulff, G.; *Micromol. Chem.* **1977**, 178, 2817.

76. Ramstrom, O.; Ye, L.; Mosbach, K.; *Chem & Biol.* **1996**, 3, 471

77. Toshifumi, T.; Jun, H.; *J. Chromatogr. B.* **1999**, 728, 1.

78. Lepsito, M.; Sellergren, B. J.; *Org. Chem.* **1989**, 54, 6010.

79. Sellergren, B.; Lepsito, M.; Mosbach, K.; *J. Am. Chem. Soc.* **1988**, 110, 5853.

80. Sabourin, L.; Ansell, R. J.; Mosbach, K.; Nicholls, I. *Anal. Commun.* **1998**, 35, 285.

81. Ansell, R. J.; Mosbach K.; *Anal. Commun.* **1998**, 35, 1611.

82. Lei Y.; Peter, A.; Cormack, G.; Mosbach, K.; *Anal. Commun.* **1999**, 36, 35.

83. Watanabe,M.; Akahoshi, T.; Tabata Y.; Nakayama, D.; *J. Am. Chem. Soc.* **1998**, 120, 5577.

84. Fery-Forgues S.; Fayet J.; Lopez J. P.; *J. Phtochem.photobiol. A.* **1993**, 70, 229.

85. Pokrajac M.; Varagic V. M.; *Acta. Pharm. Jugosl.* **1983**, 33, 23.

86. Nilsson, K.; Lindell, J.; Norrlow, O.; Sellergren, B.; *J. Chromatogr.* **1994**, 680, 57.

87. Lee B.L.; Jacob P.; Benowitz N.L.; *J. Chromatogr.* **1989**, 494, 109.

88. Desage M.; Soubeyrand J.; Soun A., Brazier J. L.; Georges, Y.; *J. Chromatogr.* **1984**, 336, 285.

89. Mirfazaelian, A.; Goudarzi, M.; Tabafabaiefar, M.; Mohmoudian, M. J.; *Pharm Pharmaceut. Sci.* **2002**, 5, 131.

90. Dockendorff, B.; Holman, D.A.; Christian, G.D.; Ruzicka, J.; *Anal. Commun.* **1998**, 35, 357.

91. Choi, H. S.; Kim, J. M.; Lee K. J.; Bae, Y. C.; *J. Appl. P. Sci.* **1998**, 69, 799.

92. Fan, W. Ph.D. Dissertation, University of New Hampshire, Durham, NH, **2003**

Reproduced with permission of the copyright owner. Further reproduction prohibited without permission.

93. Hee, C. K.; Rimmer, S.; Shaw, D.A.; Sautar, I.; Swanson, L.; *Macromolecules,* **2001**, 34, 7544.

94. Kaval, N.; Ph.D. Dissertation, University of New Hampshire, Durham, NH, **2002**

95. Young, C.M.; Greenaway, F.T.; *Macromolecules*, **1986**, 19, 484.

96. Carl, P. J.; Larsen, S. C.; *J. Catal*, **1999**, 182, 208.

97. Seitz,W. R.; Rooney M. T. V.; Miele, E. W.; Wang, H.; Kaval, N.; Zhang, L.; Doherty, S.; Milde, S.; Lenda, J.; *Analytica Chemica Acta*, **1999**, 400, 55.

98. Rooney, M. T, Ph.D. Dissertation, University of New Hampshire, **1996**

99. Pan, S, M.S. Thesis, University of New Hampshire. **1992**

100. Zhang, Z.; Shaksher Z.;Seitz, W. R.; *Mikrochemica Acta*, **1995**, 121, 41.

101. Miele, E.W.; Ph.D. Dissertation, University of New Hampshire. **1999**

102. Kunio, E.; *J. Colloid Interface Sci.* **2001,** 241, 1

103. Polymer Handbook (3rd Ed.), Brandrup, J.; Immergut.; Wiley Interscience, Toronto:**1989**

104. Macgregor, R. B.; *Nature* **1986,** 319, 90

105. Lancet, D.; Pecht, I.; *Biochemistry*, **1977,** 16, 5150

106. Chee, C. K.; Rimmer, S.; Souter,I.; Swanson, L.; *Polymer*, **2001**, 42, 5079

107. Uchiyama, S.; Santa, T.; Imai, K.; *Anal. Chem,* **2001**, 73, 2165

108. Akimitsu, K.; Toshifumi, T.; Jun, M.; Kazunori I.; Kazuyoshi, Y.; Isao, K.; *Anal. Lett*, **1996**, 7, 1107

Reproduced with permission of the copyright owner. Further reproduction prohibited without permission.